



INSTITUTE FOR DEFENSE ANALYSES

**The UXO Classification Demonstration  
at San Luis Obispo, CA**

Shelley Cazares  
Michael Tuley

September 2010  
Approved for public release;  
distribution is unlimited.  
IDA Document D-4148  
Log: H 10-000937



*The Institute for Defense Analyses is a non-profit corporation that operates three federally funded research and development centers to provide objective analyses of national security issues, particularly those requiring scientific and technical expertise, and conduct related research on other national challenges.*

**About This Publication**

This work was conducted by the Institute for Defense Analyses (IDA) under contract DASW01-04-C-0003, Task AM-2-1528, "Surface and Buried UXO Detection," for the Strategic Environmental Research and Development Program (SERDP) and Environmental Security Technology Certification Program (ESTCP). The views, opinions, and findings should not be construed as representing the official position of either the Department of Defense or the sponsoring organization.

**Copyright Notice**

© 2010, 2011 Institute for Defense Analyses  
4850 Mark Center Drive, Alexandria, Virginia 22311-1882 • (703) 845-2000.

This material may be reproduced by or for the U.S. Government pursuant to the copyright license under the clause at DFARS 252.227-7013 (NOV 95).

INSTITUTE FOR DEFENSE ANALYSES

IDA Document D-4148

**The UXO Classification Demonstration  
at San Luis Obispo, CA**

Shelley Cazares  
Michael Tuley



## **EXECUTIVE SUMMARY**

### **BACKGROUND**

Following a successful unexploded ordnance (UXO) classification demonstration carried out at the former Camp Sibert, AL [13], the former Camp San Luis Obispo, CA, was chosen as a second site in a series of demonstrations of increasing difficulty. The high-level goal of the demonstration was to assess the capability of classification algorithms, developed under the Strategic Environmental Research and Development Program (SERDP) and refined under the Environmental Security Technology Certification Program (ESTCP), to reliably determine which detected items could be left safely in the ground vs. which had to be dug. This demonstration represents a further step along the path to UXO classification, validation, and acceptance.

The intent of the demonstration was to evaluate, on a second and more challenging live site, those instruments and algorithms that had proven successful in the previous demonstration. As at Camp Sibert, inert UXO was seeded within the demonstration site to provide reliable statistics on classification performance. Typically, UXO might constitute fewer than 1% of the items dug on a live site, and with a budget that could support approximately 2500 excavations, seeding of UXO was necessary to allow sufficient understanding of the likelihood of false-negative classification decisions. No additional clutter was seeded.

There was also a desire in this demonstration to test emerging advanced instruments, as well as algorithms tailored to take advantage of the richer data set those instruments provide. Another important goal of the demonstration was continued involvement of the regulatory community in the design, conduct, and evaluation of all demonstrators in an effort to better understand what might be required if detected items that are classified as not hazardous were actually to be left in the ground.

The Institute for Defense Analyses (IDA) was assigned the responsibility to assist ESTCP in planning, carrying out, and scoring the classification demonstration. IDA's principal functions were to provide seed emplacement locations and burial procedures, create a master anomaly list, develop scoring protocols, score demonstrators' detection and classification results, and provide a comprehensive final report describing the

demonstration. This final technical report serves as an adjunct to the summary final report produced by ESTCP [17].

## **DATA COLLECTION**

This demonstration used seven data-collection instruments: (1) a standard EM61-Mk2 cart, (2) the Mobile Towed Array Detection System (MTADS) EM61 array, (3) MTADS magnetometer array, (4) the Man-portable Simultaneous Magnetometer and Electromagnetic System (MSEMS), (5) the MetalMapper, (6) the Time-domain Electromagnetic MTADS (TEMTADS), and (7) the Berkeley UXO Discriminator (BUD). The TEMTADS and the MetalMapper collected cued data over the entire survey area, with the TEMTADS cuing off the MTADS EM61 array anomalies and the MetalMapper off its own anomalies. The BUD collected cued data at a subset of the TEMTADS locations.

Ten different groups submitted ranked anomaly lists for classification scoring. These were the Army Corps of Engineers, Huntsville Center (CEHNC), Dartmouth, Geometrics, Lawrence Berkeley National Laboratory, NAEVA, Parsons, RML, SAIC, Signal Innovations Group, and Sky Research. Different groups provided lists for different instruments, and sometimes multiple lists used different classification algorithms for the same instrument. In all, 62 ranked anomaly lists were submitted, with multiple lists submitted by some groups for a single data set. For each list, the demonstrators specified a “don’t dig threshold.” Based on their calculations, the demonstrators believed that all locations listed above the threshold did not have to be dug because any buried items were not likely to be UXO and could therefore be left safely in the ground.

Careful steps were taken to prepare the site before data collection. After an exhaustive excavation of two 50 ft × 50 ft areas in a high anomaly concentration area of the site, 60 mm mortars, 81 mm mortars, 4.2 in mortars, and 2.36 in rockets were selected as seed items. Two hundred total seed items were emplaced, with 14 as 2.36 in rockets, 54 as 4.2 in mortars, 76 as 60 mm mortars and 56 as 81 mm mortars. In addition, during excavation for scoring, 44 additional UXO items were dug that had not been seeded. These included single instances of a 3 in Stokes mortar, a 37 mm round, and a 5 in rocket, plus additional instances of types of UXO that had been seeded. The classification demonstrators were responsible for correctly identifying the unexpected UXO types as items to be dug.

## RESULTS

Camp San Luis Obispo was chosen for this demonstration because, with more difficult terrain, steeper slopes, more types of UXO, and smaller UXO, it was a more challenging site than Camp Sibert. Results at Camp San Luis Obispo were not as impressive as results at Camp Sibert. Taking into consideration the challenges imposed by the site, however, the results of this demonstration clearly show that current classification procedures could be successful on a much more difficult site than Camp Sibert in terms of both variety of UXO and topography.

For this executive summary, only two illustrative performance curves are shown. The first, presented in Figure ES-1, provides results achieved using survey data from a standard EM61-Mk2 cart sensor that was analyzed using commercially available software (UX-Process, a module within Oasis montaj). At its “don’t dig threshold,” the performer, CEHNC, would have successfully dug all targets of interest (TOI), while leaving more than 30% of the non-TOI in the ground.

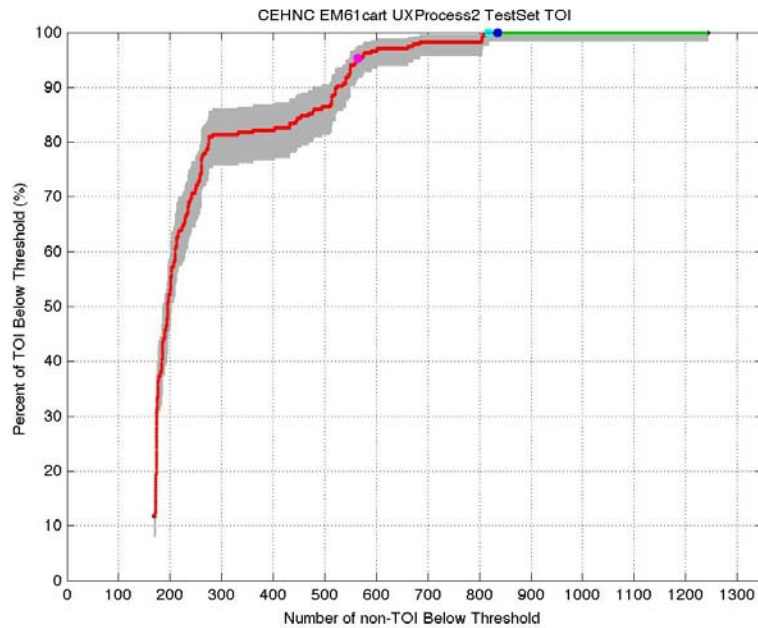


**Figure ES-1. CEHNC’s second-pass scoring results for the EM61 CART data and the UX-Process classification software. No true TOI locations rose above the don’t dig threshold (dark-blue dot).**

The second example, Figure ES-2, shows results using an advanced sensor, the MetalMapper, and custom software developed and applied by Sky Research. While the don’t dig threshold was incorrectly set, leaving two TOI in the ground, the near-vertical rise of the performance curve shows that the combination of advanced sensor data and classification algorithm could successfully distinguish most TOI from non-TOI. One of

the two TOI above threshold was a 37 mm round, which was not an expected UXO item. The other was a partial 2.36 in rocket body that also had other munition debris around it. Multiple proximate objects continue to be difficult for current classification approaches to handle, and performance improvement in that situation is an active area of research.

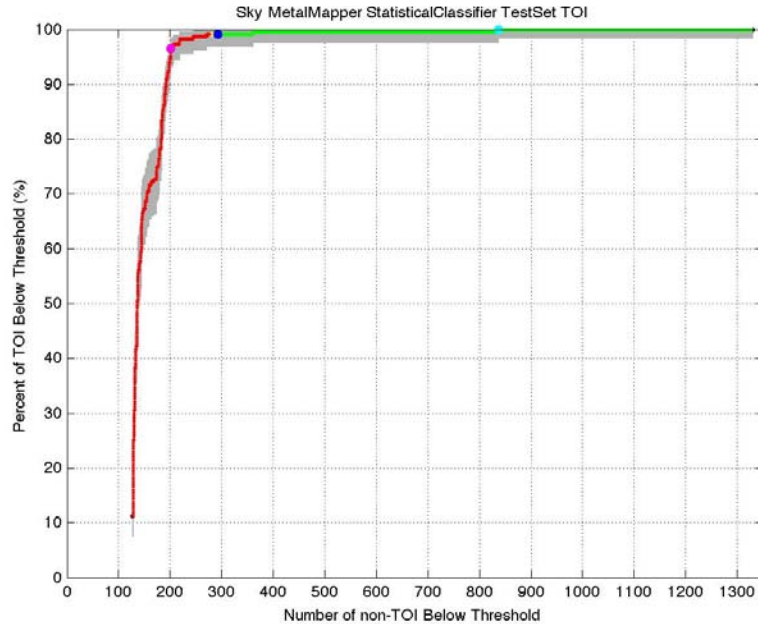


**Figure ES-2. Sky’s scoring results for the MetalMapper data and the “Statistical Classifier” classification algorithm. Two true TOI locations rose above the don’t dig threshold (dark-blue dot).**

## FINDINGS

The results described in this document provide a second confirmation that successful classification is possible on a live site using currently available instruments and software. Specific findings from this demonstration are summarized below:

- Commercially available instruments and software often led to very good classification performance. The better performers using EM61-Mk2 data and UX-Analyze or UX-Process selected “don’t dig thresholds” that would have left no true TOI in the ground while reducing the unnecessary non-TOI digs by 30% to 50%.
- In general, in spite of the EM61-Mk2’s limited decay-time coverage and having only four time gates, classification approaches based on principal polarizabilities and decay rate (size, shape, and wall thickness), or simply decay rate (wall thickness only) provided better performance than approaches based on comparisons of principal polarizability values alone (size and shape only).
- Although there were problems with a few specific true TOI locations rising well above the demonstrators’ “don’t dig thresholds,” many of the classification

performance curves for the MetalMapper and TEMTADS had a near-right-angle shape, indicating a very clear separation in feature space between true TOI and true non-TOI.

- The true TOI that challenged the advanced instruments were generally portions of 2.36 in rocket bodies close to other munitions debris. For example, location #241/1475 rose above the demonstrator's don't dig threshold on 13 of the 14 TEMTADS ranked anomaly lists and 7 of the 10 MetalMapper ranked anomaly lists (and would have been the last true TOI recovered on 2 of the 3 ranked anomaly lists where it was below the don't dig threshold). Other items causing problems were typically low SNR items, particularly partial 60 mm mortars buried deeply.
- For the commercial EMI-based instruments, even though demonstrators typically set the don't dig threshold somewhat aggressively (18 out of 28 ranked anomaly lists would have left at least one true TOI in the ground), 21 of the lists would have recovered over 98% of the true TOI, and all but 2 of the lists would have recovered over 95% of the true TOI.
- For the advanced instruments, "don't dig thresholds" were uniformly aggressive, with only 1 of the 29 ranked anomaly lists showing all true TOI correctly placed below the don't dig threshold. Nevertheless, only one of the ranked anomaly lists would have recovered fewer than 95% of the true TOI. Nineteen of the 29 would have recovered more than 98% of the true TOI.
- No clear metric indicated that either the MetalMapper or TEMTADS performed better than the other in this demonstration. Of the eight ranked anomaly lists for each instrument that were directly comparable, each proved superior on four (i.e., left fewer true TOI in the ground at the don't dig threshold). Averaged over the eight ranked lists, the MetalMapper would have left 3.9 true TOI per list in the ground; the TEMTADS would have left 3.6.



## CONTENTS

1.	Introduction.....	1
1.1	Detailed Objectives.....	2
1.2	Demonstration Motivation.....	3
1.3	General Approach.....	4
1.4	Limitations.....	8
2.	Methods.....	9
2.1	Select Site.....	11
2.2	Initial Survey.....	13
2.3	Select Areas.....	15
2.4	Excavate Sample Areas.....	15
2.5	Generate Seed Plan.....	16
2.5.1	Demonstration Area.....	16
2.5.2	Instrument Verification Strip.....	19
2.6	Emplace Seeds.....	20
2.7	Collect Survey Data.....	21
2.7.1	EM61 CART.....	21
2.7.2	EM61 ARRAY.....	22
2.7.3	MAG ARRAY.....	23
2.7.4	MSEMS.....	24
2.7.5	MetalMapper.....	25
2.8	Correct for Slope.....	26
2.9	Detect Anomalies.....	27
2.10	Generate Cued Lists.....	30
2.10.1	TEMTADS.....	30
2.10.2	BUD.....	30
2.10.3	MetalMapper.....	32
2.11	Collect Cued Data at Locations on Cued Lists.....	33
2.11.1	TEMTADS.....	33
2.11.2	BUD.....	34
2.11.3	MetalMapper.....	35
2.12	Generate Master List.....	35
2.13	Select Survey Data at Locations on Master List.....	37
2.14	Excavate.....	38
2.15	Assign Ground Truth Labels.....	38

2.15.1	Master Locations.....	38
2.15.2	MetalMapper Cued Locations.....	41
2.16	Feature extraction.....	42
2.16.1	Classify “Can Analyze” and “Cannot Analyze” Locations .....	42
2.16.2	Extract Features From “Can Analyze” Locations.....	42
2.16.3	Selecting a Subset of Features .....	44
2.17	Assign Training and Test Sets .....	45
2.17.1	Standard Training Set and Standard Test Set .....	45
2.17.2	Active Learning Training and Test Set.....	47
2.17.3	Extended Training and Test Set.....	49
2.17.4	The Second-Pass Training and Test Set.....	50
2.18	Classify Parameters.....	53
2.19	Score Classification Performance .....	56
2.19.1	Primary Scoring .....	56
2.19.2	Secondary Scoring .....	66
3.	Results and Discussion .....	69
3.1	Detection Results .....	69
3.2	Classification Results.....	72
3.2.1	Conventional Instruments .....	73
3.2.2	Advanced Instruments .....	88
4.	Findings and Conclusions .....	95
4.1	Findings.....	95
4.1.1	Detection.....	95
4.1.2	Classification.....	96
4.2	Conclusions.....	98
	Appendix A: Number of Anomalies Per Instrument .....	A-1
	Appendix B: Primary Scoring Results.....	B-1
	References.....	C-1
	Acronyms.....	D-1

## **1. INTRODUCTION**

Following a successful unexploded ordnance (UXO) classification demonstration carried out at the former Camp Sibert, AL [13], the former Camp San Luis Obispo, CA, was chosen as a second site in a series of demonstrations of increasing difficulty. The high-level goal of the demonstration was to assess the capability of classification algorithms, developed under the Strategic Environmental Research and Development Program (SERDP) and refined under the Environmental Security Technology Certification Program (ESTCP), to reliably determine which detected items could be left safely in the ground vs. which had to be dug. A 2003 Defense Science Board study noted that as much as 75% of current UXO cleanup costs might be associated with digging up nonhazardous scrap [10]. Obviously, the development, validation, and acceptance of reliable classification instruments and algorithms have the potential to significantly reduce UXO clearance costs or to allow more areas to be cleared for the same amount of funding. This demonstration represents a further step along the path to UXO classification, validation, and acceptance.

The intent of the demonstration was to evaluate, on a second and more challenging live site, those instruments and algorithms that had proven successful in the previous demonstration at Camp Sibert. As at Camp Sibert, inert UXO was seeded within the demonstration site to provide reliable statistics on classification performance. Typically, UXO might constitute 1% or less of the items dug on a live site, and with a budget that could support approximately 2500 excavations, seeding of UXO was necessary to allow sufficient understanding of the likelihood of false-negative classification decisions. No additional clutter was seeded.

There was also a desire to test emerging advanced instruments, as well as algorithms tailored to take advantage of the richer data set those instruments provide. Another important goal of this demonstration was continued involvement of the regulatory community in its design, conduct, and evaluation of all demonstrations in an effort to better understand what might be required if detected items that are classified as not hazardous are actually to be left in the ground.

Under a task titled “ESTCP/SERDP: Assessment of Traditional and Emerging Approaches to the Detection and Identification of Surface and Buried Unexploded

Ordnance,” the Institute for Defense Analyses (IDA) was assigned the responsibility to assist ESTCP in planning, carrying out, and scoring the classification demonstration. IDA’s principal functions were to provide seed emplacement locations and burial procedures, create a master anomaly list, develop scoring protocols, score demonstrators’ detection and classification results, and provide a comprehensive final report describing the demonstration. This final technical report serves as an adjunct to the summary final report produced by ESTCP [17].

## **1.1 DETAILED OBJECTIVES**

The classification study demonstration plan [1] lays out the detailed objectives of this demonstration:

1. Test and validate detection and classification capabilities of currently available and emerging technologies on real sites under operational conditions.
2. In cooperation with regulators and program managers, investigate how classification technologies can be acceptably implemented in cleanup operations.

Within each of these two overarching objectives are several technical sub-objectives:

- Test and evaluate capabilities by demonstrating and evaluating individual instrument and software technologies, as well as processes that combine these technologies. Compare advanced methods to existing practices and validate the pilot technologies for the following:
  - Ability to detect UXO.
  - Ability to identify features that distinguish scrap and other clutter from UXO.
  - Ability to reduce false alarms (items that could be left in the ground that are incorrectly classified as UXO) while maintaining a probability of detection (Pd) of UXO that is acceptable to all.
  - Ability to identify sources of uncertainty in the classification process and to quantify their impact to support decision-making, including issues such as impact of data quality due to how data are collected.
  - Ability to quantify the overall impact on risk arising from the capability to clear more land more quickly for the same investment.
  - Ability to address the issues of a dig/no-dig decision process and the related quality-assurance/quality-control issues.

- Understand the applicability and limitations of the pilot technologies in the context of project objectives, site characteristics, and suspected ordnance contamination.
- Collect high-quality, well documented data to support the next generation of signal-processing research.

This report discusses a subset of these points. The remaining points are discussed in the summary final report produced by ESTCP [17].

## 1.2 DEMONSTRATION MOTIVATION

A 2003 Defense Science Board study on UXO cleanup technologies pointed out that in a typical clearance action, more than 99% of the items dug could have been left safely in the ground [10]. It also noted that reducing the false-alarm rate from greater than 99% to a lower, yet still relatively high, number could still save much of the cost of clearance actions.

Significant progress has been made in classification technology as a result of SERDP and ESTCP funding. With the exception of the initial demonstration at the former Camp Sibert, however, testing of these approaches to date has been primarily limited to artificially constructed test sites such as those at Aberdeen Proving Ground, MD, and Yuma Proving Ground, AZ. Acceptance of classification technologies requires demonstration of system capabilities at live UXO sites under real-world conditions. Any attempt to declare detected anomalies to be harmless will require demonstrating to regulators not only individual technologies, but an entire decision-making process. This classification study was the second in a continuing effort that will span a number of years. Follow-on demonstrations already in the initial planning stage at two more sites present challenges not faced to date.

The importance of live-site testing is that the distribution of the items in the ground before testing is realistic for UXO and clutter items. While extremely valuable, areas such as the Aberdeen and Yuma Proving Grounds Standardized UXO Test Sites [16] will always be somewhat artificial because both UXO and clutter items have been emplaced in accordance with preconceived notions of how they should be distributed in type, size, and depth, as well as location. In contrast, clutter items are not emplaced at live sites such as Camp Sibert and Camp San Luis Obispo. Although it is usually necessary in live-site testing to seed the area with appropriate UXO to ensure sufficient munitions to provide reasonable statistics, the *in situ* clutter and any *in situ* UXO types are, by definition, “real” for that site.

### 1.3 GENERAL APPROACH

The ESTCP Program Office, in conjunction with IDA and the Advisory Group of local and state regulators, selected Camp San Luis Obispo for the second demonstration because it met a number of desired characteristics. Historical records showed that the portion of Camp San Luis Obispo where testing was planned likely contained 60 mm, 81 mm, and 4.2 in mortars, along with 2.36 in rockets. This made it a much more complex site than Camp Sibert, which contained only 4.2 in mortars. In addition, the site at Camp San Luis Obispo was on the side of a hill, providing more difficult topography than the earlier demonstration.

Data-collection teams initially collected magnetometer array transects (widely spaced lines of data used to assess general anomaly density in an area). Those results guided selection of approximately 30 acres for a complete electromagnetic induction (EMI) survey using a standard EM61-Mk2 cart. The cart results were used to select the specific demonstration area for the study, as well as an area for the instrument verification strip (IVS) and a test pit.

The purpose of the IVS was to confirm at the start and end of each day that all data-collection instruments were properly functioning—that is, that they provided the expected signal on all emplaced items, which included seed munitions and spheres. An exhaustive excavation was performed to clear the IVS area of all metallic items before it was seeded to ensure that only the desired signals would exist. A test pit area adjacent to the IVS was also cleared and used to collect additional training data against expected munition types.

In addition, two 50 ft × 50 ft high-density areas were exhaustively excavated to confirm the presence of the expected munitions types and to assess their depth distributions. Based on the excavation results, it appeared unlikely that UXO would be found deeper than 30 cm, and so detection thresholds were set assuming the smallest expected signal for a target of interest (TOI) at 45 cm, providing a 50% depth margin.

As noted earlier, because of the limited number of UXO typically found (often fewer than 1 out of 100 items excavated), it is usually necessary to seed demonstration sites with inert UXO to provide reasonable confidence bounds on classification performance, and seeding was necessary in this case. IDA generated a plan to seed previously fired and inert 60 mm, 81 mm, and 4.2 in mortars, as well as 2.36 in rockets, throughout the demonstration area and IVS. Parsons, the site-support contractor, followed this plan and emplaced the seeds as directed. The emplacement team took care to seed the

items at least 3 m away from each other and from other EM61-Mk2 anomalies because previous work has shown that current classification technologies cannot reliably analyze multiple closely spaced items with overlapping signatures [2, 16].

Next, the data-collection teams surveyed the demonstration area using seven data-collection instruments: (1) a standard EM61-Mk2 cart, (2) the Mobile Towed Array Detection System (MTADS) EM61 array, (3) MTADS magnetometer array, (4) the Man-portable Simultaneous Magnetometer and Electromagnetic System (MSEMS), (5) the MetalMapper, (6) the Time-domain Electromagnetic MTADS (TEMTADS), and (7) the Berkeley UXO Discriminator (BUD). The TEMTADS and the MetalMapper collected cued data over the entire survey area, with the TEMTADS cuing off the MTADS EM61 array anomalies and the MetalMapper off its own anomalies. The BUD collected cued data at a subset of the TEMTADS locations. Table 1 provides a brief description of each system, with more detail provided in Section 2.

**Table 1. Data Collection Systems**

System Name	Report Nomenclature	Sensor Description	Collection Mode
MTADS EM61 Array	EM61 ARRAY	2 m × 1 m array of 3 overlapped EM61-Mk2 time domain EMI sensors with 1 m × 1 m coils firing simultaneously.	Survey
MTADS Magnetometer Array	MAG ARRAY	Eight Geometrics G-822A cesium vapor magnetometers spaced 25 cm apart and approximately 25 cm above the ground	Survey
EM61-Mk2 Cart	EM61 CART	Standard EM61-Mk2 cart (0.5 m × 1 m coil)	Survey
MSEMS	MSEMS	EM61-Mk2 cart sensor (0.5 m × 1 m coil) operated simultaneously with a G-822A cesium vapor magnetometer	Survey
MetalMapper	MetalMapper	Three orthogonal transmit coil time-domain EMI sensor with 7 triaxial receive coils	Survey and cued
TEMTADS	TEMTADS	5×5 array of approximately 40 cm × 40 cm time-domain EMI transmit and receive coils operated multistatically	Cued
Berkeley UXO Discriminator	BUD	Three orthogonal transmit coil time domain EMI sensors with eight pairs of single-axis receive coils operating in a gradiometer mode.	Partial site cued

The data-collection teams selected detection thresholds for the survey instruments on the basis of physics-based dipole models of the smallest expected signature collected

from a horizontally placed 60 mm mortar at 45 cm depth and confirmed the validity of these thresholds using the IVS. As was recognized at the beginning of the study, different survey instruments resulted in different anomaly detection lists. That is, many items were detected by all instruments, some items were detected by more than one but not all instruments, and some items were detected by a single instrument only. IDA developed methods for reconciling the differences between individual instruments' anomaly lists to produce two cross-referenced master anomaly lists, one based on the EM61 array, cart, and MSEMS anomalies and one based on the MetalMapper. Appendix A lists the number of anomalies associated with each instrument.

Parsons, the site-support contractor, then excavated items at each location on the master anomaly lists. Based on the excavated items, the Program Office assigned ground truth labels to each location, with some locations assigned the label of "TOI" (target of interest) and other locations assigned the label of "non-TOI." IDA then separated the locations on the master anomaly lists into a Standard Training Set and a Standard Test Set.

Ten different groups submitted ranked anomaly lists for classification scoring. These were the Army Corps of Engineers Huntsville Center (CEHNC), Dartmouth, Geometrics, Lawrence Berkeley National Laboratory (LBNL), NAEVA, Parsons, RML, SAIC, Signal Innovations Group (SIG), and Sky Research. Different groups provided lists for different instruments, and sometimes multiple lists using different classification algorithms for the same instrument. In all, 62 ranked anomaly lists were submitted, with multiple lists submitted by some groups for a single data set. Demonstrator/data set combinations are denoted with an X in Table 2.

**Table 2. Data sets used by each demonstrator to provide distinct ranked anomaly lists.**

Org./Data	EM61 CART	EM61 ARRAY	MAG ARRAY	EM61 MSEMS	MAG MSEMS	Metal Mapper	TEM TADS	BUD
CEHNC	X							
Dartmouth						X	X	
Geometrics						X		
LBNL								X
NAEVA	X							
Parsons	X							
RML		X						
SAIC	X	X		X		X	X	
SIG	X	X	X	X		X	X	X
Sky	X	X	X	X	X	X	X	X

The Program Office distributed the collected data and the master anomaly lists to each demonstration team. The demonstrators also received the ground truth labels for all locations in the Standard Training Set, but remained blind to the ground truth labels for all locations in the Standard Test Set. The demonstrators used the data and ground truth labels in the training set to optimize their inversion routines and classification algorithms. Inversion routines are used to fit the data collected around each location on the master anomaly list to a dipole model to estimate parameters of the buried target. Classification algorithms are used to estimate the likelihood or probability that a buried target is a TOI based on its estimated parameters. The demonstrators then applied their optimized processes to the data in the test set while remaining blind to the ground truth labels. The demonstrators created a ranked list by arranging the locations in the test set according to their estimated probability or likelihood of being a non-TOI. Because the intent of classification is to leave non-TOI in the ground, the ranked list is ordered from 1, the item most likely to be non-TOI, to the highest number, the item most likely to be TOI. The demonstrators also specified a “don’t dig threshold” that could be applied to the ranked list, such that it was likely that all locations on the ranked list above the don’t dig threshold were non-TOI and could therefore be left safely in the ground.

IDA scored each demonstrator’s ranked list and don’t dig threshold by comparing the dig/don’t-dig label calculated for every location in the test set with its corresponding ground truth label. IDA summarized the classification performance of each instrument-algorithm combination with the metrics *Percent of TOI Below Threshold* and *Number of Non-TOI Below Threshold*. The *Percent of TOI Below Threshold* is a metric similar in concept to Pd, the probability of detection; it represents the percentage of locations with a ground truth label of “TOI” that were correctly placed below the don’t dig threshold on the ranked list. The *Number of Non-TOI Below Threshold* is simply the number of false alarms; it represents the number of locations with a ground truth label of “non-TOI” that were incorrectly placed below the don’t dig threshold on the ranked list.

IDA also revisited the choice of don’t dig threshold by retrospectively testing every possible value. For each possible value of the “don’t dig threshold,” IDA recalculated the *Percent of TOI Below Threshold* and the *Number of Non-TOI Below Threshold* and plotted these metrics against each other to form a classification performance curve, similar to a receiver operating characteristic (ROC) curve. The classification performance curves and the statistics drawn from them lead to the key findings from this demonstration. They are discussed in detail in the Results and Discussion chapter of this report.

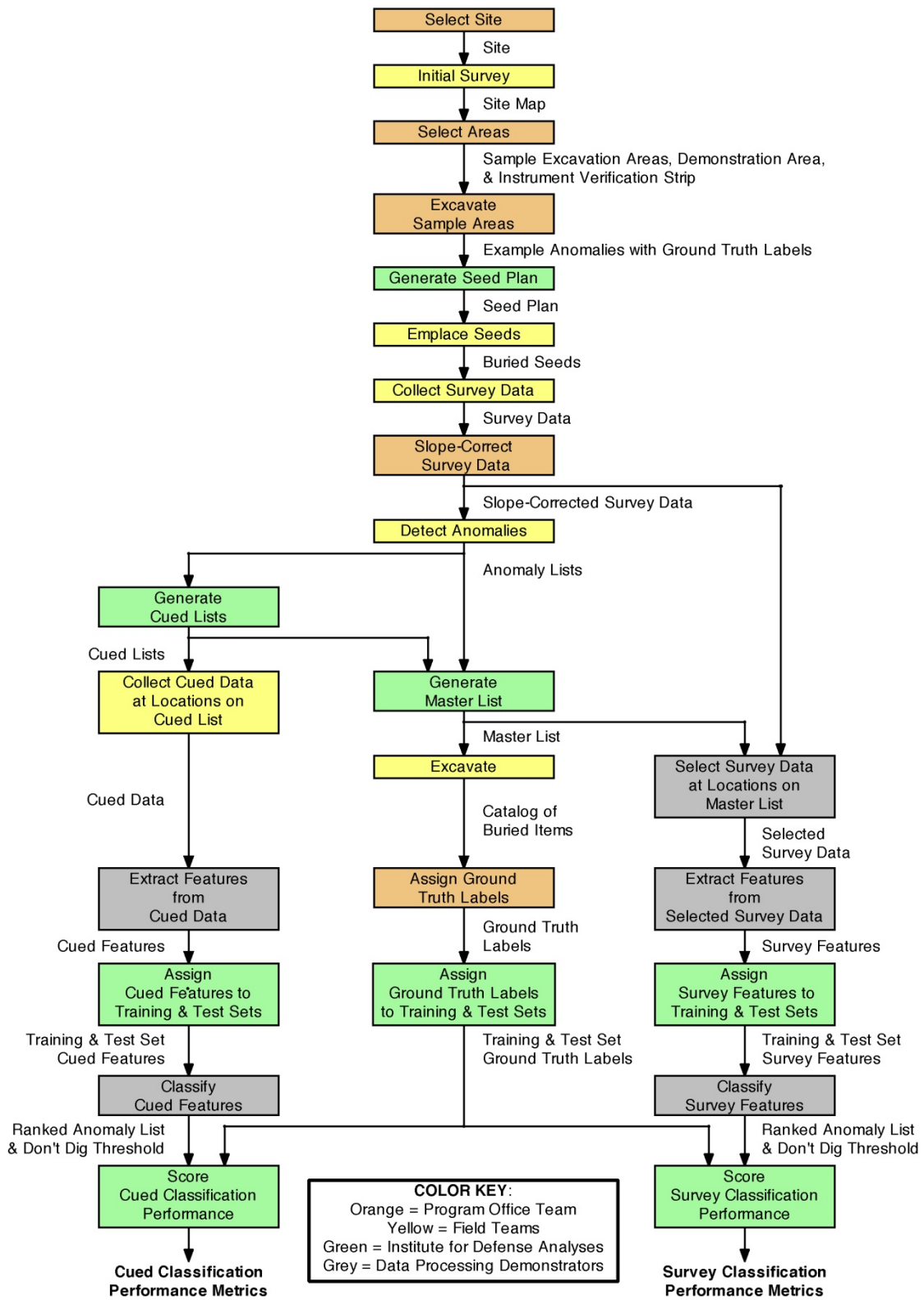
## 1.4 LIMITATIONS

A number of changes were implemented for this demonstration based on lessons learned from the former Camp Sibert [13]. Even so, several limitations remain that are the result of budget and experimental requirements:

- The primary limitation was the need to seed Camp San Luis Obispo with inert munitions to obtain reasonable classification statistics. In an ideal demonstration, the area tested would be sufficiently large that valid statistics could be gained simply from recovered intact UXO. In that case, a potentially artificial distribution of UXO density, depths, and orientations is not a concern. Although 44 true UXO that were not seed items were found in the approximately 10 acres that were excavated, that still is too small a number to provide reliable statistics, and there was no assurance at the beginning of the study that even that many would be detected. Thus, to collect data from enough recovered intact UXO for valid statistics, a very large area would have to be tested. The cost of excavating all anomalies detected in such a large area would have been prohibitive. Thus, seeding was required in this demonstration, resulting in a potentially artificial distribution of UXO density, depths, and orientations. This is a limitation that is unlikely to ever be overcome in scientific testing because of funding constraints.
- A second limitation was unexpected. The original plan had been to exhaustively excavate all anomalies that exceeded the detection threshold of all instruments. It was hoped that such an excavation would remain within the budget, allowing approximately 2500 anomalies to be dug. But a combination of geology and small anomalies resulted in far more magnetometer anomalies than could be dug within the budget (5266 anomalies above the MAG ARRAY threshold and 3389 above the MSEMS magnetometer threshold). Thus, excavation focused on those magnetometer anomalies that correlated with EMI anomalies. In addition, a number of apparently large, deep anomalies identified by the MSEMS magnetometer were excavated. Those excavations resulted in no metallic objects being found.
- A final limitation involves the subjective judgment of what constitutes a TOI when assigning ground truth labels. In this demonstration we chose a very conservative definition and treated as TOI those items that were not only clearly munitions, but those that we felt might cause the general population concern if found. Thus, a number of the 2.36 in partial rocket bodies without warheads were treated as TOI although they had been classified by the UXO technicians as nonhazardous, and those partial rockets gave the classification demonstrators significant problems. This blurs the bright binary scoring line we preferred in a scientific experiment, but appears unavoidable in the real world.

## **2. METHODS**

This chapter describes the process used to select a site for the study, select particular areas of the site as demonstration areas, emplace seed targets in the demonstration areas, collect data from the demonstration areas, detect anomalies in the collected data, provide collected data and a master list of detected anomalies to the data-processing demonstrators, and score the results of the demonstrators' classification outputs. Figure 1 is a flowchart of this process.



## 2.1 SELECT SITE

The first live-site UXO classification demonstration, held at the former Camp Sibert, AL, was intentionally chosen to provide benign terrain and geology, and it contained only one munition type, the 4.2 in mortar [13]. For the second demonstration, the ESTCP Program Office and the Advisory Group desired a site with more challenging topography and with a variety of munition types. The site chosen was the Rifle Range #13 at the former Camp San Luis Obispo, CA. The site encompasses a grassy hillside with a rock outcrop at the top and occasional isolated rocks and holes that, along with the terrain slope, made data collection significantly more difficult than at Camp Sibert. Figure 2, taken from the site inspection report [8], is a map of the former Camp San Luis Obispo, CA.

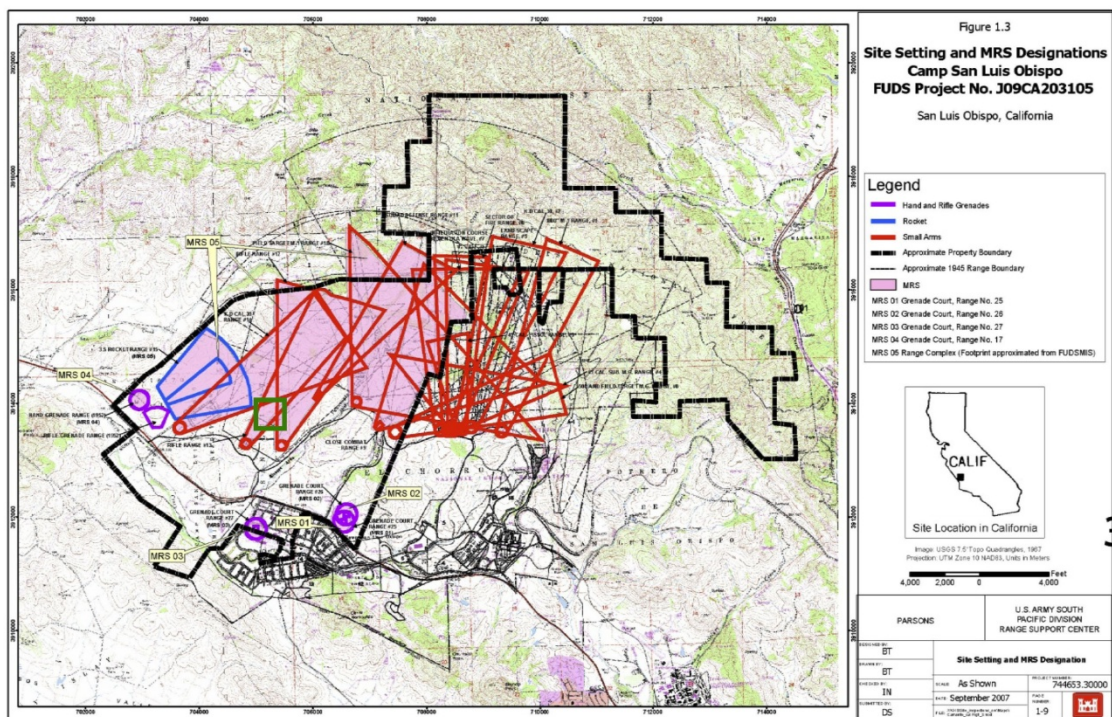


**Figure 2: A map of the former Camp San Luis Obispo, CA. Thick black lines outline the property boundary. Blue, red, and purple lines outline the ranges for different munition types, according to historical records. The small green square shows the site selected for demonstration. Taken from [8].**

Based on recommendations from the Advisory Group, criteria for the second study included multiple munition types and more challenging terrain, but still relatively benign geology. The overall site at Camp San Luis Obispo has historically included training ranges with multiple munition types (see Figure 2). Further research by the Program Office suggested that 60 mm, 81 mm, and 4.2 in mortars, along with 2.36 in

rockets, would likely be found at the particular site selected for demonstration. This site is outlined with a small green square in Figure 2. Figure 3 shows a black-and-white aerial photograph of this site, overlaid with a topographical map.

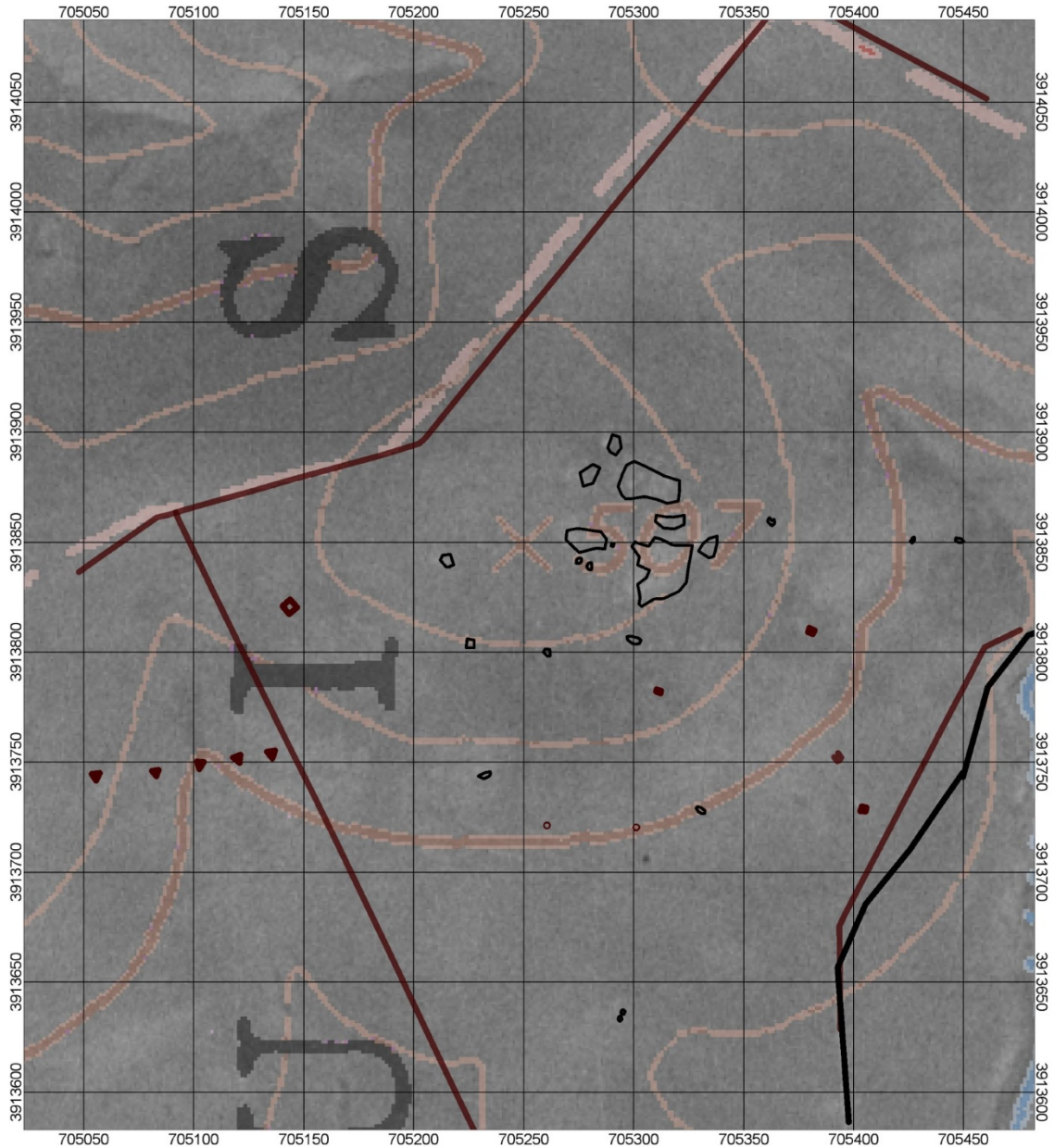


**Figure 3: An aerial photograph of the selected site overlaid with a topographical map. Thin black lines outline large rocks at the top of a hill, and the thick black line in the southeast corner indicates a road. The angled dark brown lines indicate fences, and the curved, light brown lines indicate topographical contours, representing 40 ft differences in elevation. The large gray letters and large brown numbers are part of the overlaid topographical map.**

## **2.2 INITIAL SURVEY**

A series of surveys conducted before the demonstration provided data appropriate for selecting the final demonstration area. Initially, total field magnetometer transect surveys were collected at Camp San Luis Obispo and another potential site in California. The transects at Camp San Luis Obispo covered approximately 12% of an approximate 15 ha area. Anomaly density maps were constructed from the transects and used to narrow the potential demonstration area down to approximately 12 ha, over which a 100% coverage survey was taken using an EM61-Mk2 cart-based instrument operated by NAEVA Geophysics, Inc. Figure 4 shows the EM61 survey map of the selected site. Color shadings indicate the received signal amplitude at the first time gate.

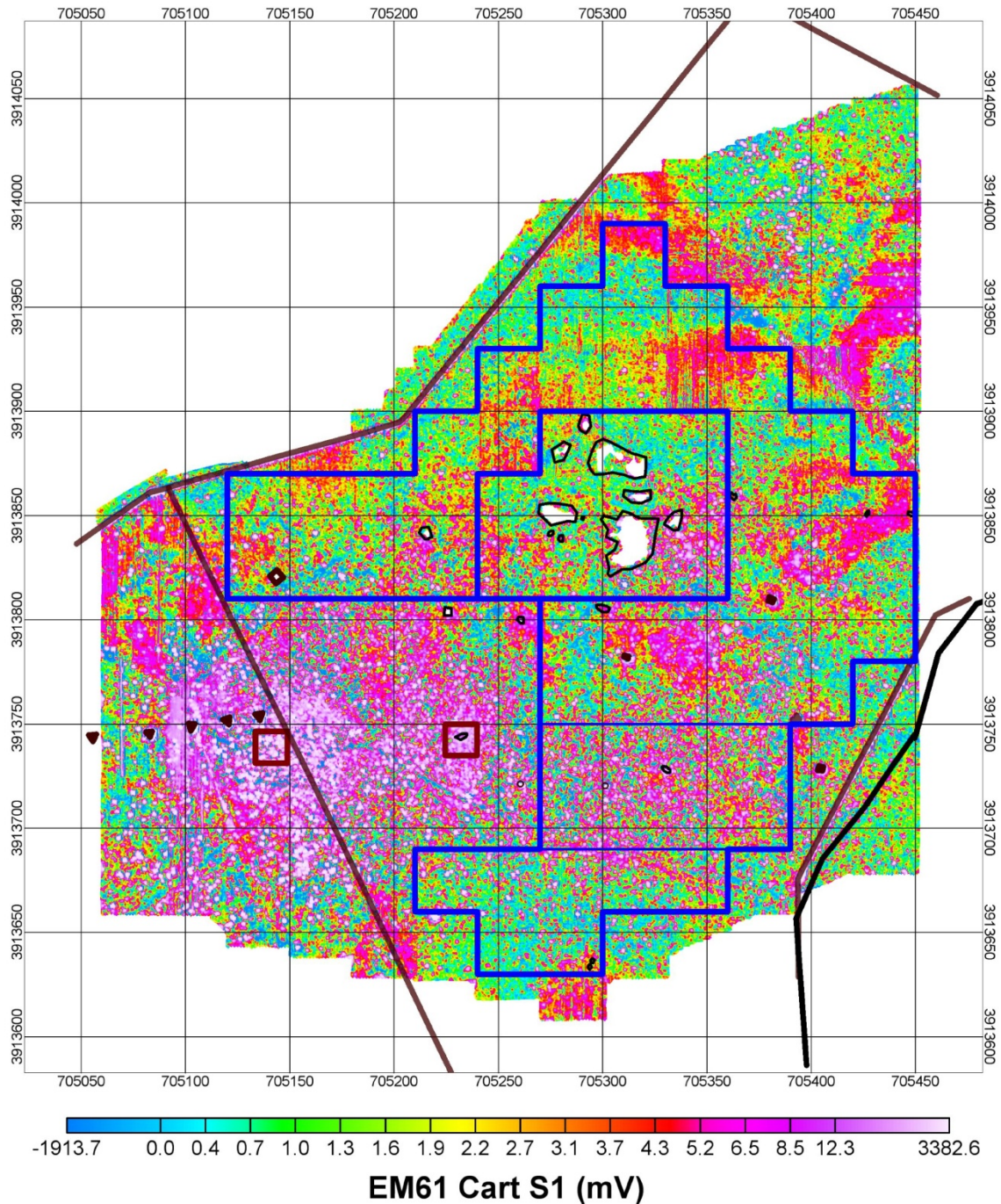


**Figure 4: The initial EM61-Mk2 cart survey map of the selected site. Colored shading indicates the sensed amplitude at the first time gate. Angled brown lines indicate fences. Thin black lines outline large rocks at the top of the hill, and the thick black line in the southeast corner indicates a road. Blue lines outline the survey area, avoiding both the rocky region at the top of the hill and the region of large positive amplitude in the southwest quadrant. The two red squares outline the two sample excavation areas, both in the region of large positive amplitude in the southwest quadrant.**

### **2.3 SELECT AREAS**

The Program Office selected four areas of the site for specific purposes: (1) the demonstration area where the classification performance evaluation would take place, (2) the instrument verification strip (IVS) where the data-collection teams would calibrate their instruments at the beginning and end of each day, (3) a test pit to allow training data on seed items to be collected, and (4) the sample excavation areas where the Program Office would confirm the existence of multiple munition types before the demonstration began. An area southeast of the road was selected for the IVS because its low anomaly density (based on EM61 CART survey) and proximity to the road would lead to a more straightforward and efficient daily instrument calibration. A contiguous region (thick blue line in Figure 4) was chosen for the demonstration area to allow efficient collection of data by the vehicle-towed sensors. The rocky outcrops at the top of the hill were avoided for the demonstration area because it would have been difficult for a number of the instruments to collect data there. Another major criterion used to select the demonstration area was that it could provide 250–500 anomalies per hectare, a density that would make it likely that most anomalies consisted of individual items, allowing a reasonable probability of classification. State-of-the-art classification technology is not advanced enough that correct classification is likely where multiple closely spaced items occur [2, 16]. To that end, the highly dense region in the southwest quadrant of Figure 4 was not used as a demonstration area. This region was selected for the two 50 ft × 50 ft sample excavation areas (red squares in Figure 4), however, because a large number of items would likely be recovered, making it easier to confirm the existence of multiple munition types.

### **2.4 EXCAVATE SAMPLE AREAS**

The Program Office team completely excavated the sample areas to help ascertain the potential munition types. The team recovered 369 total items from the two grids, all buried at 30 cm depths or shallower, with subsequent EMI interrogation not indicating more deeply buried items. In addition, the excavation team felt it unlikely that items would be found below 30 cm, given the underlying soil composition.

Recovered items included fragments from 60 mm, 81 mm, and 4.2 in mortars. Fuzes and unknown fragments were also recovered. No 2.36 in rocket fragments were identified from the sample areas, although a number of 2.36 in rocket bodies were found in the demonstration area during excavation to establish ground truth.

Once multiple munition types were confirmed at the site, the demonstration proceeded to the next step: emplacing seeds in the demonstration area and instrument verification strip.

## **2.5 GENERATE SEED PLAN**

The seed plan consisted of a list of locations where the emplacement team was instructed to bury inert munitions, called “seeds” [22]. The list was separated into two sections. The first listed 200 seeds for emplacement in the demonstration area of the site. The purpose of these 200 seeds was to guarantee the existence of a large number of TOI to ensure sufficient statistical confidence in the classification performance metrics eventually calculated at the end of the study. The second section listed 10 seeds for emplacement in the IVS. The purpose of the IVS was to allow the data-collection teams to recalibrate their instruments on a daily basis using known TOI.

### **2.5.1 Demonstration Area**

To select the intended locations of all 200 seeds in the demonstration area, IDA applied an amplitude threshold to the EM61 survey map to identify strong anomalies representing geology or items indigenous to the site. Figure 5 shows the thresholded map; blue lines outline the demonstration area. Locations with strong anomalies are shaded in pink; all other locations are shaded in light blue. IDA visually analyzed this thresholded map and manually selected 200 locations in the demonstration area that were far from each other and far from any anomalies. Anomalies were avoided since multiple closely spaced items, such as a seed emplaced next to a shell fragment, are generally difficult to separate and classify with the state-of-the-art technology [2, 16]. Black circles mark the intended locations of the seeds. Figure 6 is a close-up of the area enclosed by the black square in Figure 5. Five intended seed locations are shown; all locations are far from each other and far from any anomaly.

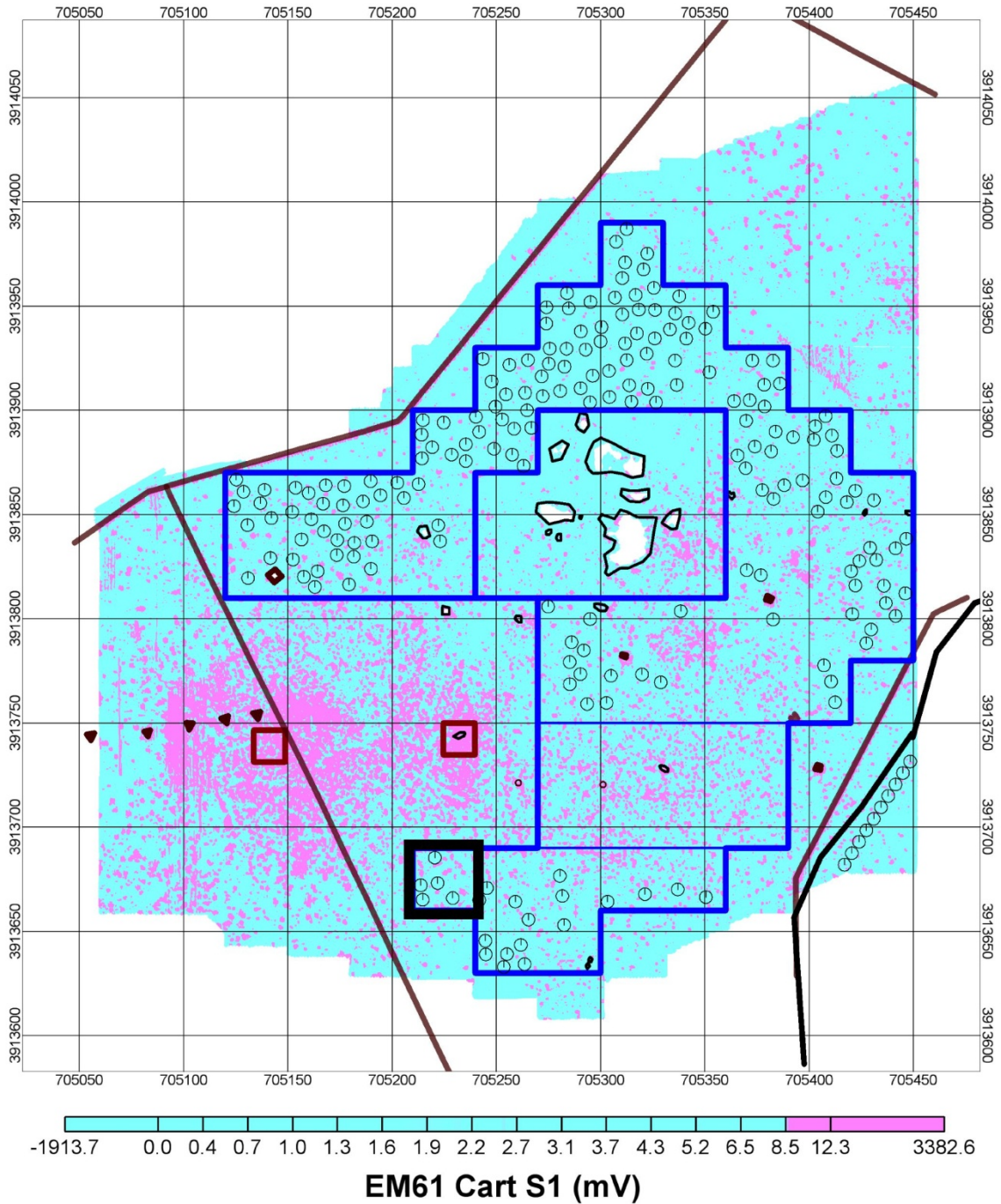


**Figure 5: The thresholded EM61-Mk2 survey map with intended seed locations. Anomaly locations with a first time gate amplitude greater than 8.5 mV are shaded in pink; all other locations are shaded in light blue. Blue lines outline the demonstration area, and the thick black line in the southeast corner indicates a road. Black circles mark the intended seed locations. Two hundred seeds were emplaced in the demonstration area, and 10 seeds formed an instrument verification strip to the southeast of the road.**

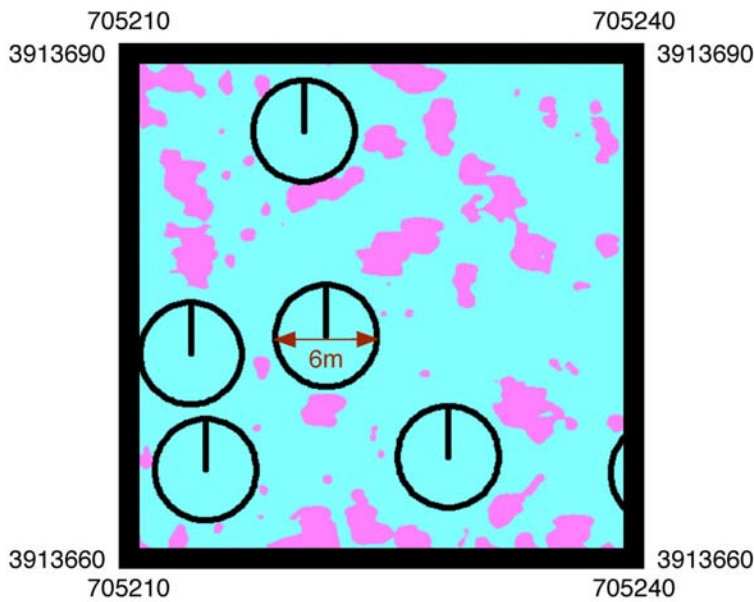


**Figure 6: A close-up of the 30 m x 30 m grid of the thresholded EM61-Mk2 survey map enclosed by the black square in Figure 5. Anomalies are common. Black circles mark the intended locations of five seeds. Each circle has a radius of 3 m. Intended locations are further than 6 m from each other and 3 m from any anomaly.**

A TOI type was then selected for emplacement at each of the 200 seed locations. The Program Office was able to obtain many mortars from munition stores across the United States, but estimated that it would only be able to obtain eleven 2.36 in rockets. Therefore, eleven of the 200 seed locations were randomly selected for the 2.36 in rockets, with the remaining 189 seed locations randomly assigned to 63 each of 60 mm, 81 mm, and 4.2 in mortars.

Next, depths were selected for the 200 seeds in the demonstration area. All seeds were initially assigned an intended depth of 30 cm because no items from the sample excavation areas were buried deeper than 30 cm, and the diggers thought it unlikely items would be buried deeper. However, the program team decided to bury five 60 mm mortars, five 81 mm mortars, and five 4.2 in mortars at 45 cm to provide some deeper targets. No 2.36 in rockets were chosen for a depth of 45 cm because there were so few of them.

Intended azimuth angles were selected for each of the 200 seeds in the demonstration area. Each seed was randomly assigned to 1 of 12 groups, regardless of its munition type. All seeds in the first group were assigned an azimuth angle of zero degrees from magnetic north. The azimuth angle of each subsequent group was incremented by an additional 30 degrees so that all seeds in the 12th group were assigned an azimuth angle of 330 degrees.

Finally, intended inclination angles were selected for each of the 200 seeds. The Advisory Group pointed out that most indirect-fire munitions settle in a downward orientation. Therefore, 140 (70%) seeds were randomly assigned a downward inclination angle, defined as within 45 degrees of pointing straight down. Similarly, 40 (20%) of the remaining seeds were randomly chosen for a “below horizontal” inclination angle, defined as within 45 degrees below horizontal. An “above horizontal” inclination was chosen for the remaining 20 (10%) seeds, defined as within 45 degrees above horizontal. Recognizing that some of the larger seeds could not be buried at a downward inclination angle without part of the seed sticking out of the ground, the inclination angles of all downward 81 mm mortars, 4.2 in mortars, and 2.36 in rockets were reset to below horizontal. Only 60 mm mortars, which were small enough to remain completely buried, were allowed to keep their initially assigned downward inclination angles.

The seed plan instructed the emplacement team to bury each seed as close as possible to its intended location, azimuth angle, inclination angle, and depth. But the plan also allowed for minor deviations, if needed. For example, the plan instructed the emplacement team to inspect the ground at an intended location with a hand-held EMI detection device before emplacing the seed to check for anomalous indigenous items or geology that, for some reason, had failed to appear on the initial EM61-Mk2 survey map. If there were no strong anomalies detected by the hand-held instrument within approximately 3 m of the intended location, the seed plan instructed the emplacement team to proceed with burying the seed. If, however, there was indeed a strong anomaly within 3 m of the intended location, the seed plan instructed the team to choose a nearby location for the seed. In another example, the seed plan instructed the emplacement team to alter the depth and orientation angles of the seed if the intended parameters did not allow at least 10 cm of dirt over the top of the buried seed. These deviations allowed for appropriate seed emplacement.

### **2.5.2 Instrument Verification Strip**

IDA and the Program Office manually selected the intended locations of the 10 seeds in the IVS. The Program Office recommended situating the strip directly across the road running through the southeast corner of the site. As shown in Figure 5, this area exhibited few anomalies representing indigenous items or geology. Furthermore, the data-collection teams could easily access this area with their instruments at the beginning and ending of each day. Based on that guidance, IDA selected a strip of land parallel to and approximately 6 m southeast of the road. The seed plan instructed the emplacement

team to first search for, and clear this strip of, indigenous items and then emplace the 10 seeds 6 m apart from each other along the strip.

TOI locations, depths, azimuth angles, and inclination angles were selected for each of the 10 seeds in the IVS. Two intended locations were chosen for each munition type (60 mm mortars, 81 mm mortars, 4.2 in mortars, and 2.36 in rockets). The remaining two locations were reserved for iron spheres (shot puts). All seeds were assigned a depth of 30 cm. One of each type of TOI was assigned an inclination angle straight down (or as close as possible while still allowing 5 cm of dirt over the top of the buried seed) because downward items generally provide the strongest signal for EMI sensors. The remaining TOI were assigned a horizontal cross-track orientation (an inclination angle directly horizontal and an azimuth angle perpendicular to the length of the strip) because horizontal cross-track items generally provide the weakest signals for EMI sensors.

## **2.6 EMPLACE SEEDS**

The emplacement team followed the instructions contained in the seed plan to emplace seeds at or near their intended locations, depths, and orientation angles, with one exception. Upon the recommendation of the Advisory Group, the Program Office instructed the emplacement team to choose five 60 mm mortars, five 81 mm mortars, and five 4.2 in mortars in the demonstration area with intended depths of 30 cm and, instead, bury them at depths of 45 cm. This doubled the number of each of these TOI types buried at deeper depths. No 2.36 in rockets were chosen for a 45 cm depth because there were so few of them. The emplacement team also made some substitutions into the types of TOI buried each intended location, resulting in fourteen 2.36 in rockets (rather than the intended 11), seventy-six 60 mm mortars (instead of the intended 63), fifty-four 4.2 in mortars (instead of 63), and fifty-six 81 mm mortars (instead of 63).

After emplacing each seed in the ground, but before covering the seed with dirt, the emplacement team recorded the following information:

- The identification number of the seed.
- The TOI type of the seed (e.g., “60 mm mortar,” “4.2 in mortar,” etc.).
- The easting, northing, and height-above-ellipsoid coordinates for the nose, center, and tail of the seed, with a surveyed point on the lip of the hole providing a depth reference.
- The azimuth and inclination angles of the seed.

- A photograph of the seed, with the identification number clearly written on the seed and a ruler clearly placed next to the seed.

Once seeds were emplaced in the ground, data collection could begin.

## **2.7 COLLECT SURVEY DATA**

The data-collection teams surveyed the demonstration area with six different data-collection instruments. This section explains the motivation for selecting the instruments and briefly describes the sensor technology employed by each. More detail can be found in the plans and reports written by the data-collection teams [4, 6, 19, 21].

### **2.7.1 EM61 CART**

The typical EMI instrument used in commercial surveys will be called the “EM61 CART” for the remainder of this document. The EM61 CART consists of a standard EM61-Mk2 sensor mounted on a two-wheel cart. This instrument employs a 1 m × 0.5 m receive coil mounted 30 cm above a second 1 m × 0.5 m coil that transmits as well as receives. The instrument may be set up with four time gates from the lower coil or with three time gates from the lower coil and the first time gate from the upper coil. The classification demonstrators preferred the first option because it provided the maximum temporal extent for assessing the decay characteristics of the components of the polarization tensor.

The operator of the instrument wears a backpack containing the sensor electronics and battery. The data-acquisition system records data (consisting of the four time gates for the lower coil) at a rate of 16 records per second and can store up to 1 million records. In typical commercial surveys, survey lines are often spaced 1 m apart. Because the purpose of this study was to collect high-quality data that could support classification, the operator was instructed to space the survey lines 0.5 m apart. Figure 7 shows the EM61 CART collecting data at San Luis Obispo.

NAEVA Geophysics, Inc., the data-collection team that operated the EM61 CART, employed a Trimble 5700 real time kinematic (RTK) differential global positioning system (DGPS) to track the position of the sensors. Figure 7 shows the DGPS antenna mounted above the center of the sensor coils, the standard configuration.



**Figure 7: A photograph of the EM61 CART collecting data at Camp San Luis Obispo.**

### **2.7.2 EM61 ARRAY**

The Multi-sensor Towed Array Detection System (MTADS), developed by the Naval Research Laboratory, was used to serially collect magnetometer and EMI data at San Luis Obispo. Each sensor mounted on the time-domain EMI version of the MTADS instrument (called the “EM61 ARRAY” for the remainder of this document) is a modification of the standard EM61-Mk2 sensor sold commercially by Geonics, Ltd. While the standard EM61-Mk2 sensor is based on a single  $1\text{ m} \times 0.5\text{ m}$  coil, the modified sensor is based on three  $1\text{ m} \times 1\text{ m}$  coils. The three overlapping  $1\text{ m} \times 1\text{ m}$  coils are mounted on the EM61 ARRAY, as shown in Figure 8.

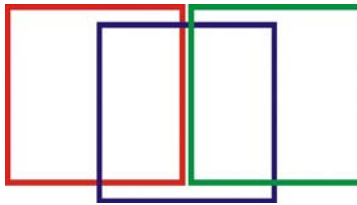


**Figure 8: A sketch of the three overlapping sensor coils mounted on the EM61 ARRAY.**

To maximize their sensitivity, the three transmitting coils are synchronized to provide as large a magnetic moment as possible. Based on the preference of the classification demonstrators, the EM61 ARRAY survey was conducted in four-gate mode, with all gates sampled on the lower coil. The sensors pulse at 75 Hz but do internal stacking and provide an output at 10 Hz, leading to a down-track sample spacing of 15 cm for the typical 1.5 m/s survey speed. Because these are vector sensors, accurate measurement of the orientation of the sensors is necessary for accurate data inversions. Therefore, three RTK DGPS receivers are used to measure both the position and orientation of the sensors at 5 Hz. A Crossbow VG300 inertial measurement unit (IMU)

also outputs the orientation of the sensors at 30 Hz. Figure 9 shows the EM61 ARRAY collecting data at Camp San Luis Obispo.



**Figure 9: A photograph of the EM61 ARRAY collecting data at Camp San Luis Obispo.**

The EM61 ARRAY has some advantages over the EM61 CART. Its three DGPS receivers allow the orientation of the sensor to be measured. Corrections can be made to any errors in the sensor’s measured position caused by the tilting of the entire instrument as it is pulled over steep terrain. The EM61 CART’s single RTK DGPS receiver does not allow such corrections. The EM61 ARRAY also provides three cross-track samples with excellent relative position accuracy. In contrast, the CART’s relative position from survey line to survey line is only as accurate as its DGPS position measurements. However, because the EM61 ARRAY’s three transmit coils fire simultaneously, items near the center of a data line are unlikely to be illuminated by magnetic field components in both horizontal directions. Hence the EM61 ARRAY must make a pair of surveys over an area in orthogonal directions to ensure sufficient information for a reliable inversion.

### **2.7.3 MAG ARRAY**

The magnetometer version of the MTADS instrument will be called the “MAG ARRAY” throughout the remainder of this document. This instrument employs eight Geometrics 822A total-field cesium vapor magnetometer sensors mounted in a linear array with 25 cm spacing. The distance of the sensors above the ground is also approximately 25 cm. The signals measured by the sensors are sampled at 50 Hz, leading to a down-track sample spacing of approximately 6 cm for the typical 3 m/s survey speed. A single RTK DGPS antenna is generally mounted over the center of the array and tracks the position of the sensors at a 5 Hz sampling rate. For this demonstration, however, a pair of DGPS antennas measured the array’s yaw and roll orientation for tilt correction.

(Pitch was neither measured nor corrected, although doing so would most likely have led to a slight improvement in the accuracy of the recorded positions.) A base station receiver placed at a surveyed monument provides DGPS corrections. Figure 10 shows the MAG ARRAY collecting data at San Luis Obispo.



**Figure 10: A photograph of the MAG ARRAY collecting data at Camp San Luis Obispo.**

#### **2.7.4 MSEMS**

Under ESTCP funding, the Man-portable Simultaneous Magnetometer and Electromagnetic System (MSEMS) was developed by Science Applications International Corporation (SAIC) to provide a cart platform capable of collecting both EMI and magnetometer data in a single pass. As shown in Figure 11, this is accomplished by mounting the magnetometer on a boom that places it 4 ft ahead of a standard EM61 Mk-2A coil. The EM61 sensor has standard wheels, so the coil is 40 cm from the ground. Only the lower coil was installed, and data were collected from the lower coil at four time gates. The carbon-fiber boom, supported by a third wheel, gives the Geometrics 822 cesium vapor total field magnetometer an effective height from the ground of 51 cm. Figure 11 shows the MSEMS collecting data at San Luis Obispo.



**Figure 11: A photograph of the MSEM collecting data at Camp San Luis Obispo.**

The MSEM collects data simultaneously by interleaving EMI and magnetometer collections. The EM61 is pulsed at a 75 Hz rate and outputs samples at a 10 Hz rate. For each pulse, after EMI primary field decay and time for the magnetometer output to settle, the magnetometer collects a static magnetic field sample. The MSEM is pushed at a speed of approximately 1 m/s, so with the differences in sample output rate, the EM61 provides a down-track sample spacing of about 10 cm while the magnetometer sample spacing is about 1.3 cm. MSEM also employs RTK DGPS, with a single antenna between the two sensors that can be seen in Figure 11.

NAEVA operated the MSEM at Camp San Luis Obispo with technical assistance from SAIC. The MSEM collected data on all grids that were scored in the demonstration. While Sky Research used the EMI and magnetometer anomaly lists for cooperative inversions (discussed later in this chapter), interference from local geology made the magnetometer data not useful in many areas. However, the MSEM pre-processing team used the magnetometer data to identify some anomalies believed to be deep, large targets. These were later dug, but no metallic objects were found.

### **2.7.5 MetalMapper**

The MetalMapper is an advanced instrument developed under ESTCP funding by Geometrics, Inc., as an enhancement to the Advanced Ordnance Locator system developed earlier by G&G Sciences and tested under Navy funding. Figure 12 shows the MetalMapper deployed on the front lift of a Kubota tractor. The MetalMapper instrument employs three 1 m × 1 m orthogonal transmit coils to illuminate all three target axes and a collection of seven three-axis receive coils arranged along the bottom of the instrument to overlap down-track and cross-track receive samples.



**Figure 12: A photograph of the MetalMapper collecting data at Camp San Luis Obispo.**

At San Luis Obispo, the MetalMapper collected survey data that were then used to identify the locations where it should return to collect high-resolution, cued data. In survey mode, only the horizontal transmit coil (producing a vertically directed magnetic field) is energized, but data are collected on all receive coils. Data are collected at a tractor speed of approximately 0.4 m/s. With a 270 Hz waveform rate and stacking to output data at a 10 Hz rate, this produces data at about a 4 cm along-track separation. Tracks were run with a 0.7 m separation. While the MetalMapper employs only a single RTK DGPS receiver and antenna, it also includes an inertial measurement unit (IMU) that allows data to be tilt corrected.

## **2.8 CORRECT FOR SLOPE**

Survey data were collected by six different sensors at San Luis Obispo: the EM61 CART, the EM61 ARRAY, the MAG ARRAY, the MSEMS EM61 and magnetometer sensors, and the MetalMapper. To produce a master anomaly list, anomaly declarations from the different sensors had to be associated. Because the site was hilly and different instruments surveyed sections in different directions, there was a concern that the combination of the terrain slope and the vertical offset of the GPS antennas from the sensors would result in position errors that would make anomaly association between sensors difficult. The solution to that problem was to slope-correct the data. That could be done with on-board information for the EM61 ARRAY, MAG ARRAY, and MetalMapper systems, which had either multiple GPS antennas or IMUs to detect the sensor orientation. Because the EM61 CART and MSEMS had a single GPS antenna, their data had to be slope-corrected based on a map of terrain slope created from the EM61 ARRAY attitude data in a two-step process [11].

The first step was to create a digital elevation map of the terrain that was free from artifacts caused by small local irregularities. This was accomplished by performing two levels of smoothing on the EM61 ARRAY GPS and IMU data. The first level used the standard Oasis montaj gridding routine to create a minimum-curvature 1 m cell grid. The size was chosen as a compromise between the down-track sample spacing of approximately 0.15 m between points and the cross-track spacing of 1.5 m. The second level of smoothing was accomplished by passing a  $9 \times 9$  cell symmetric convolution filter over the data using a standard Oasis montaj grid filter. The  $9 \text{ m} \times 9 \text{ m}$  area was chosen to encompass several array dimensions to remove any array orientation artifacts from the digital elevation map.

The second step was to calculate directional grid gradients in the positive easting and northing directions from the smoothed digital elevation map using an Oasis montaj gradient routine. This produced a gradient map for each of the two orthogonal directions, and these maps were employed for the slope-correction calculations. To apply the slope correction to the recorded position of the data, the recorded position was used to look up the gradient in each direction, and offsets in the easting and northing directions were calculated using the gradient in that direction and the height of the GPS antenna for the sensor in question. Although an iterative calculation that provided a better slope correction based on the first corrected position could have been used, the average slope correction deltas were less than 0.5 m, and it was felt that a second iteration was not necessary. Slope-corrected data were provided to the classification demonstrators for all the survey instruments and were also used in associating anomalies among the various instruments when producing the master anomaly list.

Once the survey data had been corrected for tilt, individual anomalies could be detected.

## **2.9 DETECT ANOMALIES**

A consistent procedure for anomaly declaration was employed. Anomalies for the EM61 CART were selected by NAEVA, for the MSEMS by SAIC, for the MetalMapper by Snyder Geoscience, and for the EM61 ARRAY and MAG ARRAY by the Program Office team. The major difference between the instruments was the threshold above which an anomaly was declared. This description of anomaly selection focuses on the EM61 ARRAY, MAG ARRAY, and MSEMS, but the procedure for all instruments followed the same path. More detailed information can be found in the data-collection reports for these instruments [6, 21]. Information on the EM61 CART and MetalMapper

anomaly-selection procedures can be found in the data-collection plans and reports for these instruments [4, 19].

Based on the data collected from exhaustive excavation of the sample areas and the recommendation of the Advisory Group, a maximum expected target depth of 30 cm was selected, and a 50% depth margin was applied. To determine the anomaly-detection threshold, we considered the physics-based predictions of the worst-case response (i.e., at the most unfavorable orientation for the instrument) at 45 cm depth from each of the expected munitions items. Figure 13 provides those curves for the EM61 CART and a 60 mm mortar, along with test pit measurements that show the accuracy of the worst-case prediction curves lower bounding the expected response. Note that the second time gate is selected for the plot; that gate was also used for detection processing. While the target signal is stronger in the first gate, the signal-to-noise ratio (SNR) is frequently larger in the second or third gates because of their improved immunity to motion noise.

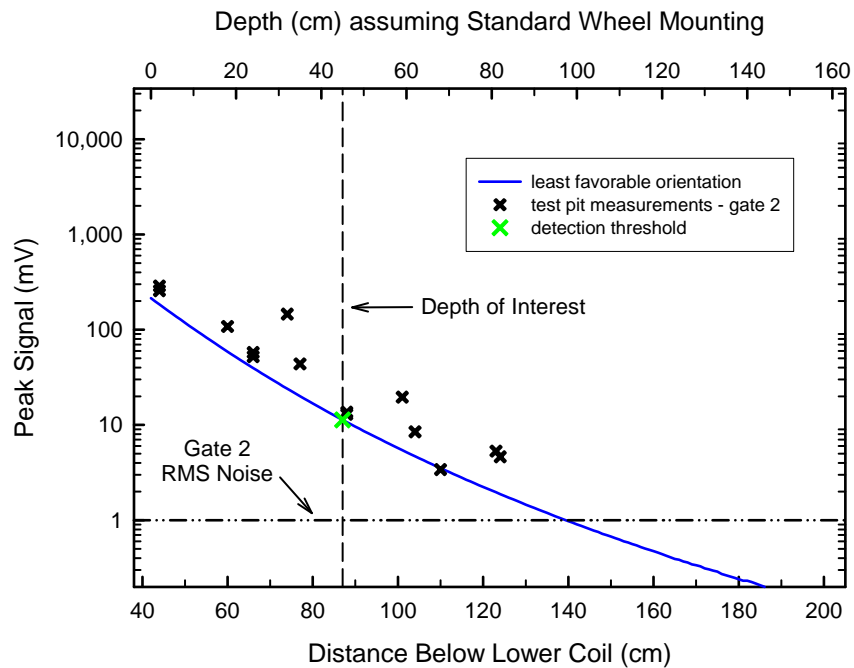


**Figure 13: The expected EM61 CART second time gate amplitude for the most unfavorable orientation as a function of distance below the transmit coil for a 60 mm mortar and measured data from the test pit.**

Given the threshold for a particular instrument, detection processing first consisted of selecting peaks in the gridded data that exceeded the chosen threshold. Other than gridding the data, no data smoothing was performed before anomaly selection. Actual anomaly selection was accomplished using the *gridpeak* function in Oasis montaj.

Once the list of anomalies and their locations was produced, the instrument data were imported into the UX-Analyze module of Oasis montaj so that the anomalies could be inverted using a dipole model. A chip of data surrounding the anomaly peak that encompassed the anomaly was either extracted automatically or a polygon surrounding the desired data was generated manually for data inversion. UX-Analyze provides a picture of the gridded data along with the match data produced by the inversion parameters; fit coherence values; and fit parameters, including the location and depth of the object. The data analyst checks those parameters as part of the overall quality-control process. If the fit location passes the quality check, it is returned as the anomaly location. For items with a poor fit, the grid location of the anomaly peak is returned instead.

For elongated items, particularly those elongated in the down-track direction, EM61-based instruments can provide a double-humped return for a single item. For this experiment, the data analyst looked at all anomalies that were within 0.6 m of each other to determine whether they came from a single item or from multiple closely spaced items. In the cases where it was judged that the returns constituted a single unique anomaly, it was treated as such on the anomaly list.

Determining anomalies for the magnetometer data followed a similar procedure as that for the EM61-based instruments, but there were differences due to the physics that determines the response for the two types of instruments. Magnetometers sense the distortion in Earth's magnetic field due to the presence of a ferrous object. For most target aspects relative to Earth's field, this distortion presents itself as a bipolar field distortion. This field distortion at the instrument can be predicted using physics models analogous to those for the EM61-based instruments. Such models were used to establish the threshold for detection by the magnetometers, using the same 50% depth safety factor as for the EMI case. Actual anomaly detection selection was based on the positive peak of the anomaly, but the anomaly location reported was that given by a dipole inversion.

Adverse geology at the Camp San Luis Obispo site caused the magnetometer threshold to be exceeded in a number of instances, many of which were not near an EMI anomaly. For that reason, the only magnetometer anomalies prosecuted in the excavation phase of the demonstration were those that associated with an EMI anomaly, plus 45 additional excavations for what the MSEM pre-processor felt might be large, deeply buried items. (The demonstrators did not attempt to classify these additional 45 anomalies, however. Furthermore, no metallic items were recovered from these anomalies during excavation.) Because the geology of the site was highly magnetic in

some areas, many more anomalies were detected in the magnetometer-based survey data than in the EM61-based data.

Once the data-collection teams had detected individual anomalies in the survey data, other data-collection teams could collect high-resolution, cued data at individual locations throughout the site.

## **2.10 GENERATE CUED LISTS**

The cued lists provided the data-collection teams with the locations of high-resolution data to be collected with the cued instruments. Three cued lists were formed, one for the TEMTADS, the BUD, and the MetalMapper, the three cued instruments used at Camp San Luis Obispo.

### **2.10.1 TEMTADS**

IDA created the TEMTADS cued list from the EM61 ARRAY anomaly list. The 1464 locations on the TEMTADS cued list corresponded to the 1464 unique anomalies detected by the EM61 ARRAY. The Program Office team fit the data from each EM61 ARRAY anomaly to a dipole model using the UX-Analyze module in Oasis montaj. IDA included an anomaly's fitted location on the TEMTADS cued list if the anomaly's data:

- Exhibited a fit coherence greater than or equal to 0.85, and
- Based on the Program Office team's visual analysis:
  - Fit well to the dipole model,
  - Appeared to represent a single buried item, and
  - Encompassed the complete anomaly.

Conversely, the location of the anomaly's peak signal was included on the TEMTADS cued list, rather than its fitted location, if the anomaly's data:

- Exhibited a fit coherence less than 0.85, or
- Based on the Program Office team's visual analysis:
  - Appeared to fit poorly to the dipole model,
  - Appeared to represent multiple closely spaced items, or
  - Did not encompass the complete anomaly.

### **2.10.2 BUD**

The BUD cued list was a subset of the TEMTADS cued list. BUD remains in the early phase of development, and its large size and weight cause difficulties in

transporting it from one cued location to another, especially over steep terrain. The Program Office decided in advance that the BUD would collect data only at locations with relatively flat terrain. To that end, two contiguous sub-areas of the site that were relatively flat were identified, and all TEMTADS cued locations in these sub-areas were assigned to the BUD cued list. Figure 14 is a topographical map of the site. Blue lines outline the survey area, and the curved light-brown lines indicate topographical contours. Orange dots show locations where both the TEMTADS and BUD collected cued data; all are within relatively flat sub-areas of the site. Purple dots show locations where only the TEMTADS collected cued data; the terrain was quite steep in these locations.

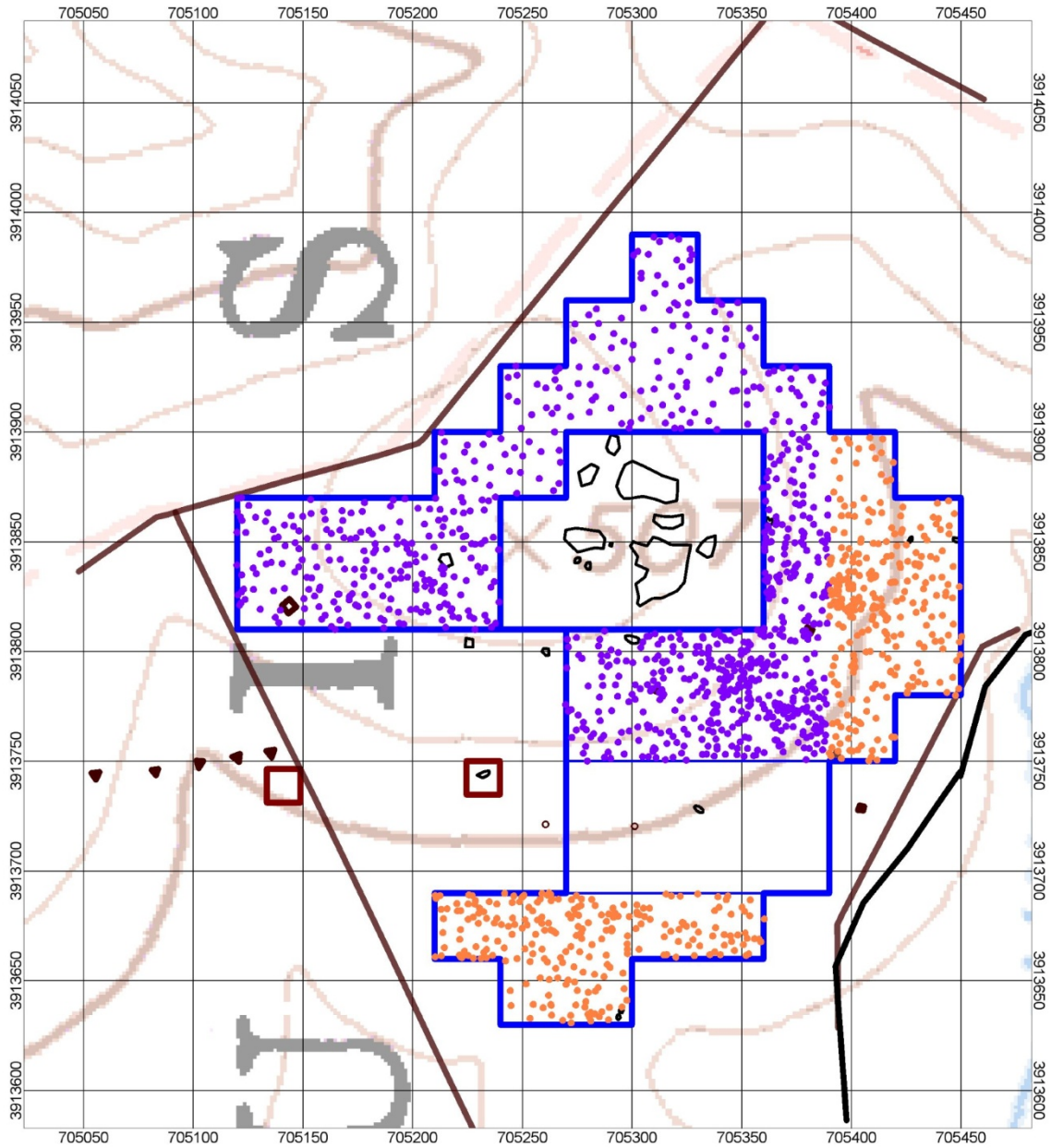


**Figure 14: A topographical map of the selected site with TEMTADS and BUD cued locations. Blue lines outline the demonstration area, and the curved light-brown lines indicate topographical contours with elevation differences of 40 ft. Orange dots show locations where both the TEMTADS and BUD collected cued data; all are within relatively flat sub-areas of the site. Purple dots show locations where only the TEMTADS collected cued data; the terrain was quite steep in these areas.**

### 2.10.3 MetalMapper

The MetalMapper data-collection team created the MetalMapper cued list independently of the TEMTADS and BUD cued lists. As discussed in the data-collection report [19], the data-collection team surveyed the site with the MetalMapper in dynamic

mode. The team detected 1617 unique anomalies in the MetalMapper survey data and included the locations of each of these anomalies on the MetalMapper cued list. Cued data were eventually collected at all 1617 locations on the MetalMapper cued list. But the classification demonstrators processed the data recorded at only 1561 cued locations because 56 locations were not excavated in time to provide ground truth labels used for optimizing the classification algorithms.

## 2.11 COLLECT CUED DATA AT LOCATIONS ON CUED LISTS

In collecting cued data, TEMTADS, BUD, and MetalMapper used different sets of cued locations. This section describes the sensor technology of the instruments. More detail can be found in the reports written by the data-collection teams [5, 14, 19].

### 2.11.1 TEMTADS

TEMTADS, an advanced sensor constructed by the Naval Research Laboratory, is based on the coils and electronics from the Advanced Ordnance Locator system, developed under Navy funding by G&G Sciences. As shown in Figure 15, TEMTADS employs twenty-five 35 cm square sensors arranged in a  $5 \times 5$  array. Each sensor consists of a 35 cm square outside transmit coil and a 25 cm square inner receive coil. The coils are mounted on 40 cm centers, forming a  $2 \text{ m} \times 2 \text{ m}$  array.

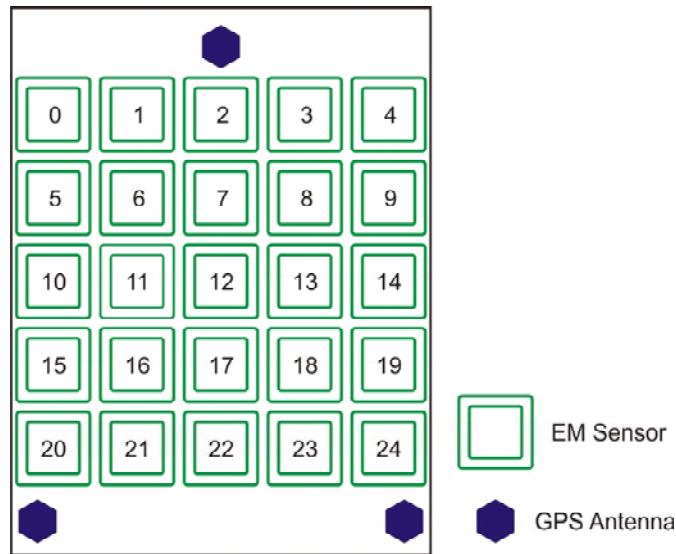


**Figure 15: A sketch of the transmit/receive coils mounted on the TEMTADS.**

Each transmit coil is sequentially pulsed, with the induced secondary field from any item below the array sensed by all 25 receive coils. This arrangement provides spatial transmit and receive diversity, along with the additional information provided by multi-static operation. As a cued sensor, TEMTADS can do sufficient signal stacking to

produce high SNR data. In addition, the increased sensitivity provided by stacking allows extension of the receiver processing time to 25 ms, giving a good sampling of the late-time decay for large, thick-walled objects. Sampling is done at 250 kHz, but data for analysis consist of 115 logarithmically spaced gates covering 40  $\mu$ s to 25 ms.

At Camp San Luis Obispo, TEMTADS collected cued data at all the unique anomaly locations produced from the EM61 ARRAY survey. The procedure was to program anomaly locations into the TEMTADS navigation software, drive the tow vehicle to place the center of the array over the anomaly, collect data, and then move to the next anomaly. Quality control checks were subsequently performed on the collected data to allow anomalies to be revisited if necessary. Figure 16 shows the TEMTADS collecting data at San Luis Obispo.



**Figure 16: A photograph of TEMTADS collecting data at Camp San Luis Obispo.**

### **2.11.2 BUD**

BUD is a next-generation instrument developed by Lawrence Berkeley National Laboratory. Its design and construction were funded by ESTCP and SERDP. BUD is still a developmental instrument and data collection is slow, so it collected data in only the cued mode. Figure 17 shows the BUD collecting cued data at Camp San Luis Obispo. For this collection, the BUD operators chose to collect data at 11 points relative to the flagged anomaly, 5 points at half-meter intervals with the center point over the anomaly, and 3 points in lines offset.



**Figure 17: A photograph of the BUD collecting data at Camp San Luis Obispo.**

The BUD consists of three orthogonal transmit coils and eight pairs of receive coils that are differenced to provide a gradiometer output. The eight pairs of receive coils are mounted diagonally across the upper and lower horizontal transmit coils to provide gradiometric samples along the three axes. In cued mode, the BUD sequentially pulses all three transmit coils to fully interrogate the source of the anomaly. The BUD samples at a rate of 250 kHz and has 35 sample gates logarithmically spaced from 153  $\mu$ s to 1387  $\mu$ s. Because the BUD remains temporarily stationary while collecting data, time is available for data stacking, and motion noise is suppressed. This leads to an improved SNR, which in turn leads to more accurate data inversions.

### **2.11.3 MetalMapper**

For this demonstration, the MetalMapper was self-cued from a list of anomalies detected in the data it collected itself in survey mode. Thus, the MetalMapper demonstration took place independently of the demonstration of the other instruments. In cued mode, the MetalMapper was driven to the anomaly location and lowered so that the bottom skids were on the ground. Data were collected by sequentially exciting each of the three transmitter coils. Data were collected at a 30 Hz rate, and 270 repetitions were stacked for each transmitter to improve SNR.

Once data were collected by all survey and cued instruments, preparations began for excavating each detected anomaly to provide ground truth for scoring.

## **2.12 GENERATE MASTER LIST**

The master list consisted of the union of all survey instruments' anomaly lists and all cued instruments' cued lists. The purpose of the master list was to develop a single

excavation list and to allow for a straightforward scoring process. The master list instructed the classification demonstrators where to extract features from the collected data; the demonstrators then classified each location based on its extracted features. The master list also instructed the excavation team where to recover buried items; the Program Office then assigned one ground truth label to each master location based on the characteristics of its recovered item or items. IDA scored the demonstrators' classification performance by comparing each location's classification output with its ground truth label.

The master list was constructed in three sequential steps. In the initial step, the first 1464 locations on the master list were defined as the 1464 locations on the TEMTADS cued list, corresponding to the 1464 unique anomalies detected by the EM61 ARRAY. In the second step, an additional 355 master locations were taken from the fitted locations of 355 of the 1552 unique anomalies detected by the EM61 CART. These 355 anomalies had fitted locations further than 0.6 m from any of the master locations from the first step. In the third step, an additional 387 master locations were added from 387 of the 1561 unique locations on the MetalMapper cued list. These 387 cued locations were further than 0.6 m from any of the master locations already designated in the first and second steps. The remaining MetalMapper anomalies fell within 0.6 m of a location added to the list in the first or second step. Thus, the master list consisted of a total of 2206 locations (1464 + 355 + 387).

The Program Office briefly considered appending additional locations to the master list in a fourth, fifth, and sixth step. The fourth step would have added an additional 614 master locations from 614 of the 2316 unique EM61 MSEMS anomalies whose fitted locations were further than 0.6 m from any of the master locations created in the first three steps. The Program Office quickly abandoned this idea due to the prohibitive cost of recovering items from over 600 additional locations. The fifth and sixth steps would have added master locations from MAG MSEMS and MAG ARRAY anomalies whose fitted locations were further than 0.6 m from any previously formed master location. This idea was also abandoned because the magnetic geology of some areas of the site made magnetometer-based survey instruments unsuitable for anomaly detection.

IDA associated each of the 2206 master locations with one or more instruments, with the exception of the MetalMapper. Specifically, a master location was associated with a cued instrument if the instrument collected cued data within 0.6 m of the master location. Similarly, a master location was associated with an EM61-based survey

instrument if there was at least one anomaly detected by the instrument whose fitted location was within 0.6 m of the master location. The same approach could not be used to associate master locations with magnetometer-based survey instruments, however, because the magnetometer-based surveys led to the detection of many overlapping anomalies. Therefore, a master location was associated with the MAG ARRAY if it had already been associated with the EM61 ARRAY. Similarly, master locations were associated with the MAG MSEMS sensor if they were already associated with the EM61 MSEMS sensor. No master locations were associated with the MetalMapper because the MetalMapper classification demonstration was held independently of the rest of the study. The table in Appendix A shows the number of locations associated with each instrument.

Once the master list was created, the classification demonstrators could begin processing data at each location on the master list.

### **2.13 SELECT SURVEY DATA AT LOCATIONS ON MASTER LIST**

Data collected with cued instruments differ in nature from data collected with survey instruments. A cued instrument collects many individual sets of data, with each set collected over one location on the instrument's cued list. In contrast, a survey instrument collects a single large set of data over the entire demonstration area of the site. In this study, the classification demonstrators had to select from this large set of survey data many individual smaller subsets of data, with each subset corresponding to one location on the master list. This process was one of the most subjective steps in the entire study.

The demonstrators selected survey data around individual master locations. First, they visually analyzed the survey data surrounding each master location associated with a given instrument. Then, they selected a polygon circumscribing the master location. The polygon was intended to capture only those data points representing the detected anomaly, so that only the data representing the anomaly, rather than background, would be analyzed further. For master locations associated with more than one survey instrument, the demonstrators selected different polygons for different instruments because the data collected by some instruments were of a higher resolution or SNR than the data collected by other instruments.

While the demonstrators were analyzing the collected data, the Program Office was taking steps to assign ground truth labels to the collected data.

## **2.14 EXCAVATE**

The excavation team recovered all items buried at the master locations. The purpose of the excavation was to gather ground truth information that could be used to score the output of the demonstrators' classification analyses. As it turned out, multiple items were recovered from some master locations, while no items were recovered from other locations. Upon uncovering an item, but before removing it from the ground, the excavation team cataloged the following information:

- The easting, northing, and depth coordinates for the center of the item, with depth measured with respect to a surveyed point on the lip of the hole.
- A description of the item (e.g., "60 mm mortar," "fin parts," "scrap metal," etc.).
- A photograph of the item, with a ruler and a small white board clearly placed next to the item. The excavation team wrote the master location's identification number on the white board. Figure 18 shows photographs of different recovered items.

The excavation team recovered all 200 seeds that had been emplaced in the survey area, along with hundreds of clutter items (including parts of previously exploded munitions), as well as 44 intact or nearly intact munitions that were indigenous to the site. Some of these indigenous munitions—one 5 in rocket, one 3 in Stokes mortar, and one 37 mm round—were unexpected because historical records did not indicate that these types of munitions had been fired at the site.

## **2.15 ASSIGN GROUND TRUTH LABELS**

The Program Office and IDA assigned a single ground truth label to each master location, as well as to each MetalMapper cued location. Each label was based on the characteristics of the item or items recovered at the location.

### **2.15.1 Master Locations**

The Program Office assigned one ground truth label to each location on the master list. Specifically, a location was labeled as "TOI" if any item recovered from the location was a seed; an intact munition indigenous to the site; or any item that a reasonable individual might suspect to be an explosive munition, based on the excavation team's description and photograph of the item. Conversely, a master location was labeled as "non-TOI" if no items recovered from the location met these criteria. In addition, all locations labeled as "TOI" were further labeled by type (e.g., "60 mm mortar," "81 mm

mortar,” etc.). As it turned out, no more than one TOI was recovered from any one location.

Some locations were difficult to label. The Program Office questioned whether a reasonable individual might suspect some partial munitions to be explosive, such as those shown in Figure 19. To settle the matter, photographs of questionable items recovered were gathered from locations that had been assigned to the Standard Training Set. (The training and test sets will be discussed later in this chapter.) These photographs were presented to both the Advisory Group and the classification demonstrators, and these groups were asked for their opinion. After much debate, the Program Office, the Advisory Group, and the classification demonstrators labeled each questionable location in the training set as “TOI” or “non-TOI.” For example, they labeled the training set location in Figure 19(a) as “TOI,” since they believed a reasonable individual would suspect the item to be an explosive munition. Much of this was because the item still retained many of its fins, which can appear dangerous to a reasonable, yet untrained, individual. The Program Office then applied the same logic to each questionable location in the test set, labeling each of these as “TOI” or “non-TOI” in a manner consistent with the training set. (The Program Office did not ask for the demonstrators’ opinions regarding the questionable locations in the test set because the demonstrators remained blind to the ground truth labels in the test set throughout the course of the study.) For example, the Program Office labeled the test set location in Figure 19(b) as “TOI” because the recovered item resembled the item shown in Figure 19(a).



Figure 18: Photographs of recovered items, including (a) a 60 mm mortar, (b) an 81 mm mortar, (c) a 4.2 in mortar, (d) a 2.36 in rocket, (e) a 5 in rocket, (f) a 3 in Stokes mortar, (g) a 37 mm round, and (h) scrap metal from a previously exploded munition.



**Figure 19: Photographs of questionable items excavated from (a) a training set location and (b) a test set location. After much debate, the Program Office, the Advisory Group, and the classification demonstrators labeled the training set location in (a) as “TOI” because they believed a reasonable individual would suspect the recovered item to be an explosive munition. To maintain consistency, the Program Office also labeled the test set location in (b) as “TOI” because the recovered item bore a close resemblance to the item shown in the first photograph.**

The Program Office erred on the side of caution when assigning ground truth labels to questionable locations, more often labeling a questionable location as “TOI” than as “non-TOI.” In a real-world situation, a partial munition that remained in the ground poses no true threat to public safety since it can no longer explode. But a reasonable individual who found the munition could perceive it as a threat, leading to costs associated with public relations and any potential police or explosive ordnance disposal response to 911 calls.

### 2.15.2 MetalMapper Cued Locations

IDA also assigned a single ground truth label to each MetalMapper cued location. The MetalMapper demonstration occurred independently of the other parts of the study, and not all MetalMapper cued locations mapped directly to a master location. Therefore, for each MetalMapper cued location, all master locations within 0.6 m of the cued location were identified. Most cued locations had only one master location within 0.6 m. These cued locations were assigned the ground truth label of the associated master location. However, some cued locations had more than one master location within 0.6 m. Only one of the associated ground truth labels were assigned to each of these cued locations, with TOI taking precedence over non-TOI. As it turned out, no cued locations were associated with more than one master location labeled as TOI.

While the Program Office and IDA assigned ground truth labels to the master locations and MetalMapper cued locations, the classification demonstrators were further analyzing the data collected at these locations.

## **2.16 FEATURE EXTRACTION**

The classification demonstrators processed the data collected at each location associated with a given instrument. First, the demonstrators classified each location as “Can Analyze” or “Cannot Analyze.” Then, they extracted features from the “Can Analyze” locations; most demonstrators extracted these features by fitting the collected data to a dipole model. Finally, they selected a subset of the extracted features on which further, more specific classification could be based.

### **2.16.1 Classify “Can Analyze” and “Cannot Analyze” Locations**

The demonstrators classified a given location as “Can Analyze” or “Cannot Analyze” based on the quality of data recorded at that location. The data recorded from most instruments at most locations were of sufficient quality for accurate feature extraction. In these cases, the demonstrators classified the locations as “Can Analyze.” In contrast, the data recorded by some instruments at some locations suffered from geolocation errors, spotty coverage, low data density, or low SNR, making it difficult, if not impossible, to extract accurate features. In such cases, the demonstrators classified these locations as “Cannot Analyze.”

Different demonstrators used different criteria for making the “Can Analyze” or “Cannot Analyze” classification. While some demonstrators used quantitative criteria, such as the fit coherence or a similar measure of how well the collected data fit to a dipole model, other demonstrators used subjective criteria, such as visual analysis of the collected data. Furthermore, in many cases, the same demonstrator classified a location as “Can Analyze” based on one instrument’s data but as “Cannot Analyze” based on another instrument’s data because different instruments have different resolutions, SNRs, etc.

### **2.16.2 Extract Features From “Can Analyze” Locations**

The demonstrators extracted features from each location classified as “Can Analyze.” Most demonstration teams extracted geophysical parameters, estimating the characteristics of the item(s) that were likely to be buried at the location, based on a dipole model of the data collected at the location. In contrast, some demonstration teams extracted features that were related to direct measurements of the collected data itself.

#### **2.16.2.1 Extract Features: Geophysical Parameters of Dipole Models**

To estimate parameters of the item(s) buried at a location, demonstrators input the data collected at the location into a geophysical inversion computer routine. This routine

fit the data to a dipole model. Parameters of the best fit dipole model were then used in classification processing.

Different demonstration teams used different inversion routines. Some routines assumed that only a single item was buried at each location, an assumption that was not always true. Other demonstrators used more complex routines that estimated the number of buried items as well as their parameters. Despite their differences, however, all inversion routines estimated intrinsic and extrinsic parameters of the buried item(s). Extrinsic parameters included a buried item's easting and northing coordinates, as well as its orientation angles and depth. Intrinsic parameters included characteristics of the buried item—size, shape, material composition, and wall thickness—regardless of where or how the item was situated. The data-processing demonstrators designed their classification algorithms to exploit the known differences in intrinsic parameters between TOI and non-TOI.

Inversion routines operating on EMI data can estimate many intrinsic parameters. For example, the inversion routines applied to standard EM61-Mk2 sensor data estimate the polarizability of the buried item along each of its three major axes ( $\beta_1$ ,  $\beta_2$ ,  $\beta_3$ ) at three or four different time gates. The amplitudes of the polarizabilities indicate the item's size, and their relative amplitudes with respect to each other indicate the item's shape. TOI tend to be ferrous bodies of revolution with one large axis and two equal, smaller axes. In contrast, non-TOI, such as munitions debris and cultural items, can be very small and are not often bodies of revolution. More advanced EMI sensors, such as those used on the TEMTADS and MetalMapper, sample the received signal at later time gates than the standard EM61-Mk2. Their inversion routines estimate the polarizabilities of the buried item over a longer span of time, such that the polarizabilities' decay rates ( $\tau$ ) can be estimated. Decay rates indicate the item's material composition and wall thickness, with TOI tending toward thicker walls than non-TOI.

Inversion routines applied to magnetometer data can estimate fewer intrinsic parameters. To estimate the three polarizabilities of a buried item—that is, to estimate its shape as well as its size—the item must be illuminated and sampled from three orthogonal directions. Magnetometers cannot always accomplish this because they rely on Earth's magnetic field to illuminate the item; there is no assurance that this field will sufficiently illuminate all three axes of the item at once (e.g., if an item was aligned with Earth's magnetic field, no information about the other two axes could be estimated). Magnetometers can only estimate the item's magnetic moment (induced plus remanent) which gives the item's effective size in the illumination direction only.

“Cooperative” inversions can also be performed using EMI and magnetometer data recorded at the same location. Although EMI inversions provide more information than magnetometer inversions, magnetometer inversions often lead to more accurate depth estimates. Cooperative inversions enjoy the advantages of both. Demonstrators first invert the magnetometer data to estimate the buried item’s depth as accurately as possible. Then, they invert the EMI data with the depth parameter of the EMI dipole model constrained to the value previously estimated using the magnetometer model. Constraining the value of one parameter reduces the number of degrees of freedom of the EMI model. If the parameter is constrained to an accurate value, the reduction in the number of degrees of freedom increases the likely accuracy of the other estimated parameters. One demonstration team, Sky Research, performed cooperative inversions in this study using the EM61 and MAG MSEM data. Other demonstrators chose not to perform cooperative inversions because the highly magnetic geology of the site made the magnetometer data difficult to analyze.

#### **2.16.2.2 Extract Features: Data-Driven**

Some demonstration teams did not estimate the characteristics of the item buried at a location. Instead, they measured the characteristics of the anomaly to which the buried item gave rise. Examples of these measurements include the peak amplitude of the anomaly, the footprint area of the anomaly, and the time decay of one channel of data recorded at the anomaly (rather than the time decay of a polarizability parameter of a dipole model that was fitted to the data). Unlike the geophysical parameters resulting from dipole model inversions, these data-driven features do not directly describe the intrinsic parameters of the buried item(s). Some have hypothesized that these data-driven features can still be used for accurate classification, however.

#### **2.16.3 Selecting a Subset of Features**

For a given instrument, the demonstrators chose a subset of the extracted features likely to best exploit the known differences between TOI and non-TOI locations. The demonstrators formed a feature vector from the chosen subset, with each element of the vector holding one of the chosen features. Some demonstrators chose a very simple subset consisting of a single feature only, such as the magnetic moment or the principal polarizability at one time gate. This resulted in a one-dimensional feature vector. Other demonstrators chose more complex subsets consisting of multiple combinations of multiple parameters, such as the ratio of a polarizability decay rate to the polarizability

amplitude. This resulted in a multidimensional feature vector. In either case, the demonstrators used the feature vectors to further classify the locations.

Before classification could proceed further, however, the collected data were separated into training and test sets.

## **2.17 ASSIGN TRAINING AND TEST SETS**

IDA assigned each master location and each MetalMapper cued location to either a Standard Training Set or Standard Test Set. Training and test sets serve complementary purposes. A training set allows demonstrators to optimize their classification algorithms using a subset of data labeled with ground truth. To that end, the Program Office released to the demonstrators all ground truth information related to the Standard Training Set locations so that the demonstrators could use these labels to optimize their algorithms. (Demonstrators could also choose to use the data and ground truth labels from the TOI seeded in both the IVS and the test pit.) The Standard Test Set allows demonstrators to test their optimized algorithms by applying the algorithms to the remaining, unlabeled data. As such, the Program Office did *not* release ground truth information related to the Standard Test Set locations. In this way, the demonstrators' analyses of the Standard Test Set locations were kept "blind."

### **2.17.1 Standard Training Set and Standard Test Set**

Most demonstrators used the Standard Training Set and Standard Test Set to optimize and test their classification algorithms. The survey site consisted of forty-five 30 m × 30 m grids. IDA selected six of these grids and assigned to the Standard Training Set all locations residing in these grids. All remaining locations were assigned to the Standard Test Set. The six Standard Training Set grids were selected from different sub-areas of the site. (Two of the six grids were located in the sub-areas of the site over which the BUD collected data, shown in Figure 14. This was done such that the training data available for BUD-related analyses were a subset of the training data used for all other instruments' analyses.) Figure 20 shows a topographical map of the site with master locations plotted as dots. (Only those master locations associated with the EM61 ARRAY are shown.) Those locations residing in the Standard Training Set grids are colored in red and green, depending on their ground truth label. The locations residing in the Standard Test Set grids are colored in black, regardless of their ground truth label.

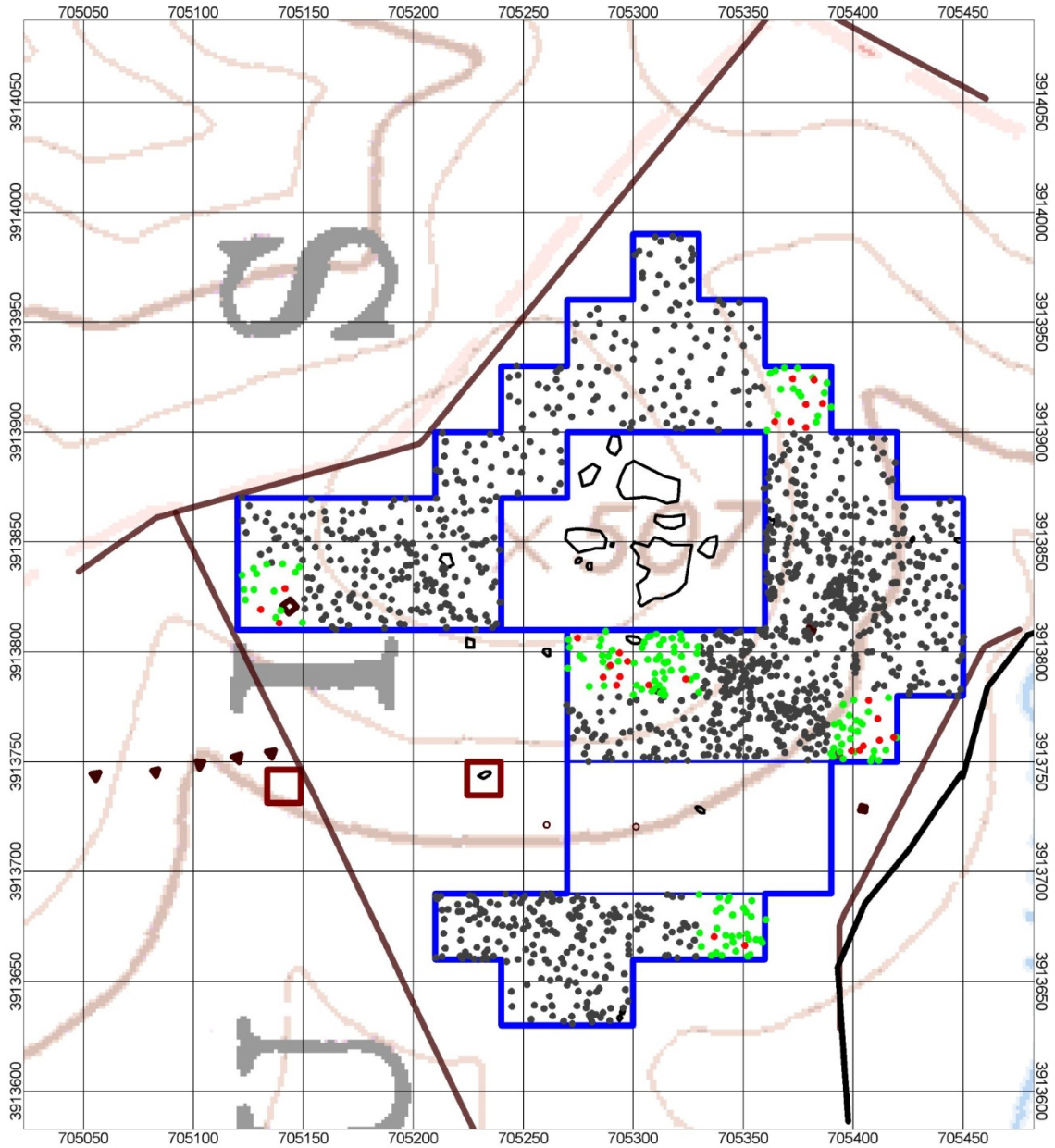


**Figure 20: A topographical map of the site with master locations associated with the EM61 ARRAY in the Standard Training Set and Standard Test Set. The blue lines outline the demonstration area. Red and green dots mark the true TOI and non-TOI locations in the Standard Training Set. Black dots mark the locations in the Standard Test Set, regardless of ground truth label.**

Unlike most demonstrators, Signals Innovations Group (SIG) used both traditional and novel techniques for training and testing their classification algorithms. The traditional technique was supervised learning; like the other demonstrators, SIG optimized its algorithms using the ground truth labels in the training set and then applied the optimized algorithms to the test set. The novel technique was semi-supervised

learning. With semi-supervised learning, SIG optimized its algorithm using labeled data from the training set, as well as unlabeled data from the test set. Then, SIG tested the optimized algorithm by applying it to *only* the unlabeled data in the test set.

### **2.17.2 Active Learning Training and Test Set**

SIG also used active learning [12]. Active learning, an alternative approach for constructing a training set, is used in conjunction with either supervised or semi-supervised learning techniques. With active learning, the training set is *not* determined in advance. Instead, all locations are initially unlabeled, and the demonstrators use information-theory metrics to identify from which locations the optimization could benefit most if ground truth labels were assigned. Ground truth labels are made available for these locations, and the algorithm is optimized (using either supervised or semi-supervised techniques). The process iterates several times until a second information-theory metric notes that little further benefit can be gained by recovering additional items.

With active learning, then, SIG itself assigned locations to the Active Learning Training Set, with all remaining locations assigned to the complementary Active Learning Test Set. SIG performed this task twice, creating one Active Learning Training Set for the EM61 ARRAY and another for TEMTADS. The two Active Learning Training Sets differed because the two instruments' data differed in resolution, SNR, etc., causing the information-theory metrics to recommend different locations on which to train. Figure 21 and Figure 22 are topographical maps of the site, with dots showing the master locations associated with the EM61 ARRAY and TEMTADS, respectively. The Active Learning Training Set locations are colored in red and green for TOI and non-TOI, respectively. Regardless of their ground truth label, the Active Learning Test Set locations are colored in black.

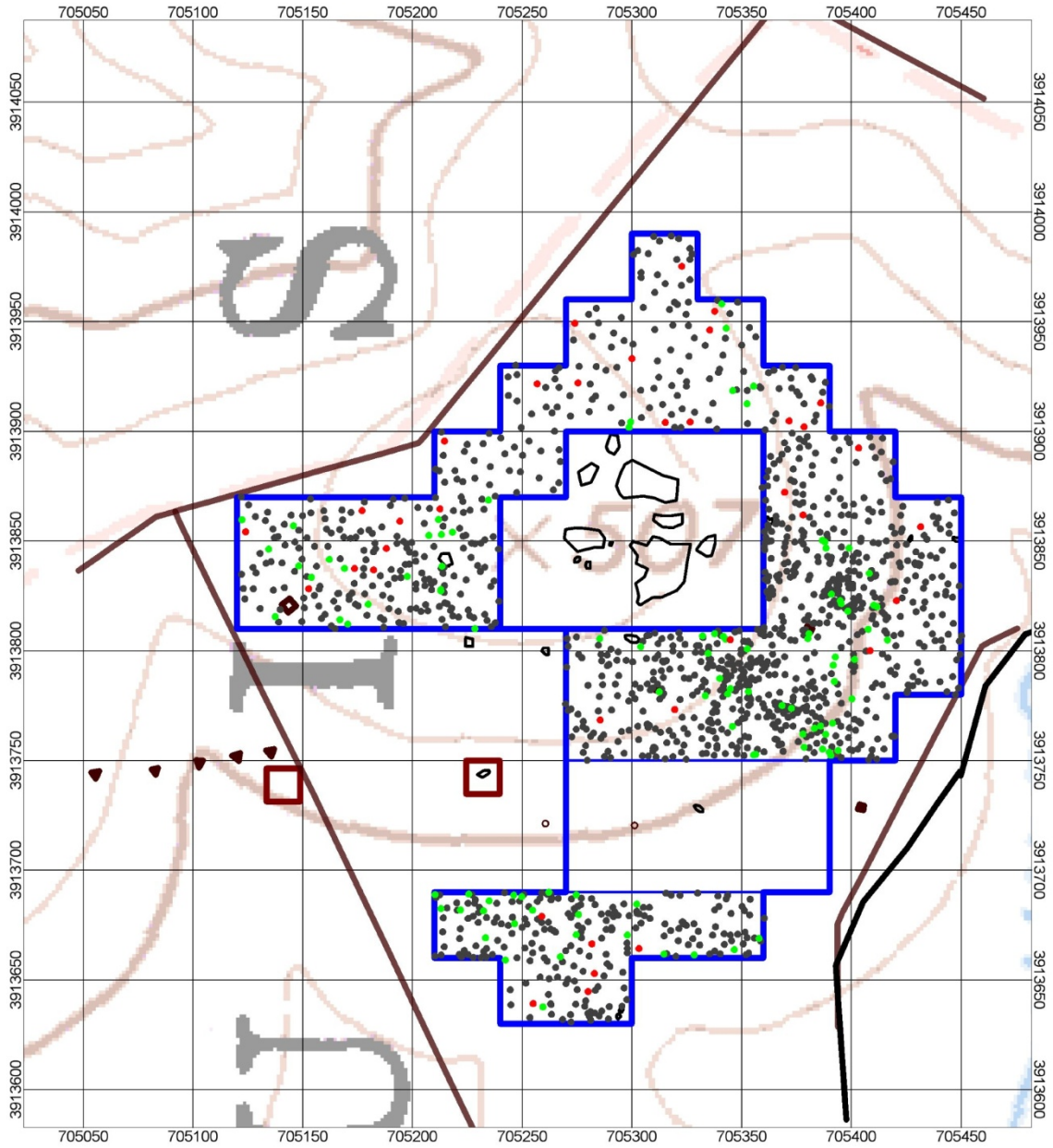


**Figure 21: A topographical map of the site with master locations in SIG's Active Learning Training Set and Active Learning Test Set for the EM61 ARRAY. The blue lines outline the demonstration area. Red and green dots mark true TOI and non-TOI locations in the Active Learning Training Set. Black dots mark locations in Active Learning Test Set, regardless of ground truth label.**

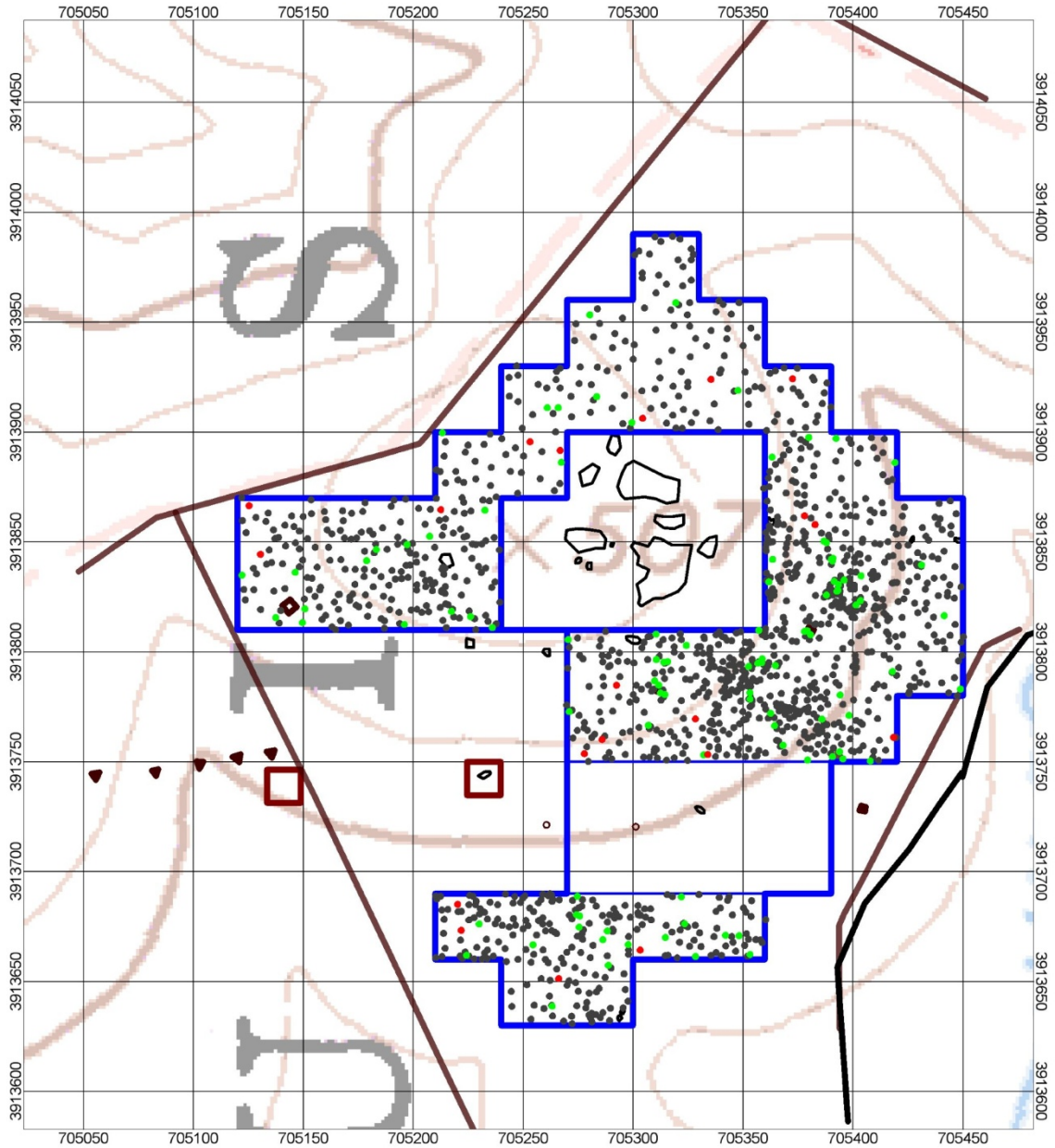


**Figure 22: A topographical map of the site with master locations in SIG’s Active Learning Training Set and Active Learning Test Set for the TEMTADS. The blue lines outline the demonstration area. Red and green dots mark true TOI and non-TOI locations in the Active Learning Training Set. Black dots mark locations in Active Learning Test Set, regardless of ground truth label.**

### 2.17.3 Extended Training and Test Set

RML Technologies compared two different sets to train and test its classification algorithm [3]. First, RML used supervised learning to optimize its algorithm using the Standard Training Set and then tested the algorithm using the Standard Test Set. RML also requested the ground truth labels of approximately 200 additional locations and

formed an Extended Training Set from all labeled locations—those in the Standard Training Set along with the additional 200 locations. The unlabeled locations formed the complementary Extended Test Set. (Note that the Extended Training Set was larger than the Standard Training Set, and the Extended Test Set was smaller than the Standard Test Set.) RML used supervised learning to re-optimize the algorithm, this time using the Extended Training Set, and retested the algorithm, this time using the Extended Test Set. Figure 23 is a topographical map of the site. Locations plotted in red and green belong to the Extended Training Set; locations plotted in black belong to the Extended Test Set.

#### **2.17.4 The Second-Pass Training and Test Set**

Finally, the U.S. Army Corps of Engineers, Huntsville Center (CEHNC) used a two-pass method for training and testing [23, 24] that mimicked what could occur in a real-world scenario. In a real-world scenario, an excavation team must classify locations into two categories, those where “items must be recovered” and those where “items may remain in the ground.” In its first pass at classification, CEHNC trained and tested its classification algorithm using supervised learning and the Standard Training Set and Standard Test Set. Then, CEHNC requested the ground truth labels for all locations in the Standard Test Set that it had classified as “items must be recovered” in its first pass. Only some of these locations were true TOI; others were true non-TOI. Based on these additional ground truth labels, CEHNC revisited the classification of all locations in the Standard Test Set for which it did not yet know ground truth (those items classified as “items may be left in the ground” during their first pass). CEHNC reclassified some of these locations in the second pass, but it was not allowed to reclassify any of the locations for which ground truth was already known. These locations remained, rightly or wrongly, in the “items must be recovered” category.

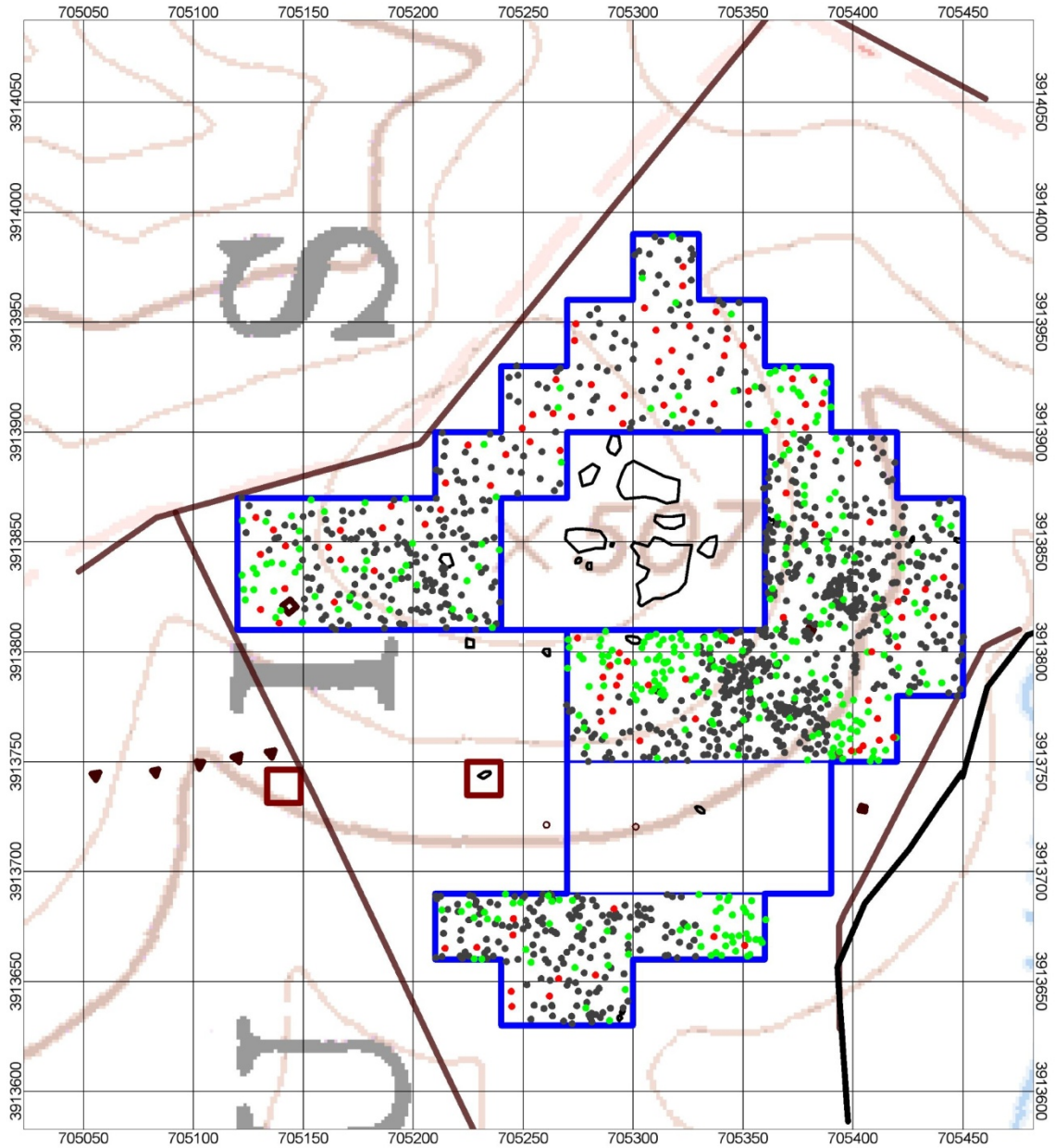


**Figure 23: A topographical map of the site with master locations in RML's Extended Training Set and Extended Test Set for the EM61 ARRAY. The blue lines outline the demonstration area. Red and green dots mark true TOI and non-TOI locations in the Extended Training Set. Black dots mark locations in the Extended Test Set, regardless of ground truth label.**

Figure 24 shows a topographical map of the site. Red and green dots indicate all locations where ground truth was available on the second pass of classification. These include all locations in the Standard Training Set and all locations in the Standard Test Set classified as "items must be recovered" on the first pass. Black dots indicate those locations where the ground truth was not yet known, which CEHNC revisited in its

second pass at classification. Note, however, that although CEHNC revisited only these locations in the second classification pass, the second-pass classification performance was scored over *all* locations in the Standard Test Set.

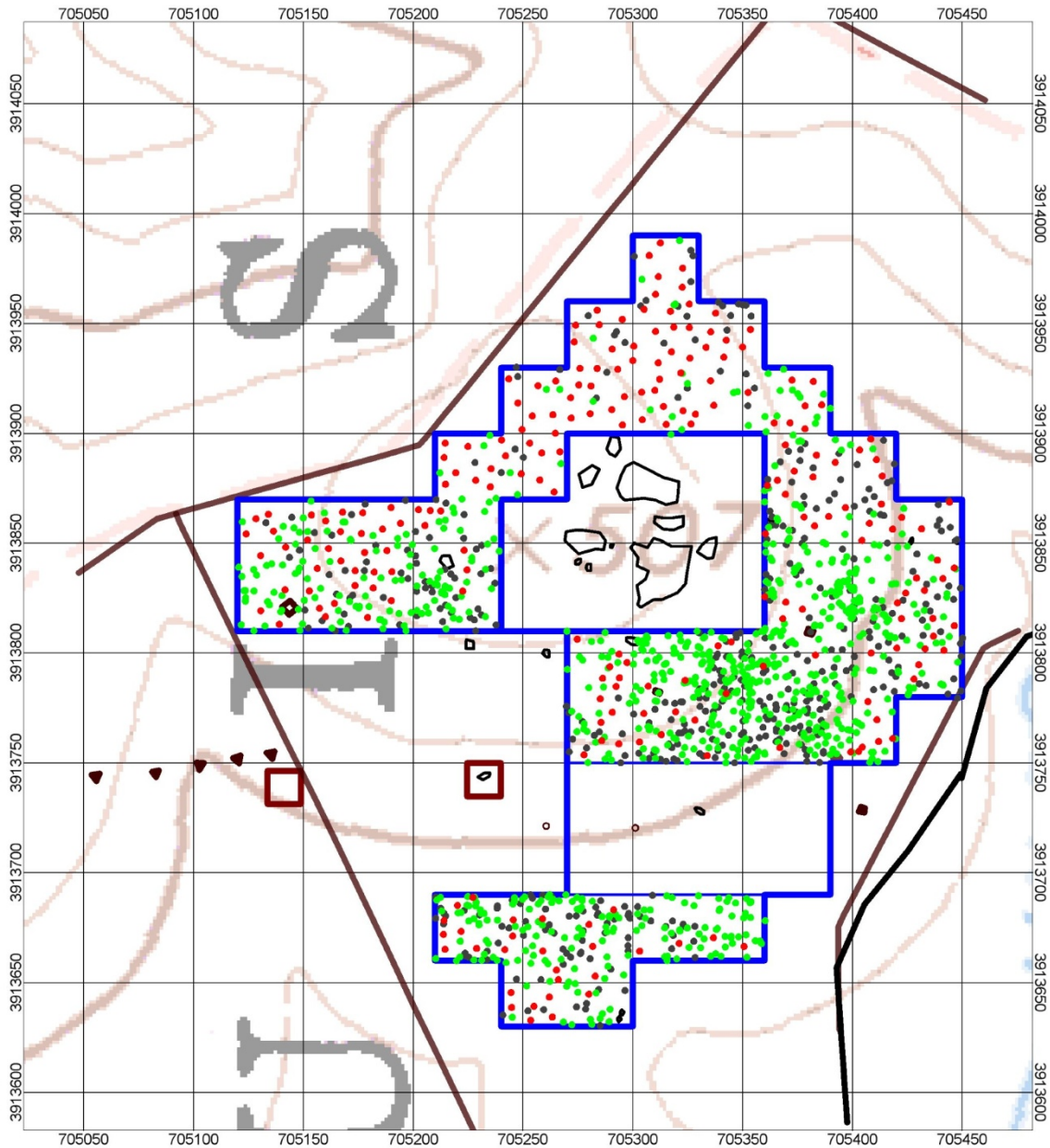


**Figure 24: A topographical map of the site with master locations in CEHNC’s Second-Pass Training Set for the EM61 CART. The blue lines outline the demonstration area. Red and green dots and mark true TOI and non-TOI locations in the Second-Pass Training Set. Black dots mark the remaining locations whose classifications were revisited in the second classification pass.**

The five training sets differed in size and character, as shown in the table in Appendix A. For example, SIG’s active learning used the smallest training sets, with the

TEMTADS' Active Learning Training Set consisting of the fewest true TOI locations. CEHNC's Second-Pass Training Set was the largest training set—ground truth labels were available for all locations in the Standard Training Set and locations in the Standard Test Set labeled as “items must be recovered” during the first pass of classification. Finally, as can be seen from Figure 20–Figure 24, the locations in the Standard Training Set were clustered into six 30 m × 30 m grids, but the locations in the other four training sets were distributed more evenly throughout the site.

## **2.18 CLASSIFY PARAMETERS**

The classification demonstrators designed algorithms to process the feature vectors extracted from the collected data. Different demonstrators used different algorithms. While some demonstrators used simple, rule-based algorithms based on quantitative thresholds defined by expert knowledge, others used more complex algorithms based on statistical classifiers or template matchers. In either case, the demonstrators extracted a feature vector from the data collected at a location and input the feature vector into the classification algorithm. The algorithm then output the location's estimated likelihood of containing TOI, or another similar decision statistic. The demonstrators used the decision statistics to construct a ranked anomaly list. A ranked anomaly list is an ordered list of all locations that were associated with a particular instrument and assigned to the applicable test set. Each demonstration team formed one ranked anomaly list for each combination of data-collection instrument and classification algorithm. Figure 25–Figure 27 show cartoons of a ranked anomaly list in various stages of construction.

In the first stage of constructing a ranked anomaly list, the demonstrators ranked the test set locations that had been classified as “Can Analyze.” The ranks were based on the decision statistics estimated by the classification algorithm, from least likely to contain TOI to most likely, as shown in Figure 25.

In the second stage of constructing a ranked anomaly list, the demonstrators further classified the “Can Analyze” test set locations. As shown in Figure 26, those locations with a low estimated likelihood of containing TOI were classified as “Likely to Contain Only Non-TOI” (green) and locations with a high estimated likelihood of containing TOI were classified as “Likely to Contain TOI” (red). Those locations with neither a high nor low estimated likelihood were classified as “Cannot Decide” (yellow).

Identification Number	Decision Statistic	Rank	Category
2	1.00	1	Can Analyze
700	0.99	2	Can Analyze
91	0.97	3	Can Analyze
1256	0.96	4	Can Analyze
2	0.90	5	Can Analyze
531	0.87	6	Can Analyze
975	0.77	7	Can Analyze
9	0.75	8	Can Analyze
483	0.71	9	Can Analyze
99	0.70	10	Can Analyze
86	0.67	11	Can Analyze
432	0.59	12	Can Analyze
785	0.31	13	Can Analyze
942	0.20	14	Can Analyze
69	0.12	15	Can Analyze

**Figure 25: A cartoon of a ranked anomaly list in its first stage of construction. “Can Analyze” locations in the test set are ranked in ascending order according to their estimated likelihoods of containing TOI, or a similar decision statistic.**

Identification Number	Decision Statistic	Rank	Category
2	1.00	1	Can Analyze: Likely To Contain Only Non-TOI
700	0.99	2	Can Analyze: Likely To Contain Only Non-TOI
91	0.97	3	Can Analyze: Likely To Contain Only Non-TOI
1256	0.96	4	Can Analyze: Likely To Contain Only Non-TOI
2	0.90	5	Can Analyze: Likely To Contain Only Non-TOI
531	0.87	6	Can Analyze: Cannot Decide
975	0.77	7	Can Analyze: Cannot Decide
9	0.75	8	Can Analyze: Cannot Decide
483	0.71	9	Can Analyze: Cannot Decide
99	0.70	10	Can Analyze: Cannot Decide
86	0.67	11	Can Analyze: Likely To Contain TOI
432	0.59	12	Can Analyze: Likely To Contain TOI
785	0.31	13	Can Analyze: Likely To Contain TOI
942	0.20	14	Can Analyze: Likely To Contain TOI
69	0.12	15	Can Analyze: Likely To Contain TOI

May leave items in the ground  
**Don't Dig Threshold**  
 Must recover items from the ground

**Figure 26: A cartoon of a ranked anomaly list in its second stage of construction. “Can Analyze” locations in the test set are further classified into three different subcategories based on their estimated likelihoods of containing TOI, or another similar decision statistic. Locations classified as “Likely to Contain Only Non-TOI,” “Cannot Decide,” or “Likely to Contain TOI” are shown in green, yellow, and red, respectively. A thick blue line indicates the “don’t dig threshold,” the boundary between the green and yellow locations. In a real-world scenario, the excavation team would begin recovering items from locations at the bottom of the list and work its way up until it reached the “don’t dig threshold.” Items buried in locations listed above the “don’t dig threshold” could remain in the ground.**

The demonstrators used different methods for selecting the boundaries between the different subcategories of a ranked anomaly list. SIG selected the boundaries by first assigning a quantitative cost to mistakenly classifying a true TOI location as “Likely to Contain Only Non-TOI” and a second cost to mistakenly classifying a true non-TOI location as “Likely to Contain TOI.” Then, SIG used information-theory metrics to

optimize the ratio of these two costs with respect to each other over the labeled locations in the training set [12]. Other demonstrators used similar, yet more subjective, methods, such as visually analyzing the spread in feature space between feature vectors extracted from the labeled locations in the training set. In any case, the boundary between the green “Likely To Contain Only Non-TOI” and the yellow “Cannot Decide” subcategories was the most important boundary because it constituted the “don’t dig threshold.”

The “don’t dig threshold” instructs stakeholders about which locations must be excavated. In a real-world scenario, an excavation team must recover the most dangerous items first—those buried in locations classified as “Likely to Contain TOI.” The excavation team must also err on the side of caution and recover items that may or may not be dangerous, those buried in locations classified as “Cannot Decide.” However, stakeholders may instruct the excavation team to leave presumably innocuous items in the ground—those buried in locations classified as “Likely To Contain Only Non-TOI.” That is, in a real-world scenario, the excavation team would begin recovering items from locations listed at the bottom of the ranked anomaly list and work its way up. Stakeholders could instruct the excavation team to cease digging once they reached the “don’t dig threshold.”

In the third and final stage of constructing a ranked anomaly list, the demonstrators focused on the test set locations classified as “Cannot Analyze.” In a real-world scenario, the excavation team must err on the side of caution and recover all possibly dangerous items, including those buried in “Cannot Analyze” locations. This means that all “Cannot Analyze” locations must be inserted into the ranked anomaly list at a point below the “don’t dig threshold.” Demonstrators were instructed to append their “Cannot Analyze” locations at the very end of the ranked anomaly list, as shown in Figure 27. The “Cannot Analyze” locations are arranged in no particular order with respect to each other because, by definition, no further information could be learned about them, including their rank or likelihood of containing TOI.

Identification Number	Decision Statistic	Rank	Category
2	1.00	1	Can Analyze: Likely To Contain Only Non-TOI
700	0.99	2	Can Analyze: Likely To Contain Only Non-TOI
91	0.97	3	Can Analyze: Likely To Contain Only Non-TOI
1256	0.96	4	Can Analyze: Likely To Contain Only Non-TOI
2	0.90	5	Can Analyze: Likely To Contain Only Non-TOI
531	0.87	6	Can Analyze: Cannot Decide
975	0.77	7	Can Analyze: Cannot Decide
9	0.75	8	Can Analyze: Cannot Decide
483	0.71	9	Can Analyze: Cannot Decide
99	0.70	10	Can Analyze: Cannot Decide
86	0.67	11	Can Analyze: Likely To Contain TOI
432	0.59	12	Can Analyze: Likely To Contain TOI
785	0.31	13	Can Analyze: Likely To Contain TOI
942	0.20	14	Can Analyze: Likely To Contain TOI
69	0.12	15	Can Analyze: Likely To Contain TOI
32	Unknown	Unknown	Cannot Analyze
33	Unknown	Unknown	Cannot Analyze
1233	Unknown	Unknown	Cannot Analyze

May leave items in the ground

**Don't Dig Threshold**

Must recover items from the ground

**Figure 27: A cartoon of a ranked anomaly list in its third and final stage of construction. “Cannot Analyze” locations in the test set have been appended to the end of the list in no particular order with respect to each other. All these “Cannot Analyze” locations share the rank of “Unknown.”**

## 2.19 SCORE CLASSIFICATION PERFORMANCE

IDA scored the demonstrators’ classification performance by comparing the demonstrators’ ranked anomaly lists with ground truth, calculating both primary and secondary performance metrics for each ranked anomaly list. Primary performance metrics summarize an instrument-algorithm combination’s ability to correctly classify locations likely to contain only non-TOI and all other locations. Primary scoring did not consider the ground truth labels of the different types of TOI; locations truly containing 60 mm mortars were considered no differently than locations truly containing 81 mm mortars, etc. Secondary scoring, however, did consider the ground truth types of TOI: locations truly containing 60 mm mortars were analyzed independently of locations truly containing 81 mm mortars, etc.

### 2.19.1 Primary Scoring

The primary classification scoring metrics were calculated for each ranked anomaly list by first counting the number of true positive (TP), false negative (FN), and false positive (FP) locations on the ranked anomaly list. (True negative [TN] locations were not counted because they were not needed to calculate the final summary statistics.) Figure 28 shows the results:

- A TP is a true TOI location that correctly fell below the “don’t dig threshold,” indicating that the demonstrators believed that the item buried at the location must be recovered.
- An FN is a true TOI location that incorrectly rose above the “don’t dig threshold,” indicating that the demonstrators incorrectly believed that the item buried at the location could be left in the ground.
- An FP is a true non-TOI location that incorrectly fell below the “don’t dig threshold,” indicating that the demonstrators incorrectly believed that the item buried at the location must be recovered.

Once these counts were tallied, two summary statistics were calculated for each ranked anomaly list, the *Percent of TOI Below Threshold* and the *Number of Non-TOI Below Threshold*.

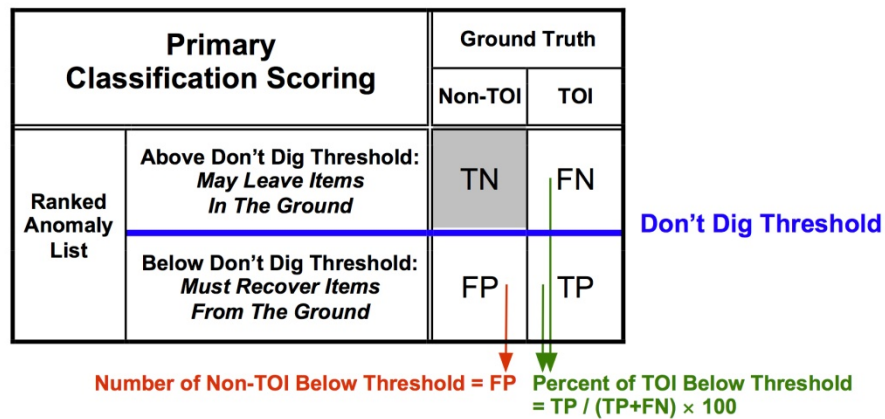


**Figure 28: Metrics used to score primary classification performance. The TOI types of the ground truth labels were not considered.**

The *Percent of TOI Below Threshold* is the most important classification performance metric to the UXO community because it is a measure of FNs. An FN could result in a true TOI being incorrectly left in the ground, with a potentially high cost to public safety. This metric is defined as the percent of true TOI locations that correctly fell below the “don’t dig threshold” and is calculated as  $[TP / (TP + FN)] \times 100$ . (This metric’s 95% confidence interval was also estimated, based on the binomial distribution.) Because this metric is a percentage, its value can range from 0% to 100%, with values near 0% indicating that almost all TOI were incorrectly left in the ground and values near 100% indicating that almost all TOI were correctly recovered. Due to the potentially high cost to public safety associated with incorrectly leaving a TOI in the ground, the UXO community requires the *Percent of TOI Below Threshold* to be at or near 100%.

The *Number of Non-TOI Below Threshold* metric is a measure of FPs, rather than FNs. An FP could result in a true non-TOI being unnecessarily recovered from the ground, but such a situation does not present a cost to public safety. FPs do have other costs, however, such as the time and money required for their recovery. Therefore, the purpose of UXO classification technology is to reduce the *Number of Non-TOI Below Threshold* while still keeping the first metric, the *Percent of TOI Below Threshold*, as close as possible to 100%.

The *Number of Non-TOI Below Threshold* is defined as the number of true non-TOI locations that incorrectly fell below the “don’t dig threshold,” calculated as simply *FP*. Although many other classification problems use a summary metric similar to *Percent of Non-TOI Below Threshold*, we focused on the more straightforward *Number of Non-TOI Below Threshold* because the number count is more easily translatable to the dollar cost of clearing the site. A simple count, the *Number of Non-TOI Below Threshold* can range from zero to the total number of true non-TOI locations associated with the instrument of interest. Values near zero indicate correct identification of almost all true non-TOI locations; the demonstrators could safely recommend that items buried at these locations be left in the ground. In contrast, values near maximum indicate the inability to correctly identify most true non-TOI locations; this could lead to the unnecessary recovery of many non-TOI. Due to the time and money required to recover items from the ground, the UXO community desires low values for this metric.

The *Percent of TOI Below Threshold* vs. the *Number of non-TOI Below Threshold* was plotted for each ranked anomaly list. Figure 29 shows a cartoon of this plot. The plotted point (large blue dot) illustrates the classification performance of the instrument-algorithm combination when the demonstrator’s chosen “don’t dig threshold” was applied to the ranked anomaly list. The 95% confidence interval (gray bar) around the *Percent of TOI Below Threshold* metric is drawn through the point.

The plot of summary metrics was used to revisit the choice of “don’t dig threshold.” The demonstrators had prospectively chosen one particular “don’t dig threshold” to apply to the ranked anomaly list. Other “don’t dig thresholds” could have been chosen instead. This was illustrated by retrospectively applying all possible “don’t dig thresholds” to the ranked anomaly list. For each possible “don’t dig threshold,” the number of TP, FN, and FP locations on the ranked anomaly list was re-tallied. Then, the *Percent of TOI Below Threshold* and the *Number of Non-TOI Below Threshold* were recalculated and plotted with respect to each other. Figure 30 shows a cartoon plot of the points from all possible “don’t dig thresholds” (black dots). Together, the points form a

classification performance curve. This curve is similar to the receiver-operating characteristic (ROC) curves often used in general classification problems. The 95% confidence intervals (vertical gray bars) around the *Percent of TOI Below Threshold* metrics are drawn through the points on the curve.<sup>1</sup>

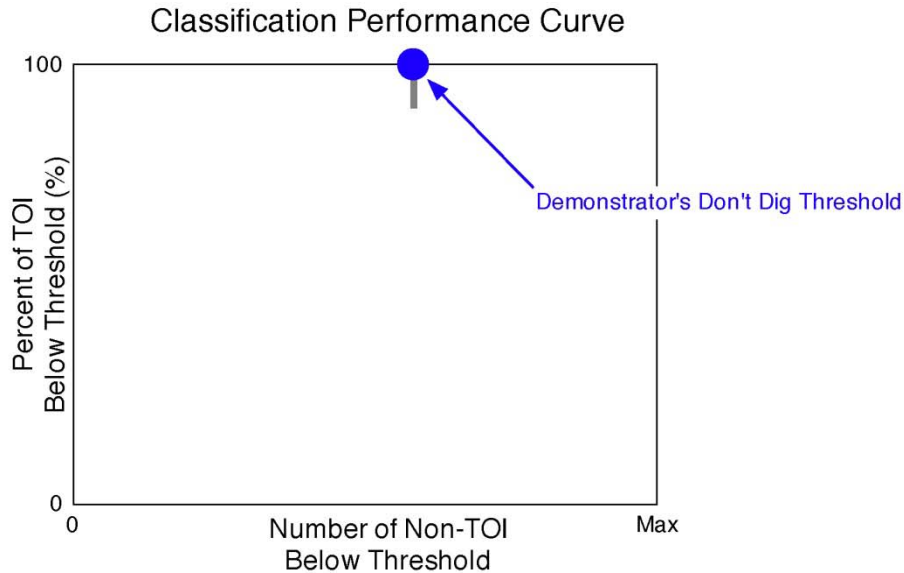


**Figure 29: A cartoon plot, showing the performance results of the demonstrator’s “don’t dig threshold” applied to a ranked anomaly list. The large blue dot illustrates the *Percent of TOI Below Threshold* vs. the *Number of Non-TOI Below Threshold* that resulted from the demonstrator’s choice of “don’t dig threshold.” The vertical grey bar illustrates the 95% confidence interval around the *Percent of TOI Below Threshold* metric.**

Figure 30 shows a cartoon of a classification performance curve with one point for every possible “don’t dig threshold.” The point in the upper right corner of the plot corresponds to the extreme situation in which the “don’t dig threshold” is applied to the very top of the ranked anomaly list, such that all locations fall below; the *Percent of TOI Below Threshold* is 100%. However, since all true non-TOI locations also fall below this “don’t dig threshold,” the *Number of Non-TOI Below Threshold* reaches its maximum value. The point in the lower left corner of the plot illustrates another extreme situation. In this situation, the “don’t dig threshold” is applied to the very bottom of the ranked anomaly list, such that no locations fall below. Both the *Percent of TOI Below Threshold* and the *Number of Non-TOI Below Threshold* are zero.

---

<sup>1</sup> Note that the 95% confidence intervals were calculated for each point independently, without any adjustments for multiple comparisons. As Macshassy and Provost explain [15], this means that one cannot infer that 95 times out of 100, every point on the curve will simultaneously lie within its own 95% confidence interval. That is, one cannot infer that 95 times out of 100, the entire curve will lie within the band generated by “smearing” the individual 95% confidence intervals.

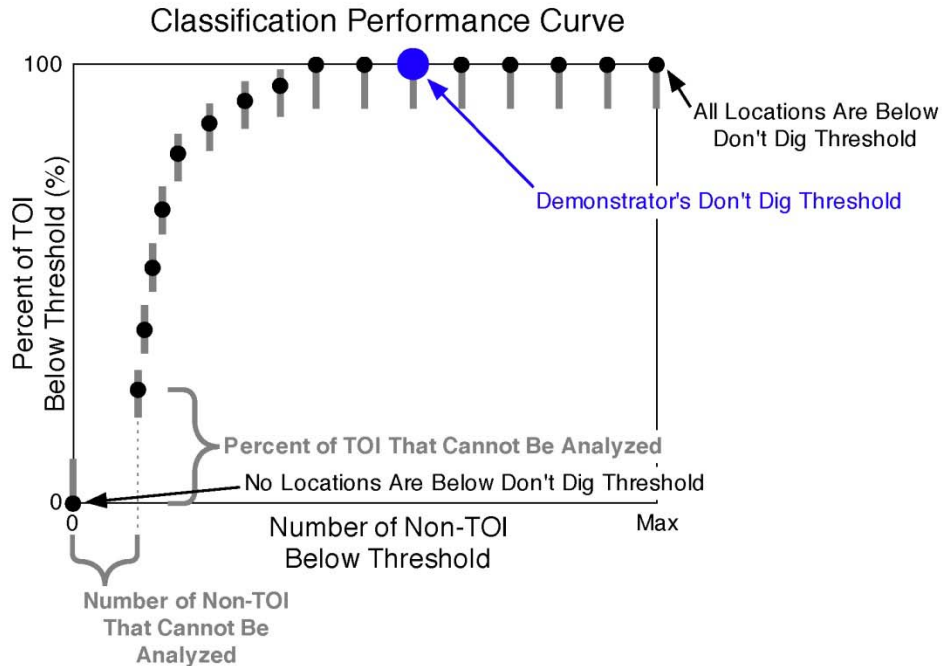


**Figure 30: A cartoon of a classification performance curve, showing the performance results of all possible “don’t dig thresholds” applied to the ranked anomaly list. The point in the upper right corner represents the extreme situation in which the “don’t dig threshold” is placed at the very top of the list, such that all locations on the list fall below. The point in the lower left corner represents the other extreme situation in which the “don’t dig threshold” is placed at the very bottom of the list, such that no locations fall below. All points between the two extremes represent possible “don’t dig thresholds.” The gap between the lower left corner and the next closest point represents the locations in the test set that the demonstrators classified as “Cannot Analyze.”**

As with ROC curves, the points of a classification performance curve are not always equally spaced. All points on the curve lying between the two extreme corners represent possible “don’t dig thresholds,” with one possible “don’t dig threshold” per each unique rank on the ranked anomaly list. Some locations on the list may share the same rank if they are considered equally likely to contain TOI. Therefore, these locations must fall, together, either above or below any given “don’t dig threshold;” a “don’t dig threshold” cannot be placed between them. These groups of identically ranked locations lead to gaps between the points in the curve. This is particularly true of the test set locations classified as “Cannot Analyze” and appended to the bottom of the ranked anomaly list. By definition, the data collected at these locations could not be analyzed, and therefore the classification algorithm could not estimate the locations’ likelihoods of containing TOI nor any other similar decision statistic. Therefore, all “Cannot Analyze” test set locations share the rank of “unknown,” and a “don’t dig threshold” cannot be placed between them. This causes a gap between the point at the origin and the next

closest point, as shown in Figure 30. This next point corresponds to the situation where the “don’t dig threshold” is placed directly between the “Can Analyze” and “Cannot Analyze” locations on the ranked anomaly list. Only the “Can Analyze” locations rise above the “don’t dig threshold,” and only the “Cannot Analyze” locations fall below. In this situation, if Y% of all true TOI locations are classified as “Cannot Analyze” and therefore fall below the “don’t dig threshold,” then the *Percent of TOI Below Threshold* is equal to Y%. Similarly, if X of the true non-TOI locations are classified as “Cannot Analyze” and therefore fall below the “don’t dig threshold,” then the *Number of Non-TOI Below Threshold* is X.

Figure 31 shows a similar plot of the cartoon curve, this time with the possible “don’t dig thresholds” colored according to the demonstrator-declared category into which they fell. The demonstrators classified each “Can Analyze” location on the ranked anomaly list into three subcategories: “Likely to Contain Only Non-TOI” (green), “Likely to Contain TOI” (red), and “Cannot Decide” (yellow). The colored points on the curve occur at the corresponding “don’t dig thresholds”. By definition, the demonstrator’s chosen “don’t dig threshold” (large blue dot) lies between the green and yellow points because this “don’t dig threshold” was defined as the boundary between the “Likely To Contain Only Non-TOI” and the “Cannot Decide” subcategories.

Each ranked anomaly list’s classification performance curve was examined to identify what would have been the best possible choice of “don’t dig threshold” for that ranked anomaly list. Choosing the “don’t dig threshold” is a critical step in UXO classification. A “don’t dig threshold” placed near the top of the ranked anomaly list leads to a high *Percent of TOI Below Threshold* (a desirable outcome) but also a high *Number of Non-TOI Below Threshold* (an undesirable outcome). Conversely, placing the “don’t dig threshold” near the bottom of the ranked anomaly list leads to a low *Percent of TOI Below Threshold* (an undesirable outcome) but also a low *Number of Non-TOI Below Threshold* (a desirable outcome). The best possible “don’t dig threshold” lies somewhere in between.

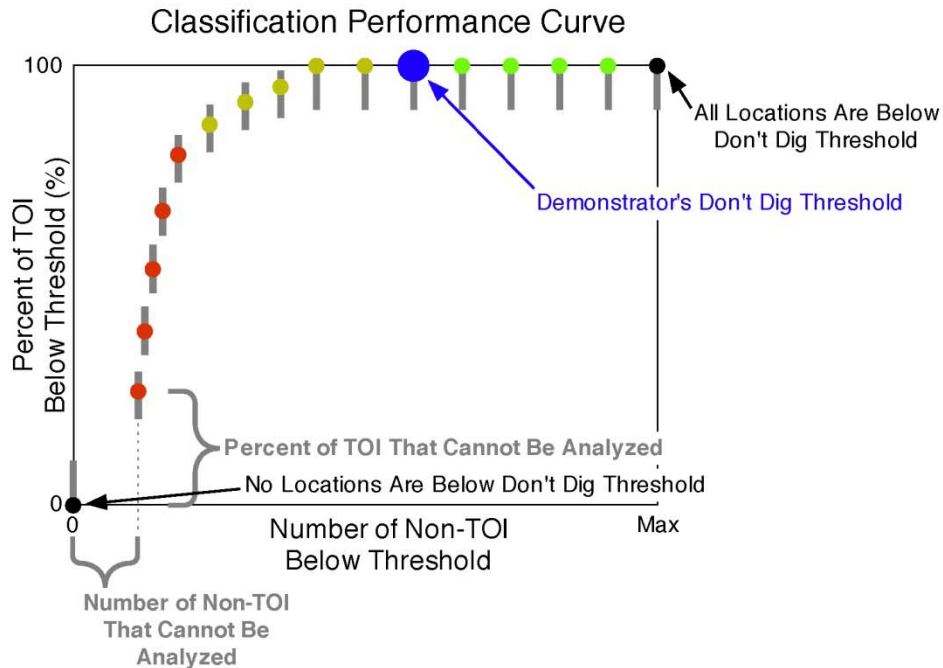


**Figure 31: A cartoon of a classification performance curve, noting in which categories the possible “don’t dig thresholds” fell on the ranked anomaly list. Points colored in green, yellow, and red correspond to “don’t dig thresholds” that fell in the “Likely to Contain Only Non-TOI,” “Cannot Decide,” and “Likely to Contain TOI” categories, respectively. By definition, the demonstrator’s “don’t dig threshold” lies between the green and yellow points.**

For this analysis, two possible definitions of the “best possible” “don’t dig threshold” were considered. According to one definition, this “don’t dig threshold” is that which would have resulted in the fewest *Number of Non-TOI Below Threshold* while the *Percent of TOI Below Threshold* was held at 100%. This “don’t dig threshold” could have minimized the cost of recovering items while leaving no true TOI in the ground. The large light-blue dot in Figure 32 corresponds to this “don’t dig threshold”. The second definition is more relaxed. This “don’t dig threshold” would have resulted in the fewest *Number of Non-TOI Below Threshold* while the *Percent of TOI Below Threshold* was held at 95%, minimizing the cost of recovering items while leaving only 5% of the true TOI (the most difficult to identify) in the ground. Figure 32 illustrates this “don’t dig threshold” with a large pink dot.

The purpose of a classification performance curve is to illustrate the classification performance of an instrument-algorithm combination over the test set. However, the classification performance curve in Figure 32 does not take the amount of training data required into account. Curves like this can be compared to each other only if they are based on same-sized training and test sets. In this study, though, different demonstrators

used different training and test sets. Some demonstrators built their ranked anomaly lists from locations in the Standard Test Set, but others, such as SIG and RML, built some of their ranked anomaly lists from locations in the Active Learning Test Sets or the Extended Test Set [3, 12]. Test sets differed in both size and character, as shown in Figure 20–Figure 24. These differences in test sets led to inherent differences in the *Number of Non-TOI Below Threshold* calculated for each ranked anomaly list. An instrument-algorithm combination could have more easily achieved a low *Number of Non-TOI Below Threshold* with a test set that contained fewer true non-TOI locations to begin with.

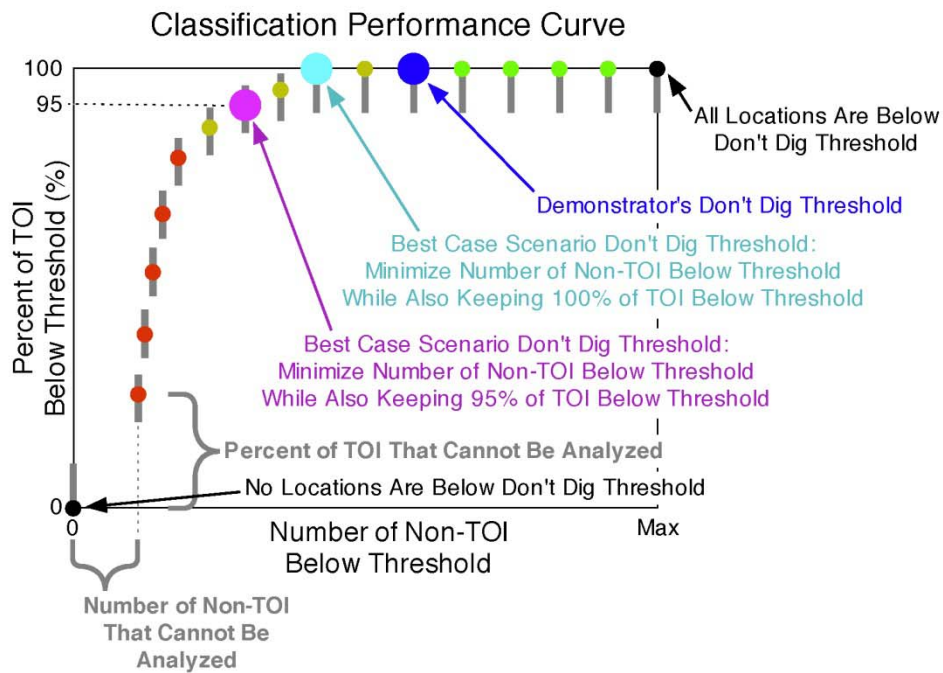


**Figure 32: A cartoon of a classification performance curve, showing the retrospectively chosen best possible “don’t dig thresholds.” The large light-blue dot represents the “don’t dig threshold” that would have minimized the *Number of Non-TOI Below Threshold* while also keeping the *Percent of TOI Below Threshold* at 100%. The large pink dot represents the “don’t dig threshold” that would have also minimized the *Number of non-TOI Below Threshold*, while ensuring that the *Percent of TOI Below Threshold* was greater than 95%.**

The classification performance curves were altered so that they could be compared with each other even if based on different-sized training and test sets. In a real-world situation, all locations in the training set must be excavated to obtain ground truth information that the demonstrators could use to optimize their classification algorithms. This is true regardless of which “don’t dig threshold” is eventually applied to the ranked anomaly list. Therefore, the training set locations were treated as though they were appended to the very bottom of the ranked anomaly list, below even the most extreme

“don’t dig threshold,” as shown in Figure 33. The summary classification performance statistics were then recalculated, incorporating the locations in the training set into the tallied TP, FN, and FP counts.

Identification Number	Decision Statistic	Rank	Category
2	1.00	1	Can Analyze: Likely To Contain Only Non-TOI
700	0.99	2	Can Analyze: Likely To Contain Only Non-TOI
91	0.97	3	Can Analyze: Likely To Contain Only Non-TOI
1256	0.96	4	Can Analyze: Likely To Contain Only Non-TOI
2	0.90	5	Can Analyze: Likely To Contain Only Non-TOI
531	0.87	6	Can Analyze: Cannot Decide
975	0.77	7	Can Analyze: Cannot Decide
9	0.75	8	Can Analyze: Cannot Decide
483	0.71	9	Can Analyze: Cannot Decide
99	0.70	10	Can Analyze: Cannot Decide
86	0.67	11	Can Analyze: Likely To Contain TOI
432	0.59	12	Can Analyze: Likely To Contain TOI
785	0.31	13	Can Analyze: Likely To Contain TOI
942	0.20	14	Can Analyze: Likely To Contain TOI
69	0.12	15	Can Analyze: Likely To Contain TOI
32	Unknown	Unknown	Cannot Analyze
33	Unknown	Unknown	Cannot Analyze
1233	Unknown	Unknown	Cannot Analyze
77	N/A	N/A	N/A
43	N/A	N/A	N/A
5	N/A	N/A	N/A
954	N/A	N/A	N/A

**Figure 33: A cartoon of a ranked anomaly list, altered to allow comparisons between different-sized training and test sets. Training set locations have been appended to the end of the list. The decision statistic, rank, and category of the training set locations are not applicable (N/A) because all training set locations are excavated.**

Training set locations were reflected in the recalculated counts of TP, FN, and FP. All locations in the training set that happened to be true TOI contributed to the TP count, the number of true TOI locations that correctly fell below the “don’t dig threshold.” Similarly, all locations in the training set that happened to be true non-TOI contributed to the FP count, the number of true non-TOI locations that incorrectly fell below the “don’t dig threshold.” These contributions led to a uniform shift of the classification performance curve away from the origin, as shown in Figure 34. (The shape of the curve was unaltered.) For example, if Y% of the true TOI locations were assigned to the training set, then these Y% must always fall below the “don’t dig threshold,” regardless of which “don’t dig threshold” is used. Therefore, the *Percent of TOI Below Threshold* can never be less than Y%. Similarly, if X of the true non-TOI locations were assigned to the training set, then these X locations must always fall below the “don’t dig threshold” as well. In this way, the *Number of Non-TOI Below Threshold* can never be less than X. Thus, the gap between the origin and the lower left end of the shifted classification performance curve represents the locations in the training set. The smaller the gap, the

smaller the training set. In either case, all curves based on the same instrument now have the same maximum value for the *Number of Non-TOI Below Threshold*. This allows an apples-to-apples comparison between instrument-algorithm combinations based on different training and test sets.

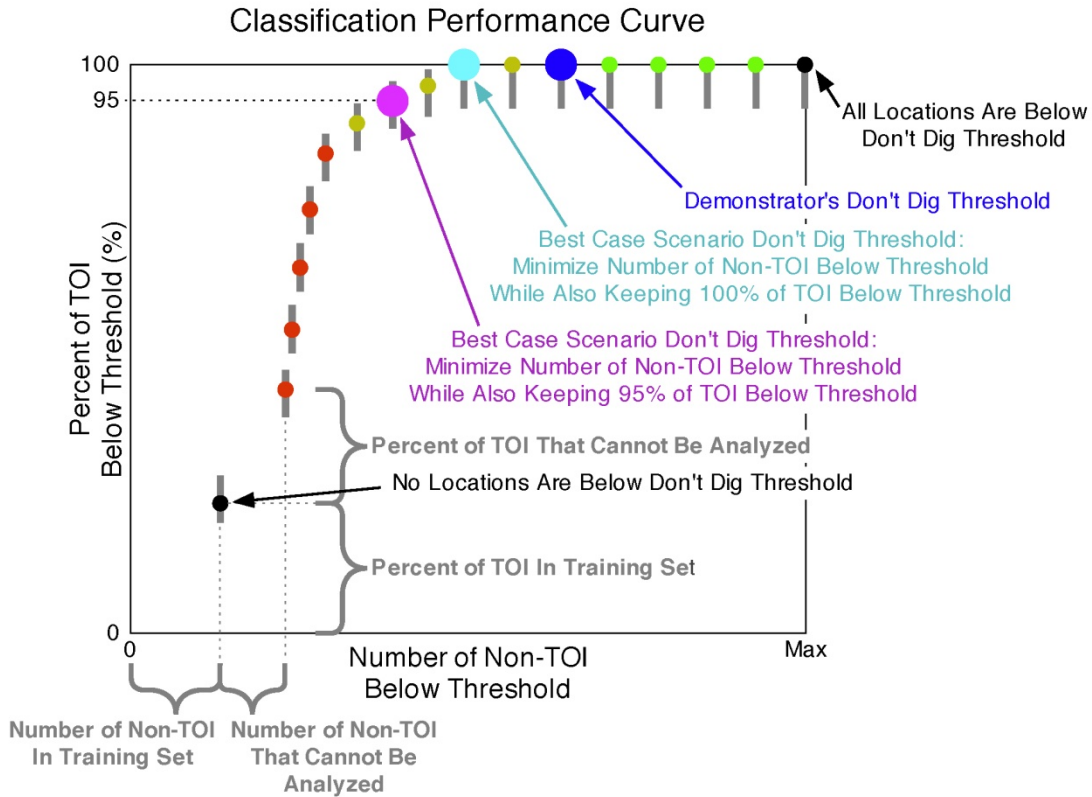


**Figure 34: A cartoon of a classification performance curve, where the locations in the training set have been included in the calculations of the plotted metrics. The gap between the origin and the black dot in the lower left corner represents the locations in the training set.**

The classification performance curves were further adjusted so that all curves could be plotted on the same horizontal scale, regardless of which instrument-algorithm combination was used to generate the ranked anomaly list. This adjustment was necessary because different instruments had different maximum values for the *Number of Non-TOI Below Threshold*. Figure 35 shows a cartoon of a curve with the horizontal axis ranging from zero to "Overall Max," a value at least as large as the largest number of true non-TOI locations associated with any instrument used in this study.

Finally, the primary classification performance of each instrument-algorithm combination was rescored for only those locations contained in the sub-areas of the site where the BUD collected data. Figure 14 shows these sub-areas in orange. The resulting

performance metrics and curves could be directly compared with the metrics and curves calculated for the BUD. In this way, the BUD's performance could be directly compared with other instruments' performances.

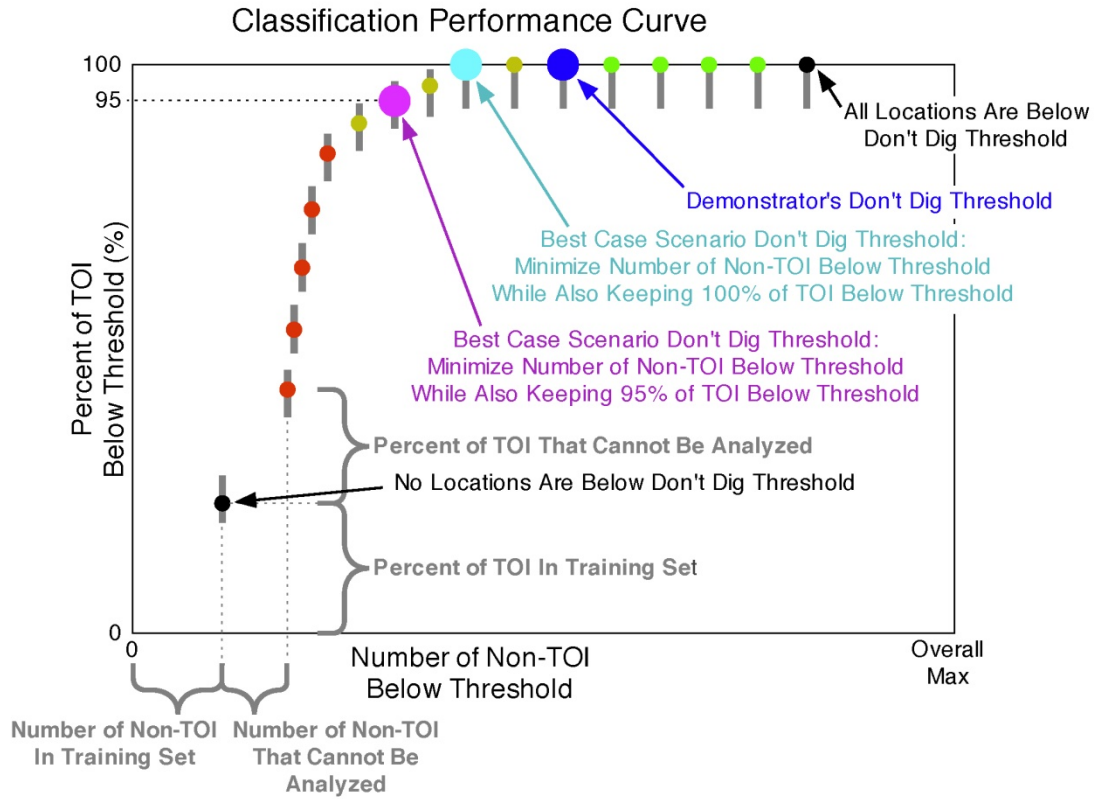


**Figure 35: A cartoon of a classification performance curve, with the horizontal axis adjusted to provide a consistent scaling across all instrument-algorithm combinations.**

### 2.19.2 Secondary Scoring

The secondary classification scoring metrics were also calculated for each ranked anomaly list, this time considering the ground truth labels between different types of TOI. As was done with primary classification scoring, the number of FP locations on the ranked anomaly list were counted. In contrast to primary scoring, however, simple counts of TP and FN locations were not tallied. Instead,  $TP_{60}$  and  $FN_{60}$  locations, true 60 mm mortar locations that fell below and above threshold, respectively, were counted. Similar counts were tallied for each type of TOI, as shown in Figure 36.

Several summary statistics were calculated for secondary classification scoring. First, the *Number of Non-TOI Below Threshold* was calculated as *FP*, as was done during primary scoring. During primary scoring, the *Percent of TOI Below Threshold* was also calculated, regardless of TOI type. In secondary scoring, however, more specific metrics

were calculated, taking note of each type of TOI. For example, the *Percent of 60 mm Below Threshold* is given as  $[TP_{60} / (TP_{60} + FN_{60})] \times 100$ , indicating the percentage of true 60 mm mortar locations that correctly fell below the “don’t dig threshold.” This metric ranges from 0% to 100%; the UXO community desires values near 100%. Similar metrics were calculated for all other types of TOI—81mm mortars, 4.2 in mortars, 2.36 in rockets, 5 in rockets, 3 in Stokes mortars, and 37 mm rounds.

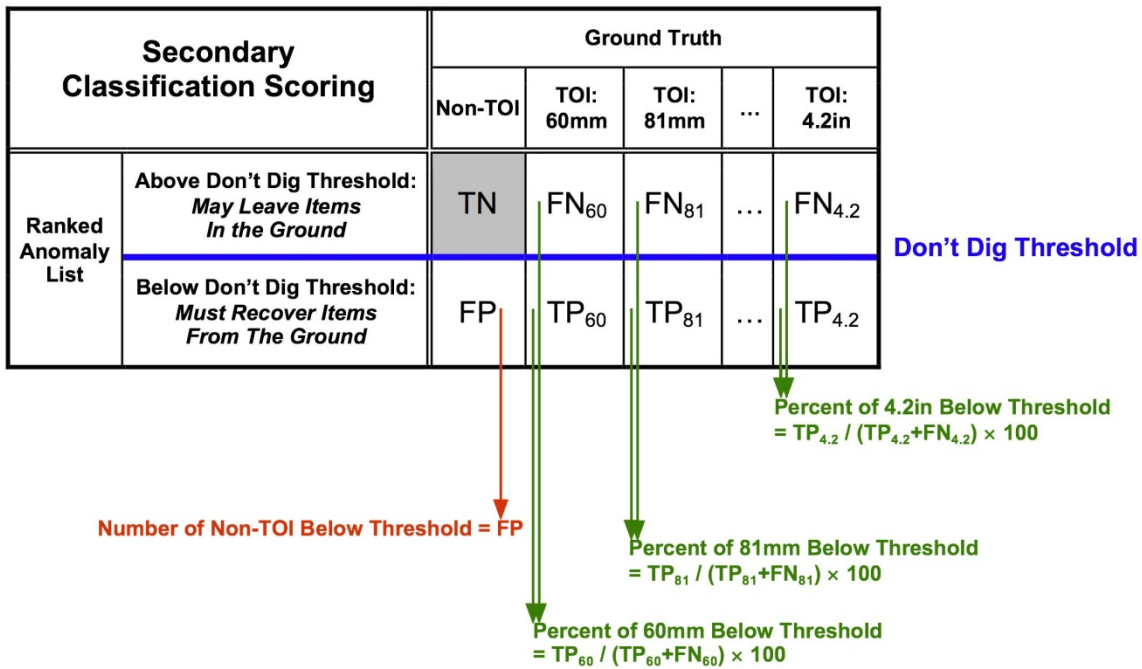


**Figure 36: Metrics used to score secondary classification performance. The TOI types of the ground truth labels were considered. Each location on a ranked anomaly list was compared with its ground truth label and tallied toward a particular count. As in primary scoring, an FP location is a true non-TOI location that incorrectly fell below the “don’t dig threshold.” TN locations were not counted. The *Number of Non-TOI Below Threshold* is calculated as FP. In contrast to primary scoring, true TOI locations were tallied as either  $FP_i$  or  $FN_i$ , where  $i$  refers to the TOI type of the ground truth label. For example, a  $TP_{60}$  location is a true 60 mm mortar location that correctly fell below threshold, and an  $FN_{60}$  location is a true 60 mm mortar location that incorrectly rose above threshold. The *Percent of 60 mm Below Threshold* is a summary statistic specifying the percentage of true 60 mm mortar locations that correctly fell below threshold. Similar statistics are calculated for other TOI types.**

To summarize the secondary classification performance metrics, several additional curves were created for each ranked anomaly list. The first curve indicated how well the instrument-algorithm combination classified true 60 mm mortars vs. non-TOI and was a plot of the *Percent of 60 mm Below Threshold* vs. the *Number of Non-TOI Below Threshold*. The other curves indicated how well other true TOI types were classified vs. non-TOI. These secondary curves shared many characteristics with the

single primary curve depicted in Figure 35. That is, the “Cannot Analyze” and training set locations were represented as gaps between the origin and the lower left end of the curve. Each point of the curve was also colored in based on the category in which it fell, and the retrospectively identified best possible “don’t dig thresholds” were included. However, the secondary curves did exhibit some differences from the primary curve. They had a coarser resolution because they were created from fewer locations, and therefore fewer possible “don’t dig thresholds”, than the primary curve. The secondary curves also showed longer 95% confidence intervals because each secondary curve was based on fewer true TOI locations than the primary curve.

Finally, as was done in primary scoring, the secondary classification performance of each instrument-algorithm combination was rescored over only those locations contained in the sub-areas of the site over which the BUD collected data. This allowed for a direct comparison between the BUD and the other instruments.

### **3. RESULTS AND DISCUSSION**

After a brief discussion of detection performance, this chapter focuses on the results obtained by the various combinations of data-collection instruments and classification algorithms. The intent is to provide results and discussion that highlight the performance of commercial or commercial-like instruments based on the EM61-Mk2 and magnetometer sensors coupled with commercial software and contrast those results with results achieved by advanced instruments coupled with software programs specifically designed to capitalize on the richer data sets that the advanced instruments provide.

#### **3.1 DETECTION RESULTS**

Although the demonstration at Camp San Luis Obispo was designed principally as a classification demonstration, understanding TOI detection performance is particularly important because the detection thresholds were based on the signals expected from the TOI/depth combination giving the smallest signal for each given instrument. In general, that was a horizontal, cross-track 60 mm mortar at a depth of 45 cm (the expected deepest depth of 30 cm plus a 50% margin). Note that in setting the detection threshold, predictions of the signature for complete 60 mm mortars were typically used, but many of the seed items were mortars that were missing the nose fuze and the tail boom, significantly reducing their signatures.

As shown in Figure 37, Camp San Luis Obispo was not good site for the use of magnetometers because of the areas of high geologic background. Nevertheless, using a 0.75 m detection halo, the MAG ARRAY detected all the emplaced seeds that it was able to survey, missing only one seed between two rocks where it was unable to maneuver. In a real clearance action, the missed area would have been covered by a hand-held instrument or cart. But as shown in the table in Appendix A, this detection performance was at the cost of over 5200 detected anomalies, compared with the 1464 unique anomalies that exceeded the detection threshold for the EM61 ARRAY, whose much cleaner anomaly map is shown in Figure 38. By the time the MSEMS magnetometer data collection was completed, the decision had been made to score only those magnetic anomalies that coincided with EMI anomalies. Therefore, no scoring of the MSEMS magnetometer anomalies against the emplaced seeds was done.

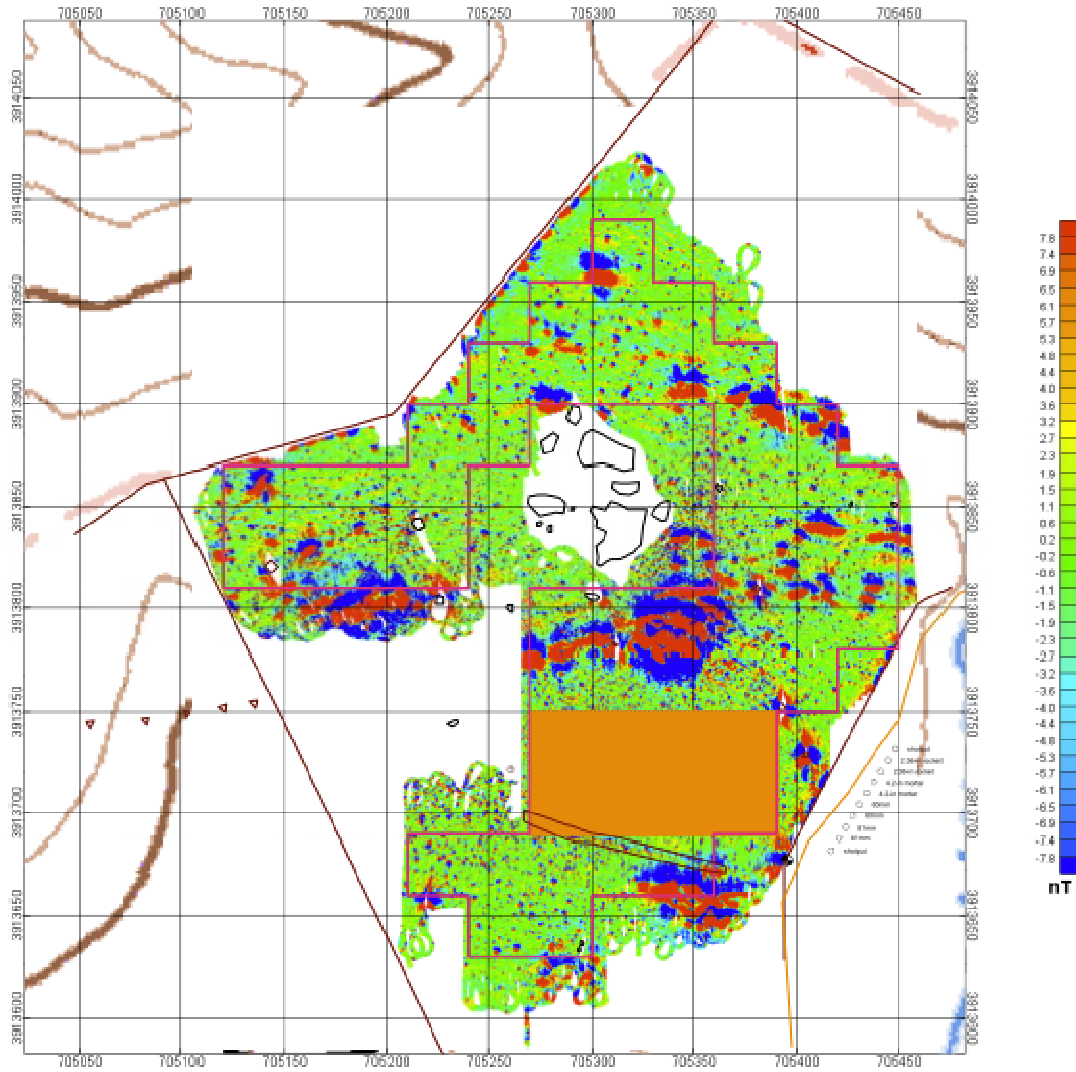


**Figure 37: MAG ARRAY survey map of the demonstration area at Camp San Luis Obispo. The orange shaded area is the vehicular area that was not scored, and the black outlined area is the access path into the site. Taken from [6].**

Using the same 0.75 m detection halo to associate anomalies with recovered items, the MSEMS EM61 detected all the emplaced seeds. The EM61 ARRAY missed the seed that was buried between two rocks. The EM61 CART missed calling detection on one seed item, a near-horizontal 60 mm mortar round missing the nose and tail boom and buried at 30 cm. The detection threshold for the EM61 CART, set based on a complete 60 mm mortar, was 11.3 mV. The partial round was just under the threshold, at 10.7 mV. This result emphasizes that for an expected signal-based threshold, care must be taken to understand all possible TOI. The conclusion is further reinforced by the fact that the MetalMapper missed detecting four seeds in its survey. All were partial 60 mm rounds, three that were near horizontal and buried at 30 cm, and one that was vertical and

buried at 45 cm. One of the missed 60 mm mortars buried at 30 cm was the same seed missed by the EM61 CART.

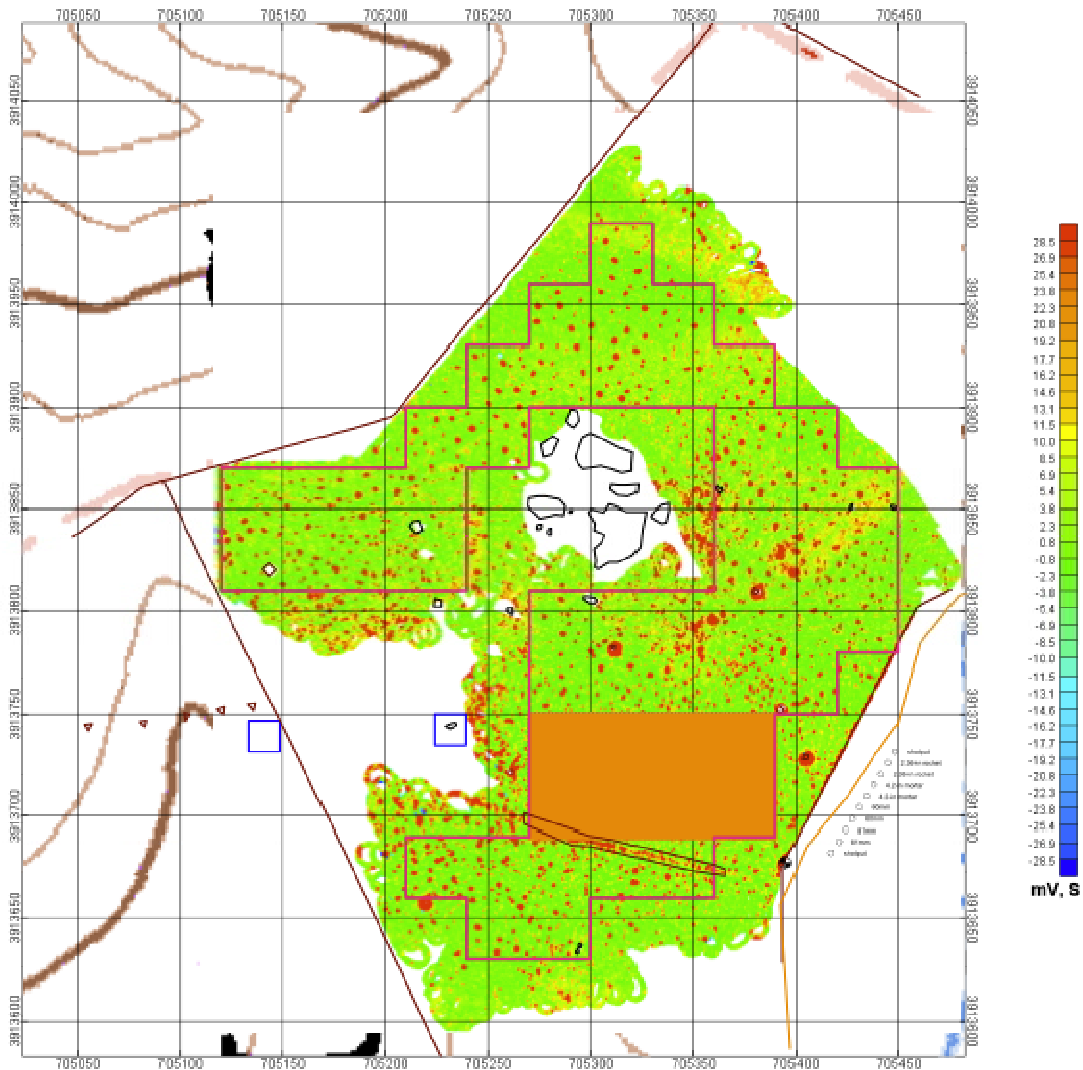


**Figure 38: EM61 ARRAY survey map for the demonstration area at Camp San Luis Obispo. The orange shaded area is the vehicular area that was not scored, and the black outlined area is the access path into the site. Taken from [6].**

The classification demonstrators analyzed only those anomalies that were detected by a given instrument. For a given instrument, the classification demonstrators arranged all test set anomalies detected by the instrument onto a ranked anomaly list. IDA appended the training set anomalies detected by the instrument to the bottom of the ranked anomaly list and then scored the list against ground truth.

## 3.2 CLASSIFICATION RESULTS

The classification demonstrators submitted 62 separate ranked anomaly lists based on different combinations of data-collection instruments and classification algorithms. This section discusses a representative set of those combinations, with the primary scoring results of all ranked anomaly lists provided in Appendix B. Appendix C is a CD with the complete scoring results.

Results are grouped by the type of instrument (conventional or advanced) and type of algorithm (commercial or custom) used to generate the ranked anomaly list. The commercial software algorithms available within Oasis montaj, UX-Process and UX-Analyze, currently handle only data collected by conventional sensors (e.g., the EM61-Mk2 and magnetometers). Classification efforts employing data from the advanced instruments used custom algorithms developed by the classification demonstrators themselves.

Results are presented in a series of classification performance curves. Each curve plots the *Percent of TOI Below Threshold* vs. the *Number of Non-TOI Below Threshold* for every possible “don’t dig threshold” that could have been applied to the ranked anomaly list. The demonstrator’s prospectively chosen “don’t dig threshold” is shown as a dark-blue dot on each curve. The demonstrators classified all locations that rose above this “don’t dig threshold” as “Likely to Contain Only Non-TOI.” In a real-world scenario, items buried at these locations could be left in the ground, but those that fell below the “don’t dig threshold” would have to be dug. True TOI locations that rose above the demonstrator’s “don’t dig threshold” were incorrectly classified.

On the curves, a light-blue dot marks the retrospective “100% don’t dig threshold.” This is the threshold that would have minimized the *Number of Non-TOI Below Threshold* while holding the *Percent of TOI Below Threshold* at 100%. By definition, no true TOI locations would have risen above the “100% don’t dig threshold.” Finally, a pink dot marks the retrospective “95% don’t dig threshold.” This is the value that would have minimized the *Number of Non-TOI Below Threshold* while the *Percent of TOI Below Threshold* was held greater than 95%. By definition, 5% (approximately 9 to 11, depending upon the instrument) of the true TOI locations would have risen above this threshold.

Each classification performance curve has an accompanying table. Listed in blue with an asterisk are any true TOI locations that rose above the demonstrator’s “don’t dig threshold.” Listed in pink without asterisks are those true TOI locations that fell between

the demonstrator’s prospective “don’t dig threshold” and the retrospective “95%” “don’t dig threshold.” In most cases, however, the demonstrator’s “don’t dig threshold” happened to be placed above the “95%” “don’t dig threshold” on the ranked anomaly list. But if the demonstrator’s “don’t dig threshold” was so poorly chosen that it was placed below the “95%” “don’t dig threshold,” then only those true TOI locations that rose above the “95%” “don’t dig threshold” are listed in the accompanying table. In all cases, the tables list the true TOI locations in the same order as they appeared on the ranked anomaly list, from least to greatest likelihood of containing TOI. The tables are included to provide a sense of what types of TOI proved troublesome to particular instrument-algorithm combinations and to help understand whether certain types of TOI were problematic for all combinations.

### **3.2.1 Conventional Instruments**

We define conventional instruments here as the instruments based on EM61-Mk2 sensors or cesium vapor magnetometers. The EM61 CART, the EM61 ARRAY, the MAG ARRAY, and the MSEMS fall into this category. This section focuses on two classification approaches. The first applies the inversion and classification algorithms residing in Oasis montaj to the data collected by conventional instruments. These results illustrate capabilities that might be demonstrated by a commercial UXO clearance contractor employing readily available commercial equipment and software. The second approach uses data collected by the conventional instruments but with more advanced classification techniques. These results show the extent to which more sophisticated processing can make up for some of the shortcomings of the conventional instruments.

#### **3.2.1.1 Conventional Instruments with Commercial Classification Software**

To be successfully transitioned to the UXO community at large, classification processing will have to be applied by UXO contractors using widely available instruments and software. The NAEVA results shown here illustrate current capabilities at Camp San Luis Obispo, where NAEVA both collected and analyzed the EM61 CART data.

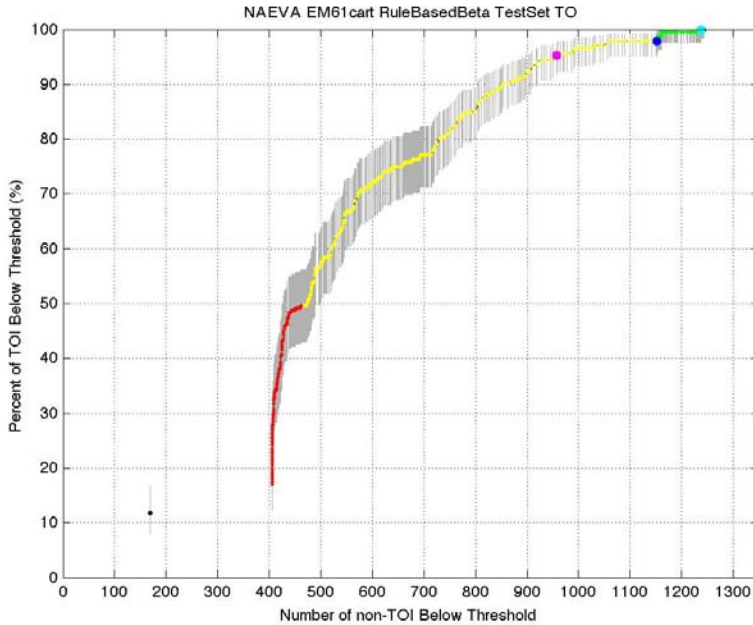
All three of the EM61-Mk2 instruments at Camp San Luis Obispo were set up in the four-time-gate mode to collect logarithmically spaced time gates out to approximately 1 ms [4, 6, 21]. Because of the single transmit and receive polarization, multiple spatially separated samples are required to ensure interrogation of all three target axes. UX-Analyze, one of the Oasis montaj modules, allows inversion of spatial data to determine the principal polarizabilities ( $\beta_1$ ,  $\beta_2$ ,  $\beta_3$ ) at each of the time gates. Because a TOI is

typically a body of revolution, with one large  $\beta$  value and two equal but smaller  $\beta$  values, the polarizabilities can be used to provide classification information. Polarizability decay rates ( $\tau$ ) between gates can also be calculated.

Figure 39 illustrates NAEVA's results using a technique that looks only at the  $\beta$  values. In the figure, the large number of "Cannot Analyze" locations are represented by the large gap between the dot in the lower left corner of the plot and the red end of the curve. Because the  $\beta$  determination requires data from multiple spatial locations, it is vulnerable to position noise. Hence, a large number of inversions did not converge. For those that did converge, the classification algorithm was able to state with confidence that very few of them were "Likely to Contain TOI." Instead, most were classified as "Cannot Decide." Even then, five true TOI locations incorrectly rose above the demonstrator's prospective "don't dig threshold." Three of the five contained relatively large items (4.2 in mortars). Based on geophysical models, it is estimated that 4.2 in mortars at depths near 30 cm would exhibit signatures with a surface footprint wider than the 0.5 m lane spacing used by the EM61 CART. Thus, the signatures of these large items must have been recorded by more than one pass of the cart. The necessity to stitch together multiple passes for the inversion adds to the potential of relative position noise to degrade the solution for the  $\beta$  values.

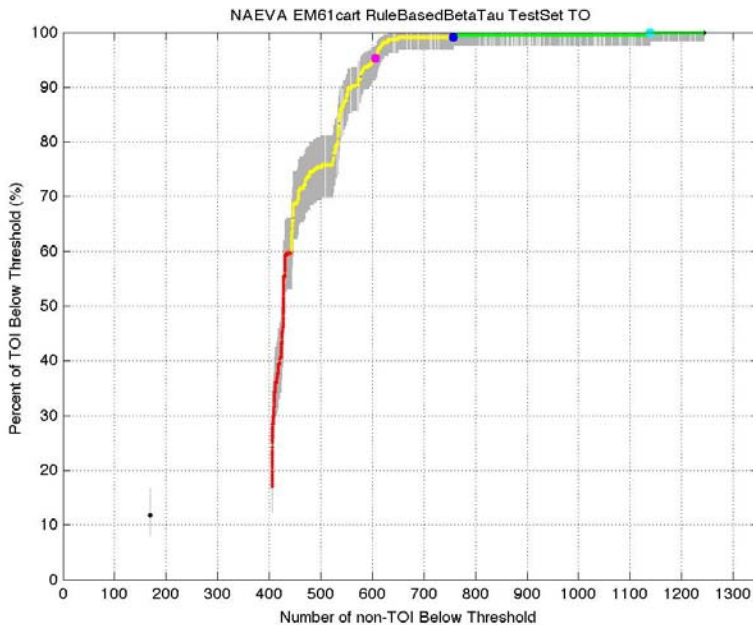
Contrast the results in Figure 39 with those in Figure 40, which use the same data set but employ an algorithm that uses the  $\beta$  and the  $\tau$  information to make a classification decision. The number of "Cannot Analyze" locations remains essentially the same, but the number of locations classified as "Likely to Contain Only Non-TOI," those locations rising above the demonstrator's "don't dig threshold," increases dramatically. Of the locations above the demonstrator's "don't dig threshold," only two are true TOI.

Figure 41 is a performance curve provided by NAEVA in a retrospective analysis. For this case, the demonstrators used time-decay parameters that did not depend on the relative positions of data points [18]. Note that the number of "Cannot Analyze" locations was dramatically reduced. At the demonstrator's "don't dig threshold" (dark-blue dot), the *Percent of TOI Below Threshold* was 100% and the *Number of Non-TOI Below Threshold* was reduced from its maximum value by more than 500 (the horizontal distance between the dark-blue dot and the green end of the curve). This means that by applying the demonstrator's "don't dig threshold" to the ranked anomaly list, over 500 unnecessary digs (44%) could have been avoided without leaving a single true TOI in the ground.



True TOI Locations Above Don't Dig Threshold	
Master ID	Ground Truth
326*	4.2*
404*	4.2*
365*	4.2*
304*	60*
188*	2.36*
367	60
66	60
79	60
290	60
197	60
249	60

Figure 39: NAEVA’s primary scoring results for the EM61 CART and the “Rule Based Beta” classification algorithm. Five true TOI locations incorrectly rose above the prospective “don’t dig threshold” (dark-blue dot).



True TOI Locations Above Don't Dig Threshold	
Master ID	Ground Truth
326*	4.2*
404*	4.2*
60	60
1456	60
59	60
1108	60
160	60
275	60
1483	60
443	60
19	60

Figure 40: NAEVA’s primary scoring results for the EM61 CART and the “Rule Based Beta Tau” classification algorithm. Two true TOI locations incorrectly rose above the prospective “don’t dig threshold” (dark-blue dot).

Parsons also employed target-decay parameters for its classification algorithm. While Parsons was significantly more conservative than NAEVA in setting the prospective “don’t dig threshold,” the shape of the curve (Figure 42) is very similar to

that of Figure 41. Furthermore, no true TOI locations rose above their “don’t dig threshold.”

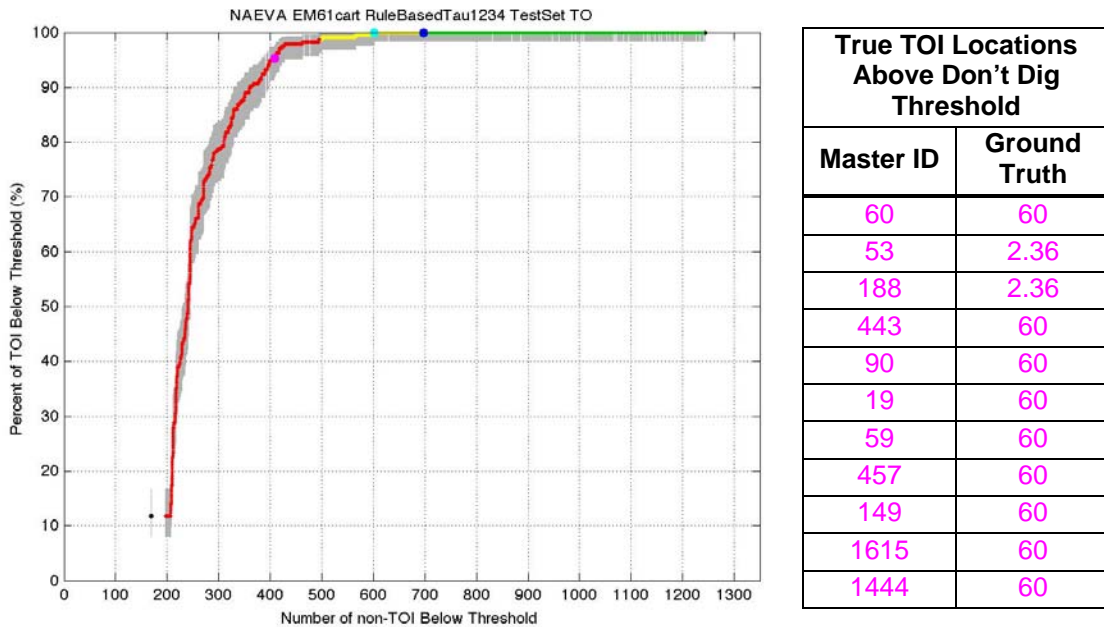


**Figure 41: NAEVA’s primary scoring results for the EM61 CART and the “Rule Based Tau 1234” classification algorithm in a retrospective analysis. No true TOI locations rose above the prospective “don’t dig threshold” (dark-blue dot).**

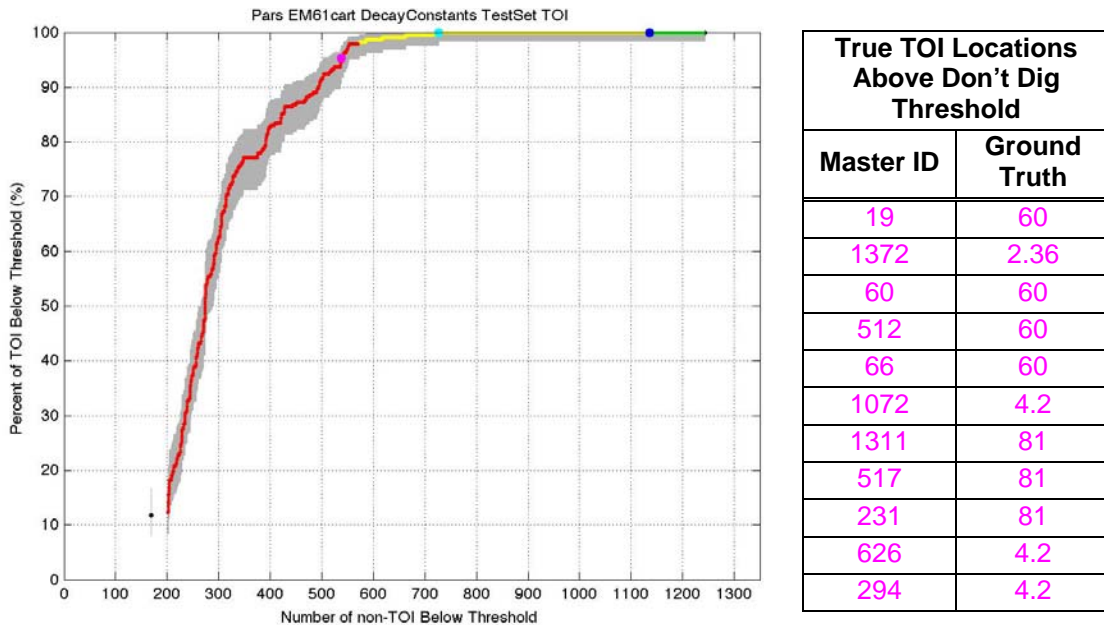


**Figure 42: Parson’s primary scoring results for the EM61 CART and the “Decay Constants” classification algorithm. No true TOI locations rose above the prospective “don’t dig threshold” (dark-blue dot).**

The Corps of Engineers, Huntsville Center (CEHNC) also applied the Oasis montaj commercial software to the EM61 CART data. For this case, the analysts used a

two-pass process for classification [23, 24]. In the first pass, they submitted a ranked anomaly list containing all locations assigned to the Standard Test Set. They requested ground truth information on all locations that fell below their prospective “don’t dig threshold,” because in a real-world scenario, this information would be available post-dig and could be used as a quality-control tool. In the second pass, they reassessed the position of their “don’t dig threshold” based on the new ground truth information. Specifically, they used the new information to adjust their classification rules regarding size,  $\tau$ , and SNR. As a result, some of the remaining unlabeled locations in the test set were moved from the “Likely to Contain Only Non-TOI” to the “Likely To Contain TOI” categories. These locations were effectively moved below the revised “don’t dig threshold,” along with all other locations already placed there during the first pass of classification. The analysts considered conducting a third classification pass and requested the ground truth information of all new locations placed under the revised “don’t dig threshold.” Analysis of this information showed that a third pass was not needed.

Figure 43 shows the results of their first classification pass. One 60 mm mortar incorrectly rose above the demonstrator’s initial “don’t dig threshold” (listed in blue with an asterisk in the table). Figure 44 is a photograph of this particular item. The TOI is missing its fuze and tail boom, giving rise to a significantly lower signal and resulting in a lower aspect ratio than a complete 60 mm mortar. This type of TOI challenged a number of the demonstrators, particularly when the items were relatively deep and exhibited a low SNR.

In the second pass of classification, no true TOI rose above the demonstrator’s revised “don’t dig threshold,” as shown in Figure 45. The revised threshold (dark-blue dot) was near optimum, as it was very close to the retrospective “100%” “don’t dig threshold” (light-blue dot). The demonstrator’s revised “don’t dig threshold” would have left no true TOI in the ground while avoiding approximately 400 unnecessary digs. Note that in the second classification pass, all 11 items that rose above the retrospective “95%” “don’t dig threshold” were 60 mm mortar rounds missing their fuze and tail booms, a type of TOI that proved difficult to classify for many demonstrators. The ability to obtain the ground truth information from the first pass of classification clearly helped the analysts understand the characteristics of the items close to the initial “don’t dig threshold,” allowing successful adjustment of the threshold for the second pass.

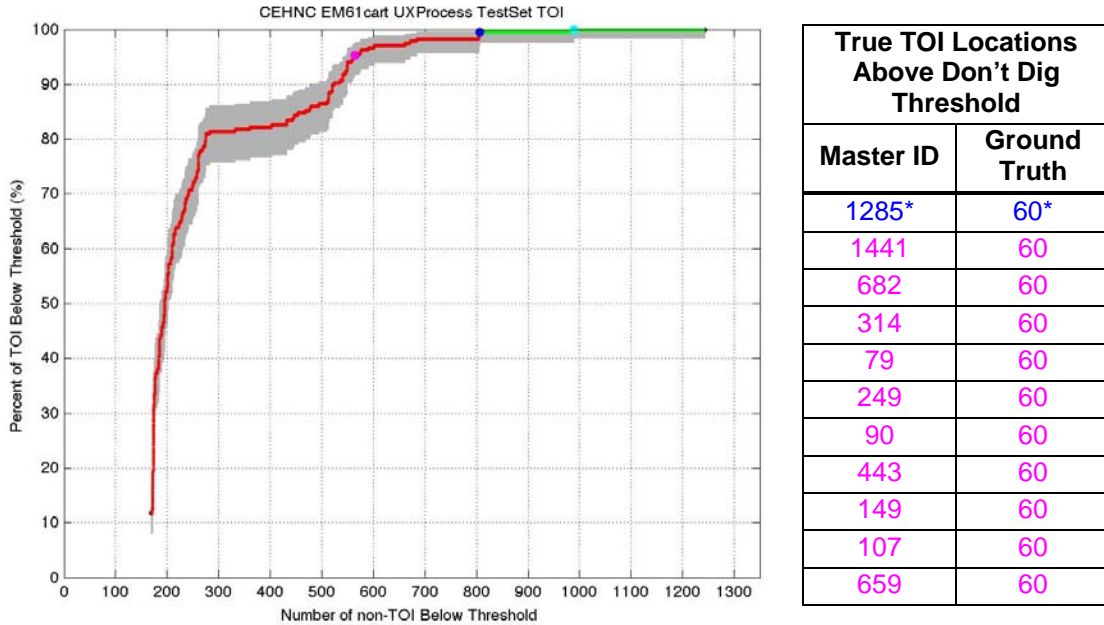


Figure 43: CEHNC's primary scoring results for the EM61 CART and the UX-Process classification software, first pass. One true TOI location incorrectly rose above the demonstrator's prospective "don't dig threshold" (dark-blue dot).

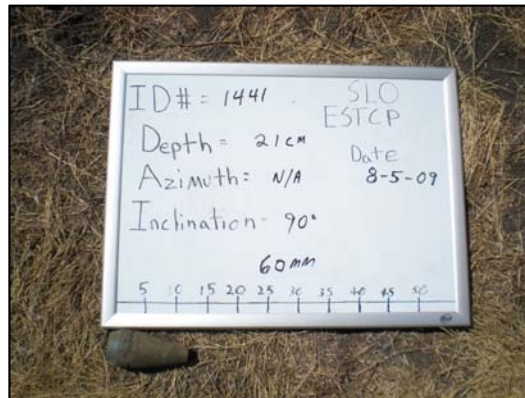
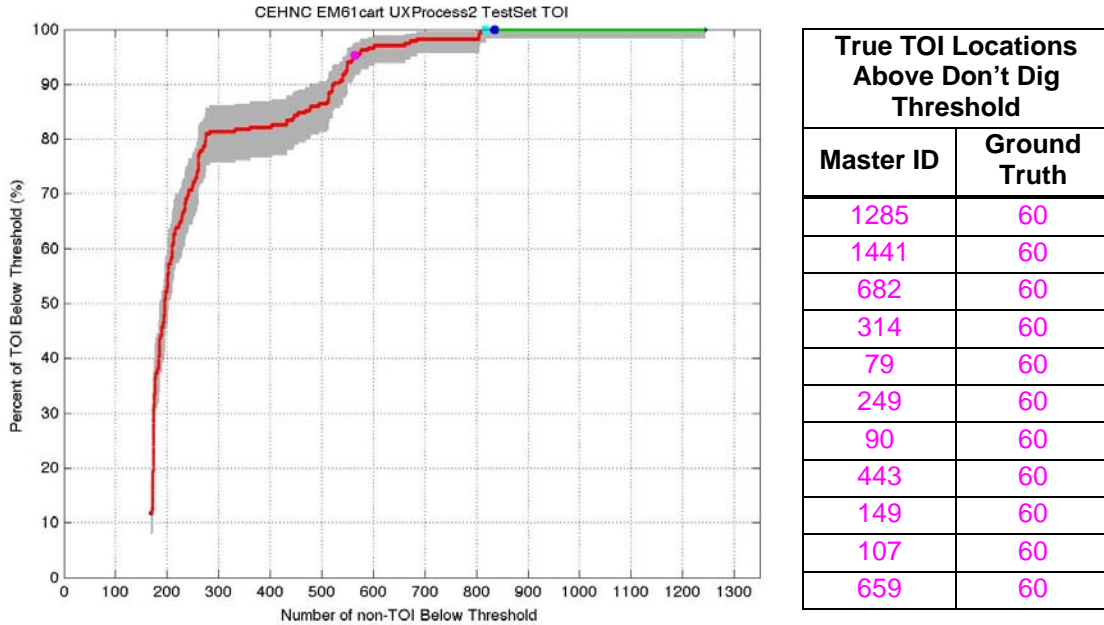
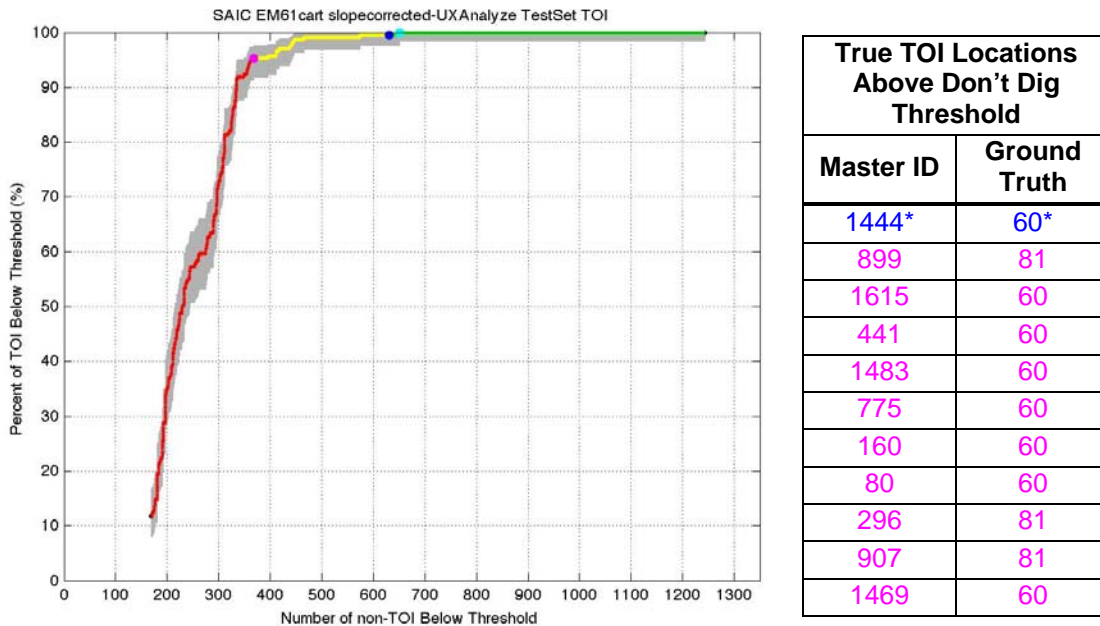


Figure 44: The TOI recovered from location #1285, a 60 mm mortar missing the fuze and tail boom. The TOI recovered from location #1444 was similar.



**Figure 45: CEHNC’s primary scoring results for the EM61 CART and the UX-Process classification software, second pass. The software was optimized over the Standard Training Set *plus* the subset of the Standard Test Set that had fallen below the demonstrator’s “don’t dig threshold” during the first classification pass. The optimized software was then re-applied to the entire Standard Test Set. No true TOI locations rose above the demonstrator’s revised “don’t dig threshold” in the second classification pass (dark-blue dot).**

A final example of commercial software combined with EM61 CART data was produced by SAIC, who did much of the work to implement classification algorithms into Oasis montaj and thus is likely the organization most familiar with that software and its use. Figure 46 shows the performance results obtained using a generalized likelihood ratio test (GLRT) classifier based on item size and decay characteristics. The one true TOI location just above the prospective “don’t dig threshold,” location #1444, contained a 60 mm partial round that looks identical to the one shown in Figure 44. In its demonstration report [9], SAIC notes that the true TOI recovered from location #1444 met the size characteristic of “Likely to Contain TOI,” but its rapid decay moved it into the “Likely to Contain Only Non-TOI” category. Upon reexamining the EM61 CART data, it appears that a small object recovered near the true TOI and within the polygon of inverted data might have artificially reduced the apparent decay rate sufficiently to move the true TOI into the “Likely to Contain Only Non-TOI” region of feature space. Anomalies representing multiple closely spaced items challenged the demonstrators in the Camp San Luis Obispo study and are the subject of ongoing research. Comparing these SAIC results to the NAEVA results in Figure 41 shows very similar curves, but with SAIC choosing a somewhat more aggressive “don’t dig threshold.”



**Figure 46: SAIC’s primary scoring results for the EM61 CART (after slope correction) and the UX-Analyze classification software. One true TOI location incorrectly rose above the prospective “don’t dig threshold” (dark-blue dot).**

Because the survey instruments were tilted when collecting data on the side of the hill at Camp San Luis Obispo, the Program Office used slope-corrected data to determine anomaly locations and to correlate items among instruments to create the master anomaly list. As an analysis excursion, SAIC applied its UX-Analyze processing to both slope-corrected and non-slope-corrected versions of the EM61 CART data, as shown in Figure 46 and Figure 47. In this case, the slope correction made very little difference in the performance, with both ranked anomaly lists having the same 60 mm partial mortar round incorrectly rising above the demonstrator’s “don’t dig threshold.” Furthermore, the majority of the TOI between the demonstrator’s “don’t dig threshold” and the “95%” “don’t dig threshold” was common to both ranked anomaly lists.

The results at Camp San Luis Obispo based on the use of the EM61-Mk2 data and commercial inversion and classification software are encouraging. Performance curves clearly indicate that this combination of commercial instruments and algorithms has significant classification capability against the TOI types encountered. While occasional problems were seen with larger TOI (4.2 in and 81 mm mortars), most problems involved the small 60 mm rounds that were missing the fuze and tail boom.

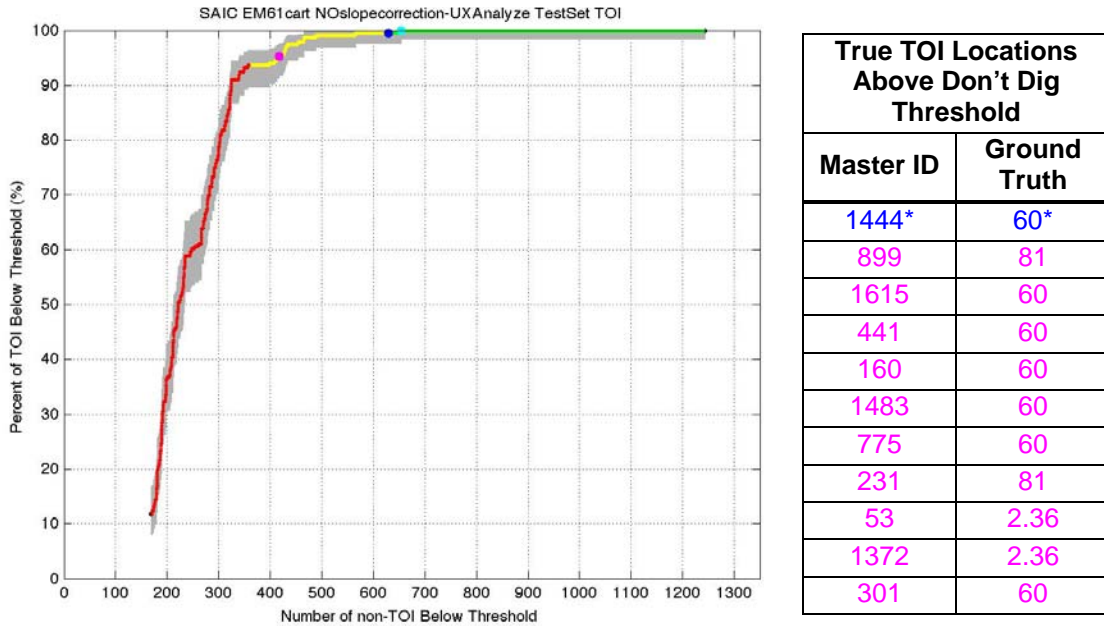


**Figure 47: SAIC’s primary scoring results for the EM61 CART (*before* slope correction) and the UX-Analyze classification software. One true TOI location incorrectly rose above the prospective “don’t dig threshold” (dark-blue dot).**

### 3.2.1.1 Conventional Instruments with Custom Classification Software

A number of the demonstrators also produced ranked anomaly lists based on the conventional instruments but using their own inversion and classification algorithms. Results were mixed. The best cases showed results significantly better than those obtained using UX-Process or UX-Analyze. In general, however, the results were no better than those obtained using commercial software and were often worse. Figure 48 shows what is arguably the best performance curve produced from an EM61-Mk2 instrument. SIG produced this list using the EM61 MSEMS data and a parameterized neighborhood-based classification (PNBC) algorithm for semi-supervised learning. As shown by the curve, this instrument-algorithm combination would have avoided over 800 unnecessary digs (67%) while leaving no true TOI in the ground. Note that the last 11 true TOI recovered (listed in the table) would have been 60 mm mortars, most of which were missing the fuze and tail boom.

Only one demonstrator, Sky Research, performed cooperative inversions of the EM61 and MAG MSEMS data. Figure 49 shows the performance curve resulting from applying their decay-rate algorithm to features extracted from the MSEMS data using cooperative inversions. Sky’s “don’t dig threshold” would have avoided about 700 unnecessary digs (55%) while leaving no true TOI in the ground. Note, though, that this

55% reduction is smaller than the 67% reduction shown in Figure 48, in which the EM61 MSEMS data was inverted alone.

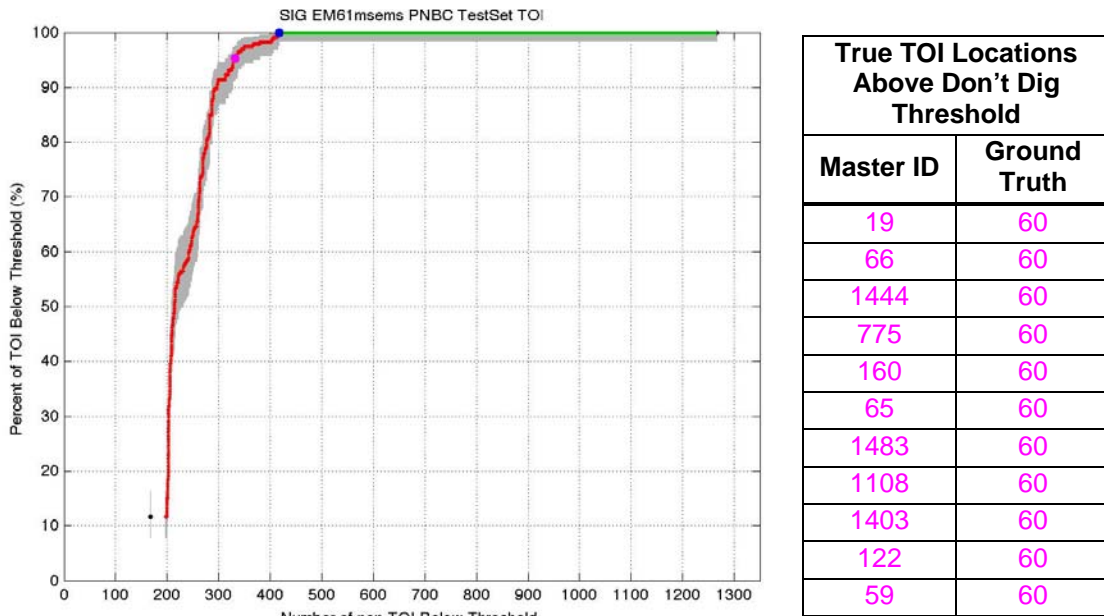


**Figure 48: SIG's primary scoring results for the EM61 MSEMS and the PNBC semi-supervised learning classification algorithm. No true TOI locations rose above the prospective "don't dig threshold" (dark-blue dot).**

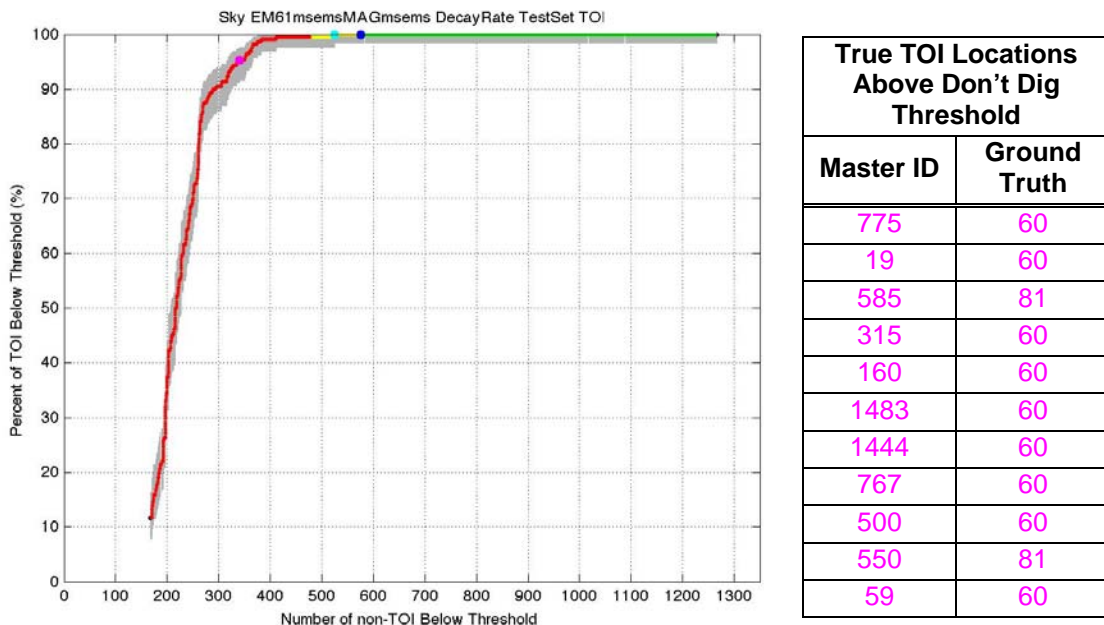


**Figure 49: Sky's primary scoring results for cooperative inversions of the EM61 MSEMS and MAG MSEMS sensors and the "Decay Rate" classification algorithm. No true TOI locations rose above the prospective "don't dig threshold" (dark-blue dot).**

Sky Research also applied its time-decay algorithm to the EM61 CART data, leading to very good results. As Figure 50 shows, this algorithm-instrument combination

would have also avoided approximately 700 unnecessary digs (56%) while leaving no true TOI in the ground. Most of the last true TOI recovered (listed in the table) would have been 60 mm mortars. Four of these same TOI were also listed for Figure 48.

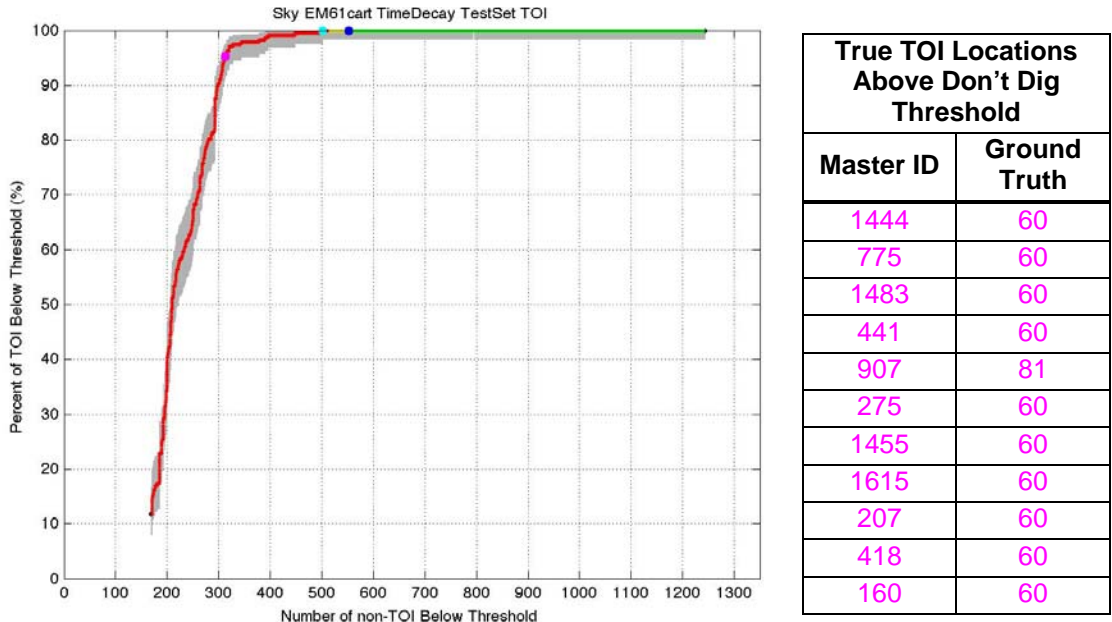


**Figure 50: Sky’s primary scoring results for the EM61 CART and the “Time Decay” classification algorithm. No true TOI locations rose above the prospective “don’t dig threshold” (dark-blue dot).**

In general, the results for the EM61 ARRAY at Camp San Luis Obispo were somewhat poorer than those for the cart-based instruments, in spite of its larger transmit moment and better sensor-to-sensor relative position precision along a survey line. This is most likely due to motion noise from towing the ARRAY across terrain with potholes and rocks. For example, Sky Research applied the same algorithm to the ARRAY data (Figure 51) that it had applied to the CART data (Figure 50). One 60 mm partial round—the same one as for the SAIC analysis of CART data—fell just above the prospective “don’t dig threshold.” According to Sky’s demonstration report [7], residual misfit (data minus model) plots of the true TOI recovered from location #1444 show a small area of high misfit to the right of the target in both the CART and ARRAY data. This bolsters SAIC’s contention that the inverted data included a small piece of scrap in addition to the 60 mm partial round [9]. For Sky’s analysis of the ARRAY data, most of the items between the prospective “don’t dig threshold” and the retrospective “95%” “don’t dig threshold” were 81 mm mortars, rather than the 60 mm partial rounds in SAIC’s analysis.

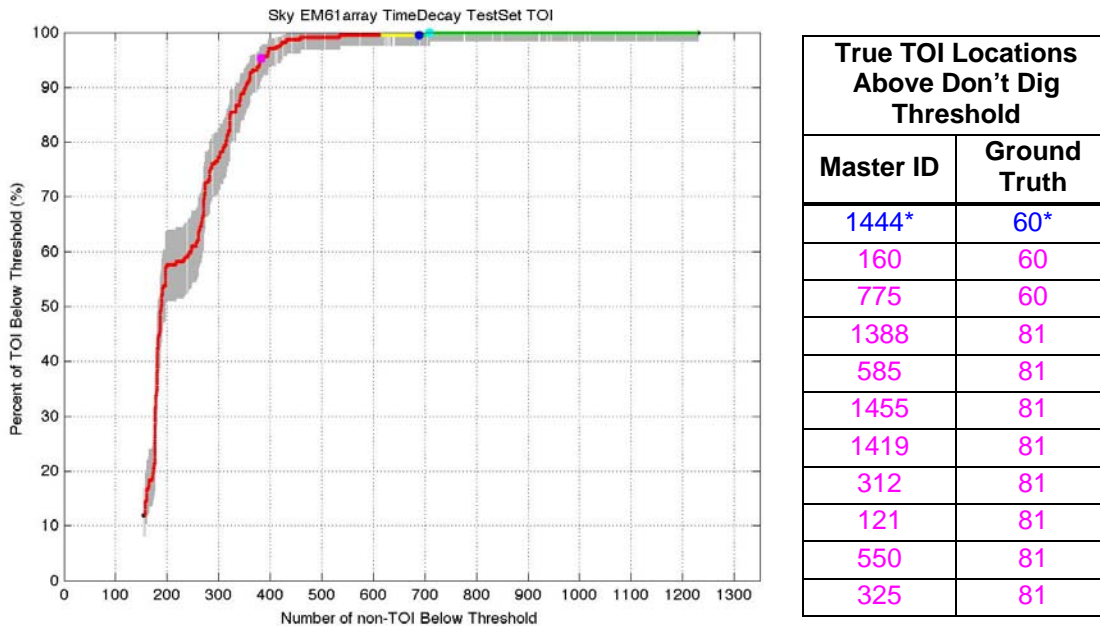
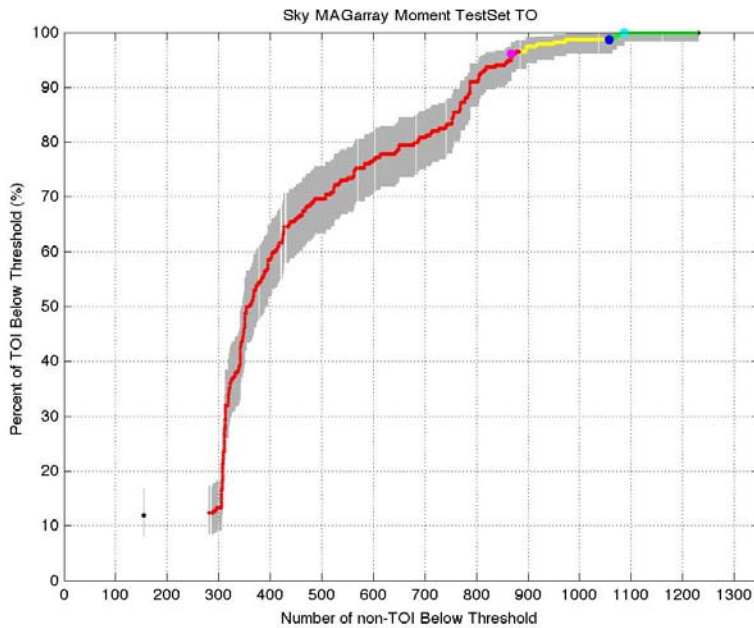


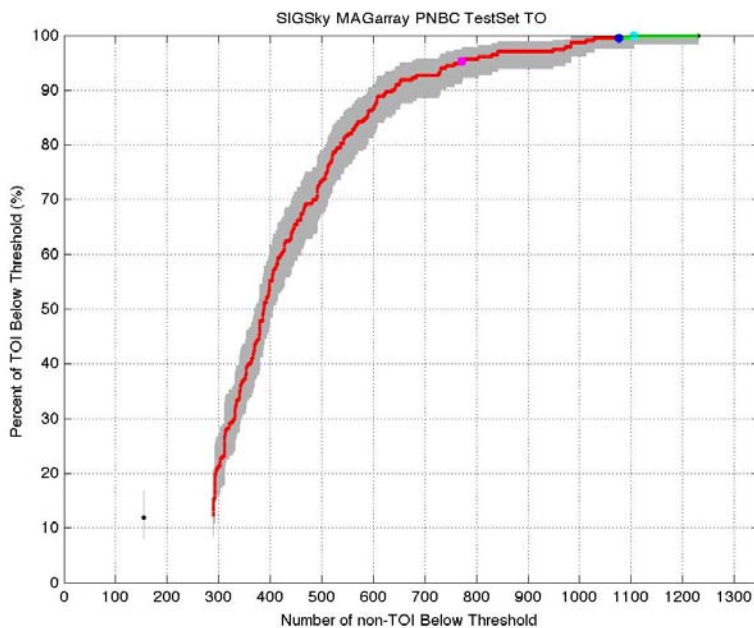
**Figure 51: Sky’s primary scoring results for the EM61 ARRAY and the “Time Decay” classification algorithm. One true TOI location rose above the prospective “don’t dig threshold” (dark-blue dot).**

The final conventional instruments used at Camp San Luis Obispo were the MAG ARRAY and the magnetometer sensor on the MSEMS. Because of adverse geology and the very large number of magnetometer anomalies, the magnetometers were only scored against their threshold crossings that were common with EMI anomalies. Figure 52 shows the results of a Sky analysis of the MAG ARRAY data, where only target size (magnetic moment) was used to rank the targets. Three of the smaller true TOI (60 mm mortars) incorrectly rose above the prospective “don’t dig threshold;” two of those were partial rounds employed as seed items. At the same time, fewer than 200 unnecessary digs (14%) could have been saved. This was the best of the magnetometer curves, demonstrating that more sophisticated algorithms were not the solution to poor magnetometer performance. Figure 53, the second-best curve, results from SIG applying its PNBC algorithm to magnetic parameters provided by Sky. One true TOI location rose above the demonstrator’s “don’t dig threshold” while only approximately 150 unnecessary digs (13%) were saved. Appendix B shows the remaining performance curves based on magnetometer data. They are significantly worse than these two, with some approaching the chance diagonal. With size as the major feature available from magnetometer data, it is clear that for sites like Camp San Luis Obispo, with multiple types of TOI of various sizes, magnetometers do not make successful classification sensors.



True TOI Locations Above Don't Dig Threshold	
Master ID	Ground Truth
600*	60*
1108*	60*
776*	60*
19	60
732	60
275	60
249	60
207	60
103	60

**Figure 52: Sky's primary scoring results for the MAG ARRAY and the "Moment" classification algorithm. Three true TOI locations rose above the prospective "don't dig threshold" (dark-blue dot).**



True TOI Locations Above Don't Dig Threshold	
Master ID	Ground Truth
600*	60*
1108	60
776	60
103	60
732	60
464	2.36
19	60
1189	81
708	60
15	60
192	60

**Figure 53: SIG's primary scoring results for the MAG ARRAY and the PNBC semi-supervised learning classification algorithm. (Sky estimated the parameters input to the algorithm.) One true TOI location incorrectly rose above the prospective "don't dig threshold" (dark-blue dot).**

An additional objective of this demonstration was to provide a second test of the active-learning concept. Active learning uses information-theoretic techniques to pick those training data that can provide the most information to a classifier. The objective of

active learning is to use a smaller set of training data to produce classification results that are as good as or better than those results obtained from the full set of training data [12]. The technique was applied in the Camp Sibert demonstration, but did not result in superior classification performance over standard training techniques [13]. Because Camp Sibert contained only one TOI type with size as an excellent discriminant, it perhaps did not provide enough opportunity for active learning to display an improved performance over standard training methods. Thus, SIG was tasked to test its active-learning techniques against the more challenging data set at Camp San Luis Obispo.

Figure 54 and Figure 55 show the performance curves for SIG’s analysis of EM61 ARRAY data using a relevance vector machine (RVM) supervised learning classifier optimized over the Standard Training Set and the Active Learning Training Set, respectively. In this case, active learning fared much more poorly than standard training. Although active learning used fewer training data, that advantage was almost offset by an increased number of “Cannot Analyze” locations, as demonstrated by the red sections of both curves ending in approximately the same place. In addition, active learning resulted in 43 true TOI locations rising incorrectly above the prospective “don’t dig threshold” (only the first 11 are listed in the table). In contrast, only three true TOI rose above threshold for standard training.

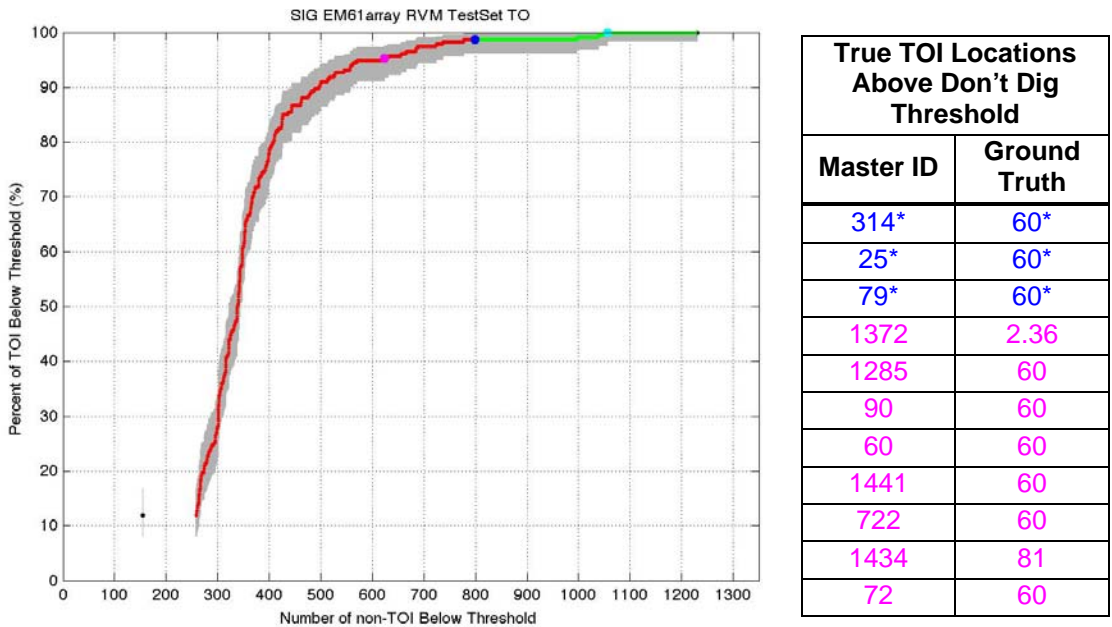


**Figure 54: SIG’s primary scoring results for the EM61 ARRAY and the RVM supervised learning classification algorithm. The algorithm was optimized over the Standard Training Set and applied to the complementary Standard Test Set. Three true TOI locations incorrectly rose above the prospective “don’t dig threshold” (dark-blue dot).**

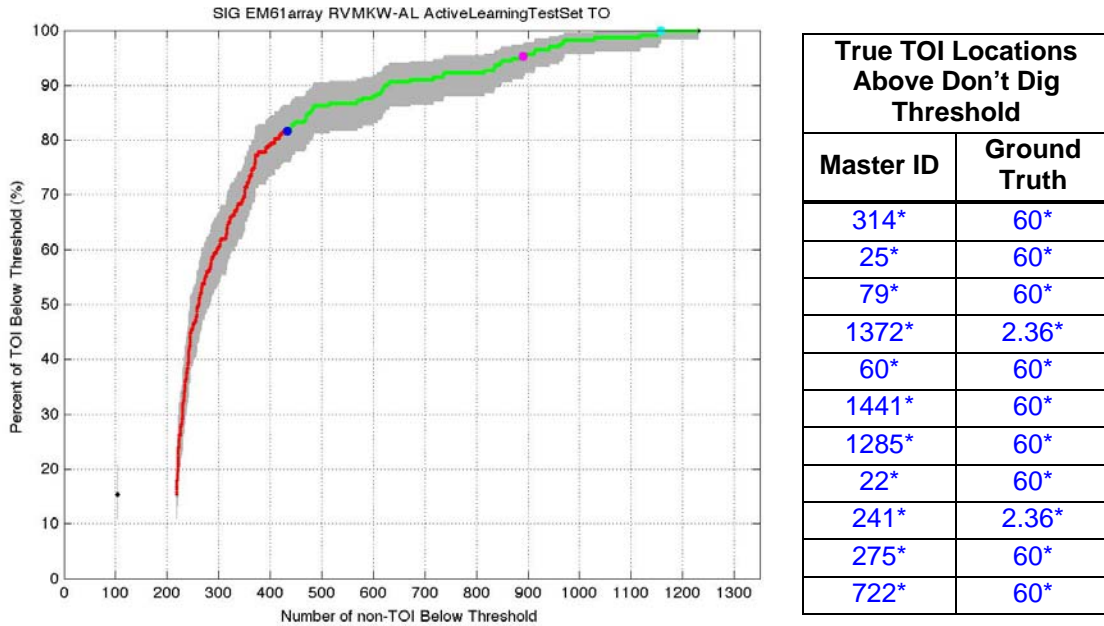


**Figure 55: SIG’s primary scoring results for the EM61 ARRAY and the RVM supervised learning classification algorithm. The algorithm was optimized over the Active Learning Training Set and applied to the complementary Active Learning Test Set. Forty-three true TOI locations rose above the prospective “don’t dig threshold” (dark-blue dot), the first 11 of which are listed in the table.**

SIG also provided some ranked anomaly lists produced with its classification algorithms operating on inversion parameters provided by Sky, an organization with significantly more experience inverting geophysical data. Figure 56 is directly comparable to Figure 54. On the surface, there is not much difference between the shapes of the two performance curves or the threshold placement, although the Sky-inverted data does put one fewer true TOI above the “don’t dig threshold.” However, the Sky inversions do result in almost 100 fewer “Cannot Analyze” locations, and the true TOI nearest the top of the ranked anomaly list is almost 200 ranks further down the list for the Sky inversions than for SIG’s own inversions. In addition, one of the true TOI above threshold was recovered from location #1285, the partial 60 mm mortar round shown in Figure 44; this location challenged many of the demonstrators and was considered particularly difficult to classify correctly. Thus, the choice of the polygon used to circumscribe the anomaly and the data-processing routine used to invert the circumscribed anomaly do affect the performance of this classification algorithm.

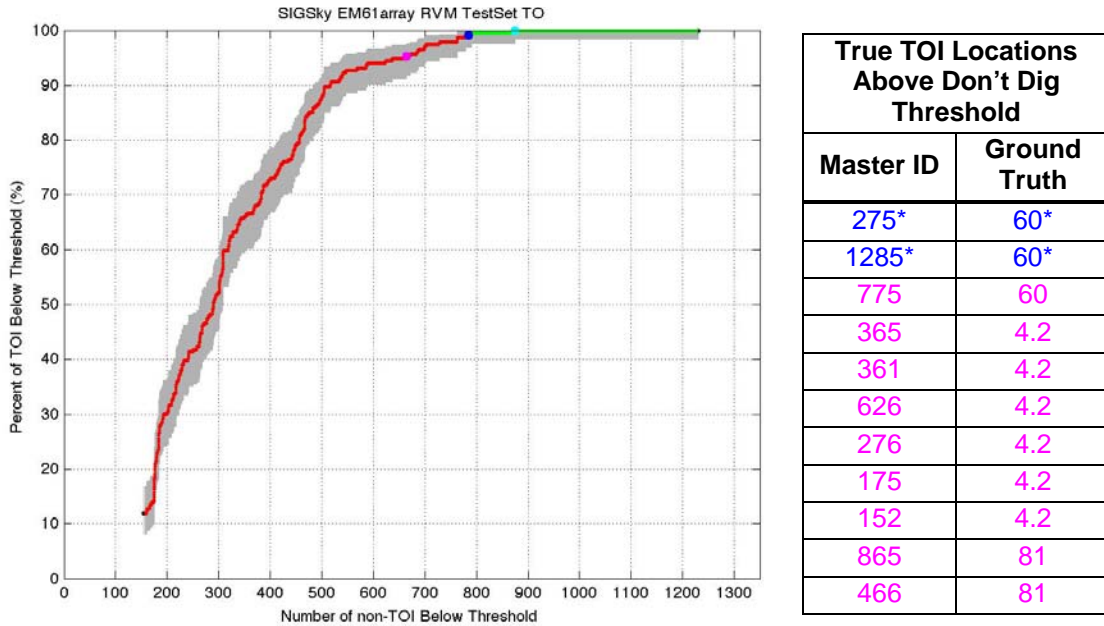
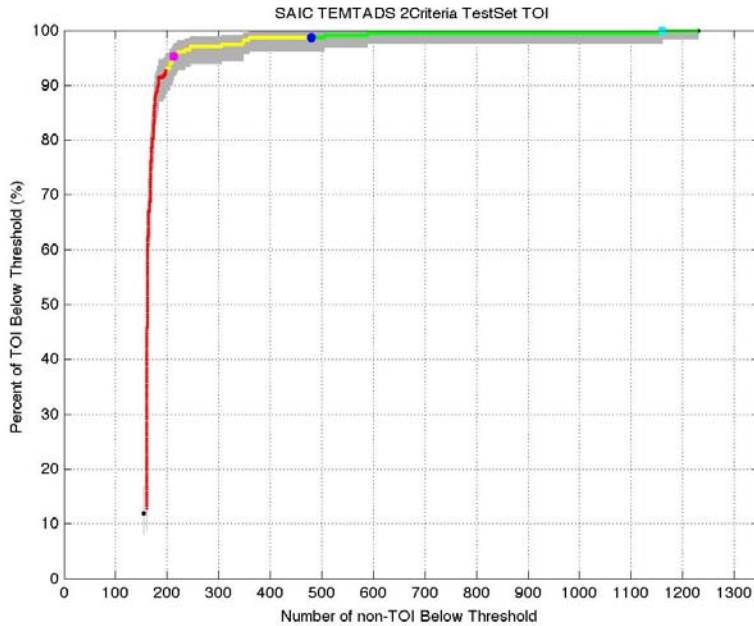


**Figure 56: SIG’s primary scoring results for the EM61 ARRAY and the RVM supervised learning classification algorithm. (Sky estimated the parameters input to the algorithm.) The algorithm was optimized over the Standard Training Set and applied to the complementary Standard Test Set. Two true TOI locations incorrectly rose above the prospective “don’t dig threshold” (dark-blue dot).**

### 3.2.2 Advanced Instruments

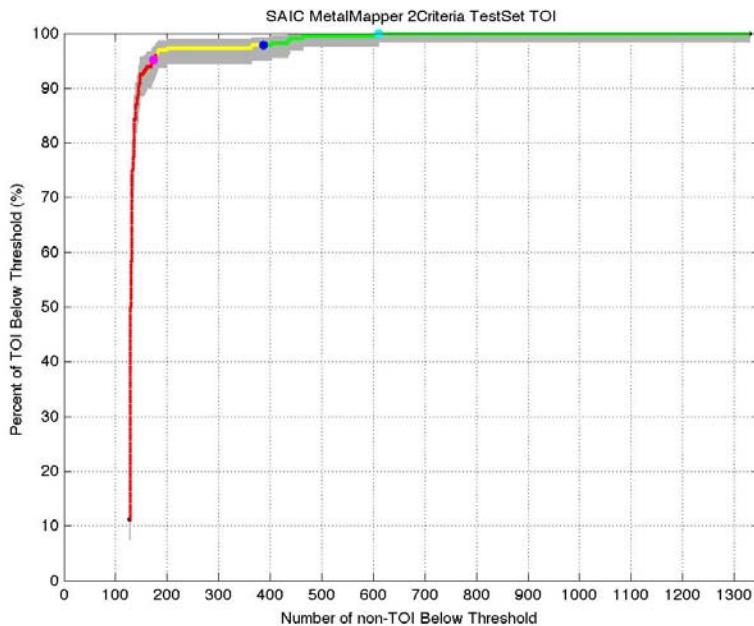
Two advanced instruments, the TEMTADS and the MetalMapper, collected cued data over the entire demonstration area at Camp San Luis Obispo. The TEMTADS cued off the EM61 ARRAY anomalies; the MetalMapper was self-cued. As such, the cued data locations are not identical, but they are comparable, and it is useful to look at results employing the same classification algorithm applied to both cued data sets.

Figure 57 and Figure 58 illustrate the results obtained by SAIC for the two instruments using its “2 Criteria” algorithm. The two criteria were the amplitude of the largest beta value ( $\beta_1$ ) as well as the ratio of  $\beta_1$  to the second largest value ( $\beta_2$ ). Both parameters were evaluated in all time gates. The classification procedure employed a library match algorithm [9]. The results for the two instruments are similar, and as is the case for most of the classification performance curves for these two instruments, both have a very steep initial slope. This indicates that most true TOI were easily distinguished from true non-TOI. However, for both instruments, the prospective “don’t dig threshold” was set too aggressively and would have incorrectly left some true TOI in the ground.



True TOI Locations Above Don't Dig Threshold	
Master ID	Ground Truth
241*	2.36*
444*	2.36*
711*	60*
103	60
79	60
90	60
1450	81
1285	60
428	3
976	60
275	60

**Figure 57: SAIC’s primary scoring results for the TEMTADS and the “2 Criteria” classification algorithm. Three true TOI locations rose above the prospective “don’t dig threshold” (dark-blue dot).**



True TOI Locations Above Don't Dig Threshold	
Master ID	Ground Truth
775*	60*
1285*	60*
1372*	2.36*
314*	60*
1469*	60*
1475	2.36
1502	37
428	3
600	60
1315	60
500	60

**Figure 58: SAIC’s primary scoring results for the MetalMapper and the “2 Criteria” classification algorithm. Five true TOI locations incorrectly rose above the prospective “don’t dig threshold” (dark-blue dot).**

Failure analyses focused on the true TOIs that appeared near the very top of the ranked anomaly lists, well into the “Likely to Contain Only Non-TOI” category. Figure 59 shows a photograph of the items recovered from location #241/1475. This location is labeled as a true 2.36 in rocket. As can be seen in the photograph, however, multiple

items were recovered from this location, including a 2.36 in rocket motor body, a handful of separate fins, and a 60 mm mortar tail boom. Multiple items were also recovered from location #444, including a 2.36 in rocket body.

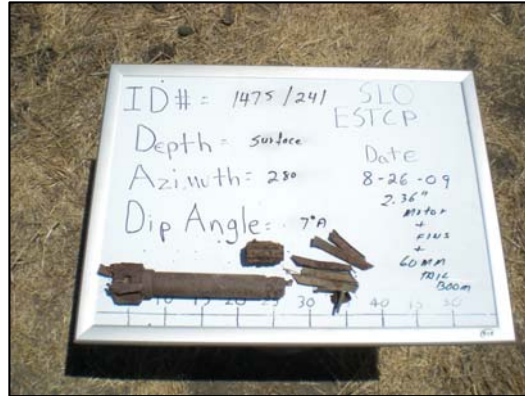


**Figure 59: Items recovered from location #241/1475. This location challenged many instrument-algorithm combinations.**

Figure 60 and Figure 61 similarly compare TEMTADS and MetalMapper results from a Sky analysis. Results are based on the primary polarization amplitude and decay parameters input into a nonparametric statistical classifier [7]. Again, location #241/1475 heads the list of true TOI that incorrectly rose above the prospective “don’t dig threshold,” with 60 mm partial rounds also causing problems. In the MetalMapper case, Sky also missed the 37 mm mortar, but in their demonstration report stated that the object’s slow decay would have allowed it to be correctly classified if Sky had expected items that small [7].

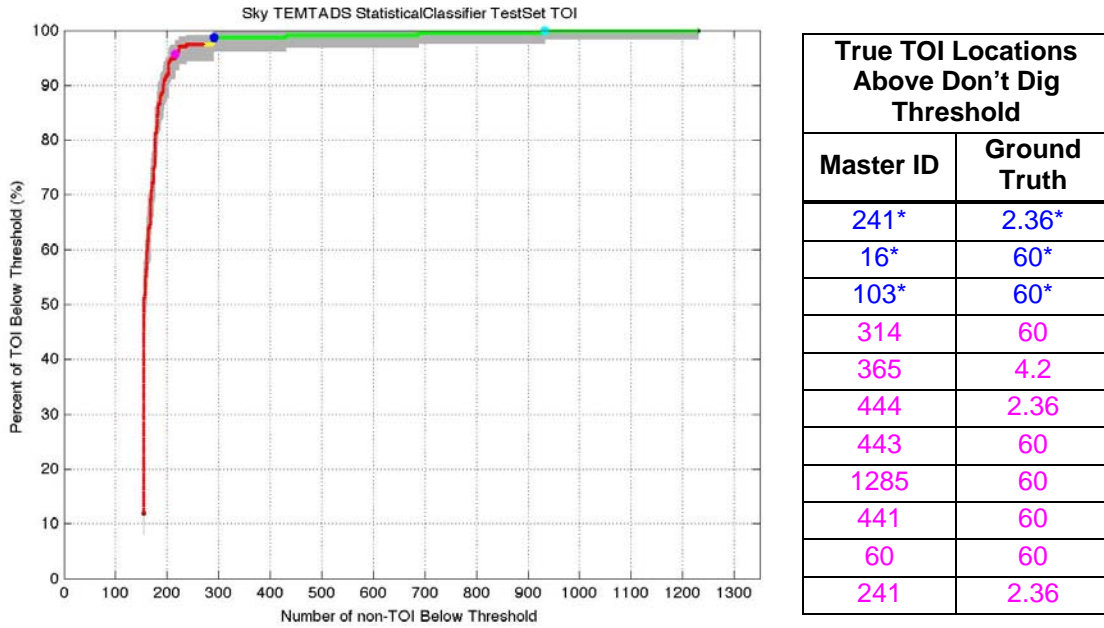


**Figure 60: Sky’s primary scoring results for the TEMTADS and the “Statistical Classifier” classification algorithm. Three true TOI locations incorrectly rose above the prospective “don’t dig threshold” (dark-blue dot).**

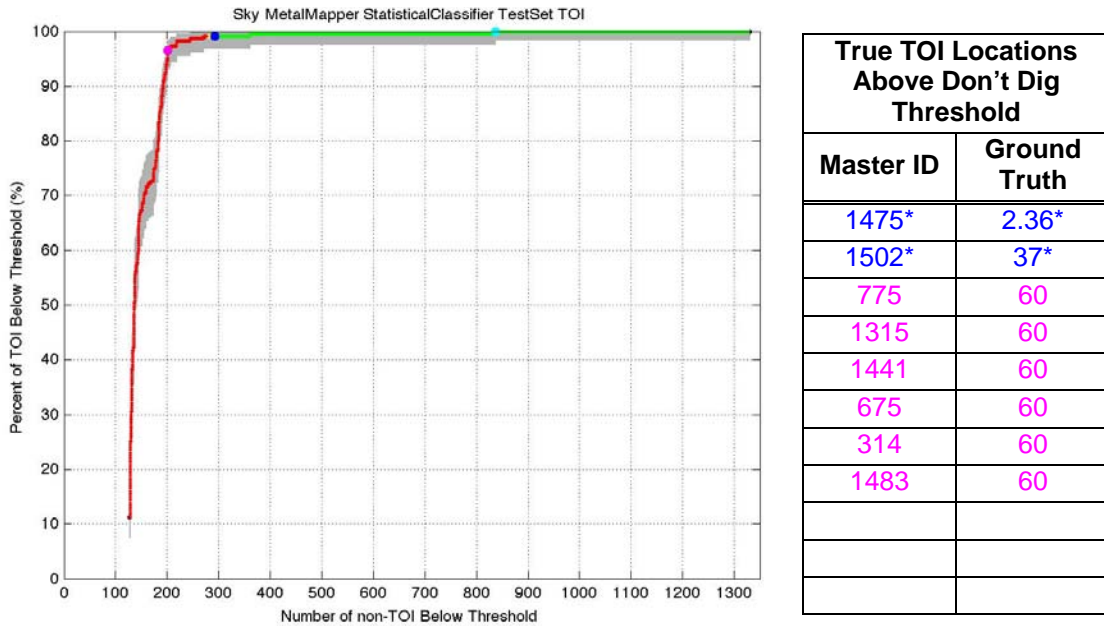


**Figure 61: Sky’s primary scoring results for the MetalMapper and the “Statistical Classifier” classification algorithm. Two true TOI locations incorrectly rose above the prospective “don’t dig threshold” (dark-blue dot).**

Geometrics, the developer of the MetalMapper, obtained similar results, as shown in Figure 62. The Geometrics classifier used a three-stage process. The first stage tested whether the SNR was sufficient and whether a reasonable inversion fit to the data was obtained. The second stage classified as “Likely to Contain Only Non-TOI” any locations

for which the inverted size parameter was significantly smaller than a 60 mm mortar (the smallest expected TOI on the site). This resulted in a missed classification of the one unexpected 37 mm mortar found on the site. The final stage of the classifier employed an artificial neural network and library matching routine, where the neural network was trained on a combination of the provided training data and additional data on TOIs measured in the test pit. In addition to the 37 mm mortar, location #241/1475 and a fused 60 mm mortar with a portion of tail boom and piece of fuze also incorrectly rose above the prospective “don’t dig threshold.”

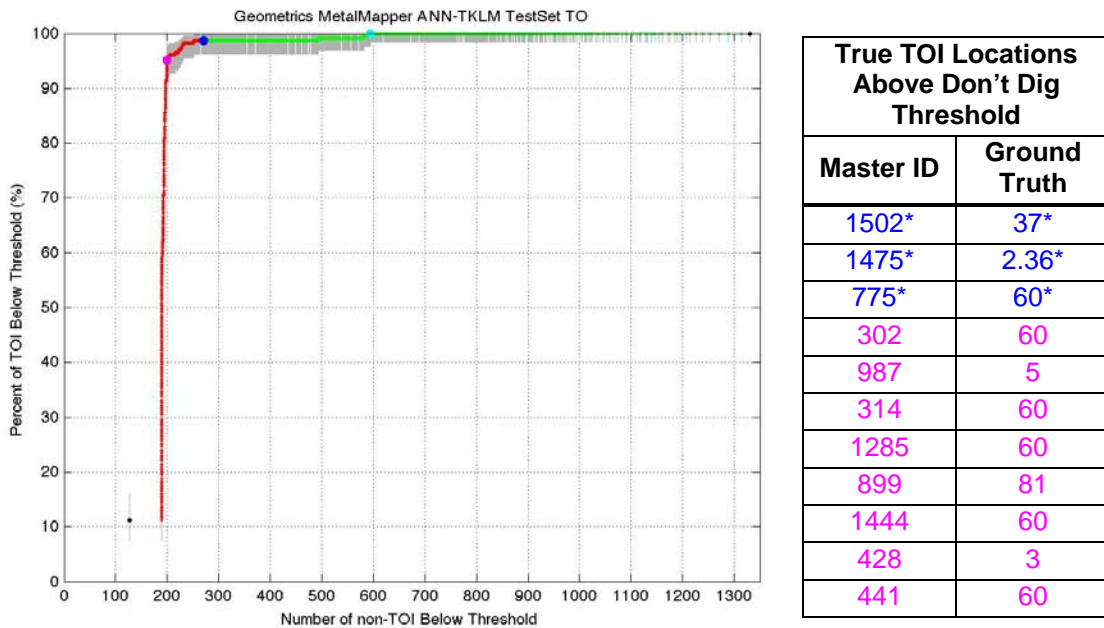


**Figure 62: Geometrics’ primary scoring results for the MetalMapper and the “ANN-TKLM” classification algorithm. Three true TOI locations incorrectly rose above the prospective “don’t dig threshold” (dark-blue dot).**

BUD was the final cued instrument used at Camp San Luis Obispo. Because of its limited mobility, BUD covered only a subset of the demonstration area. Its Standard Test Set consisted of only 473 locations, 59 of which contained true TOI. To compare, all other instruments used a Standard Test Set consisting of approximately 1300 locations, with approximately 200 containing true TOI. Hence, the error bars on the BUD performance curves are much longer than those for the other instruments. Sky produced the “best” results for the BUD data, using a probabilistic neural network (PNN) classifier applied to a feature space consisting of size and time-decay parameters from the polarizability inversions. The resulting performance curve is shown in Figure 63. The one true TOI above the prospective “don’t dig threshold” was recovered from location #241/1475, as it was for many other cases. The two true TOI locations just under the

prospective “don’t dig threshold” contained another 2.36 in rocket body accompanied by other munitions debris and a 60 mm partial round. This confirms that the same types of TOI challenged all advanced instruments.

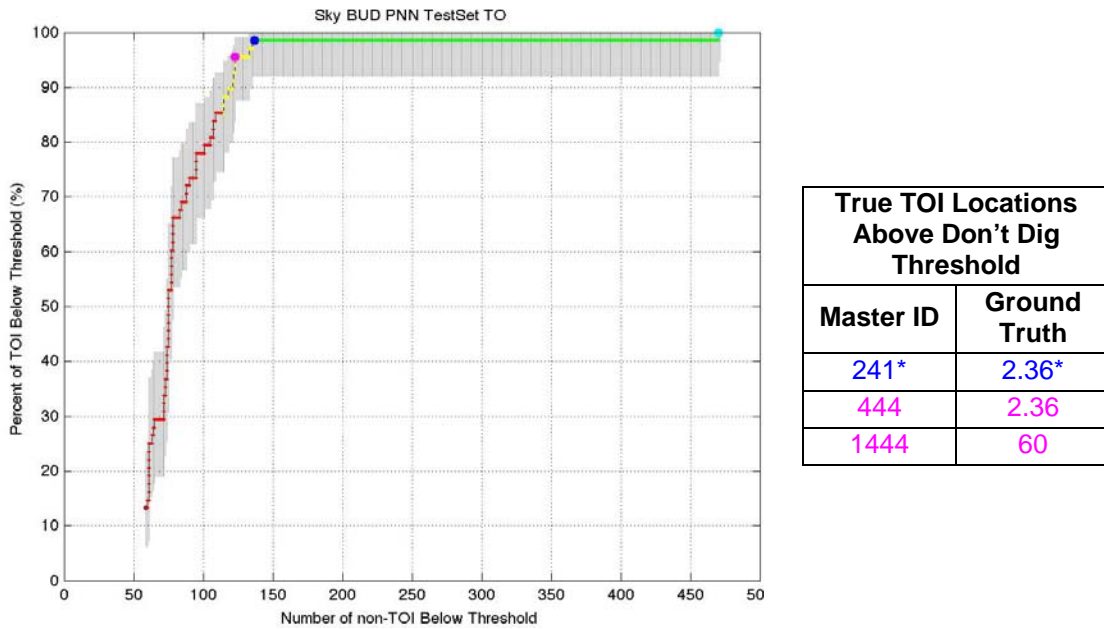


**Figure 63: Sky’s primary scoring results for the BUD and the PNN classification algorithm in a retrospective analysis. Results were scored over only the sub-areas of the site over which the BUD collected data. One true TOI location incorrectly rose above the prospective “don’t dig threshold” (dark-blue dot).**



## 4. FINDINGS AND CONCLUSIONS

### 4.1 FINDINGS

The results described in this document provide a second confirmation (to the results from Camp Sibert) that successful UXO classification is possible on a live site using currently available instruments and software. Specific findings from this demonstration are summarized below, grouped according to the stage of processing or the type of instrument or software to which they refer:

#### 4.1.1 Detection

- EMI-based instruments detected all or almost all seeds. A 0.75 m radius halo was used to associate detected anomalies with seeds. The EM61 MSEMS sensor detected all the emplaced seeds. The EM61 ARRAY missed one seed buried between two rocks where it was unable to maneuver. The missed coverage was noted, and in a real clearance action, the missed area would have been covered by a hand-held instrument or cart. The EM61 CART missed one seed, a 60 mm mortar missing the nose and tail boom. The EM61 CART's detection threshold, set based on a complete 60 mm mortar, was 11.3 mV, and the partial round was 10.7 mV, just under threshold. For detection thresholds based on the smallest signal expected from TOI, care must be taken to understand all possible TOIs. The conclusion is further reinforced by the fact that the MetalMapper missed detecting four of the seeds in its survey. All four were partial 60 mm rounds, three buried 30 cm below the surface and one buried 45 cm below the surface.
- The MAG ARRAY also detected all the emplaced seeds that it was able to survey, missing the same seed as the EM61 ARRAY. But this complete detection was at the cost of over 5200 detected anomalies, compared with the 1464 unique anomalies that exceeded the detection threshold for the EM61 ARRAY. By the time the MSEMS magnetometer data collection was completed, the decision had been made to score only those magnetic anomalies that coincided with EMI anomalies. Therefore, the MSEMS magnetometer anomalies were not scored against the seeds to determine detection performance.

## **4.1.2 Classification**

### **4.1.2.1 Commercially Available Instruments and Software**

- Commercially available instruments and software often led to very good classification performance. The better performers using EM61-Mk2 data and UX-Analyze or UX-Process selected “don’t dig thresholds” that would have left no true TOI in the ground while reducing the unnecessary digs by 30% to 50%.
- In general, in spite of the EM61-Mk2’s limited decay-time coverage and having only four time gates, classification approaches based on principal polarizabilities and decay rate (size, shape, and wall thickness), or simply decay rate (wall thickness), provided better performance than approaches based on comparisons of principal polarizability values alone (size and shape).
- In the one case where dig results were used to refine classification parameters and revise the “don’t dig threshold,” the final ranked anomaly list placed all true TOI locations below the revised “don’t dig threshold” and reduced unnecessary digs by more than 30%.

### **4.1.2.2 Commercially Available Instruments and Custom Software**

- Some results using custom software and EM61-Mk2 data were better than those using commercial software, but some were worse. The best performance curve would have reduced unnecessary digs by 67% while digging all true TOI.
- Cooperative inversion of the EM61 MSEMS and magnetometer data produced good results, reducing unnecessary digs by 56%. However, that result was not as good as the best result using EM61 MSEMS data alone, which provided the 67% reduction in unnecessary digs.
- With correct placement of the “don’t dig threshold,” the best of the magnetometer-based ranked anomaly lists could have reduced unnecessary digs by only 14%. However, all the better performing of those lists had at least one true TOI location above the “don’t dig threshold.” Note also that only those magnetometer anomalies that corresponded to EMI anomalies were included on the ranked anomaly lists and scored. If all magnetometer anomalies were included in scoring, thousands more unnecessary digs would have resulted.

### **4.1.2.3 Advanced Instruments and Software**

- While there were problems with a few specific true TOI locations rising well above the demonstrators’ “don’t dig thresholds,” many of the classification performance curves for the MetalMapper and TEMTADS had near-right-

angle shapes, indicating a very clear separation in feature space between most true TOI and non-TOI.

- The true TOI items that challenged the advanced instruments were generally portions of 2.36 in rocket bodies close to other munitions debris. For example, location #241/1475 rose above the demonstrator's "don't dig threshold" on 13 of the 14 TEMTADS ranked anomaly lists and 7 of the 10 MetalMapper lists (and would have been the last true TOI recovered on 2 of the 3 ranked anomaly lists where it was below the "don't dig threshold"). Other items causing problems were typically low SNR items, particularly partial 60 mm mortars buried deeply.
- Active learning did not enhance performance in this demonstration.

#### 4.1.2.4 "Don't dig threshold"

- For the commercial EMI-based instruments, although demonstrators typically set the "don't dig threshold" somewhat aggressively (18 out of 28 ranked anomaly lists would have left at least one true TOI in the ground), 21 of the lists would have recovered over 98% of the true TOI, and all but 2 of the lists would have recovered over 95% of the true TOI. The two lists that would have recovered fewer than 95% of the true TOI were based on a supervised learning algorithm, one optimized over the Standard Training Set and the other over the Active Learning Training Set.
- For the advanced instruments, "don't dig thresholds" were uniformly aggressive, with only 1 of the 29 ranked anomaly lists showing all true TOI placed correctly below the "don't dig threshold." However, only one of the ranked anomaly lists (based on active learning) would have recovered fewer than 95% of the true TOI. Nineteen of the 29 would have recovered more than 98% of the true TOI.
- No clear metric indicated that either the MetalMapper or TEMTADS performed better than the other in this demonstration. Of the eight ranked anomaly lists for each instrument that were directly comparable, each proved superior on four (i.e., left fewer true TOI in the ground at the "don't dig threshold"). Averaged over the eight ranked lists, the MetalMapper would have left 3.9 true TOI per list in the ground; the TEMTADS would have left 3.6.
- On the whole, the BUD performance curves did not show the near right-angle-characteristics of many of the MetalMapper and TEMTADS curves, but the overall performance was still very good. At the demonstrators' "don't dig thresholds," only one of the five BUD ranked anomaly lists would have recovered fewer than 98% of the true TOI, and that list would have recovered 95%. Again, 2.36 in rocket bodies and partial 60 mm mortar rounds were the

problem, with location #241/1475 containing the only true TOI missed on two of the lists.

#### **4.1.2.5 “Cannot Analyze” and “Cannot Decide” Locations**

- Different classification demonstrators used different criteria for placing anomalies in the “Cannot Analyze” category. The number of “Cannot Analyze” locations varied widely from instrument to instrument and among demonstrators for the same instrument. However, some trends are evident:
  - The number of “Cannot Analyze” locations at Camp San Luis Obispo was generally lower than the number at Camp Sibert.
  - The number of “Cannot Analyze” locations was generally lower for the advanced instruments than for the commercial EMI-based instruments.
  - For the commercial EMI-based instruments, demonstrators who had participated in the Camp Sibert demonstration had fewer “Cannot Analyze” locations than the new demonstrators.
  - Comparing the MetalMapper and TEMTADS using the 8 ranked anomaly lists in common, we found that the MetalMapper had fewer “Cannot Analyze” locations (2) than the TEMTADS (33) when the number of “Cannot Analyze” locations from all lists were summed.
- The number of “Cannot Decide” locations also varied among the locations, demonstrators, and algorithms, with some evident trends:
  - The advance instruments had fewer “Cannot Decide” locations than the commercial EMI-based instruments.
  - Comparing the eight lists common to the TEMTADS and MetalMapper, we found that MetalMapper typically had 50% to 75% the number of “Cannot Decide” locations than TEMTADS. However, except for the SAIC “2 Criteria” and “3 Criteria” ranked anomaly lists, where the MetalMapper “Cannot Decide” locations made up approximately 15% of the list and TEMTADS “Cannot Decide” locations made up approximately 25% of the list, the other six common lists typically had “Cannot Decide” locations as a few percent or less of the total number of locations.

## **4.2 CONCLUSIONS**

This second classification demonstration dealt with a much more difficult site than Camp Sibert in terms of number and sizes of munitions types, topography, and geography. In spite of the significantly increased difficulty, very good classification performance was achieved using both commercial instruments and classification software

and with advanced instruments and advanced processing. For the advanced instruments, false-negative calls were limited to cases where multiple items were excavated from the same location, with a single TOI among them, or where the instrument provided insufficient SNR for a satisfactory inversion. In the next demonstration, on-site quality-check procedures need to be established to ensure that satisfactory data have been collected. In addition, algorithms must be improved in post processing to identify when multiple targets are present.



## **APPENDIX A: NUMBER OF ANOMALIES PER INSTRUMENT**

This appendix lists the numbers of locations associated with each instrument. The EM61 CART, EM61 ARRAY, MAG ARRAY, and MSEMS collected survey data over the demonstration area. The data-collection teams detected anomalies in each instrument's survey data. Most anomalies detected by the EMI-based sensors were associated with a master location. The magnetometers detected very large numbers of anomalies due to the magnetic geology of the site. Therefore, the MAG ARRAY was associated with only those master locations already associated with the EM61 ARRAY, and the MAG MSEMS sensor was associated with only those master locations already associated with the EM61 MSEMS sensor. The TEMTADS collected cued data at all master locations associated with the EM61 ARRAY, and the BUD collected cued data at a subset of these locations.

This appendix also lists the number of locations assigned to different training and test sets. All master locations were assigned to either the Standard Training Set or Standard Test Set. The master locations associated with the EM61 ARRAY were also independently assigned to either an Active Learning Training Set or Active Learning Test Set, as well as to either the Extended Training Set or Extended Test Set. Similarly, the TEMTADS locations were also assigned to either an Active Learning Training Set or Active Learning Test Set. A large subset of the EM61 CART locations was assigned to a Second-Pass Training Set.

In a separate but parallel demonstration, the MetalMapper surveyed the demonstration area. The data-collection team detected anomalies in the survey data and then returned to each anomaly to collect cued data. A small percentage of cued locations were not excavated in time for classification processing. All other cued locations (the majority) were assigned to either the Standard Training Set or Standard Test Set.

**Table 1: Numbers of detected anomalies and associated master locations for each instrument. The numbers of associated master locations in four different training and test sets are shown. The numbers of true TOI and non-TOI locations are shown in red (left side of slash) and green (right side of slash), respectively.**

Instrument	Number of Detected Anomalies	Number of Associated Master Locations								
		Overall	Standard		Active Learning		Extended		Second-Pass	
			Training	Test	Training	Test	Training	Test	Training	Test
EM61 CART	1552	1479	197 28/169	1282 208/1074	-	-	-	-	1042 235/807	437 1/436
EM61 ARRAY	1464	1464	182 28/154	1282 206/1076	140 36/104	1324 198/1126	438 107/331	1026 127/899	-	-
MAG ARRAY	5268	1464	182 28/154	1282 206/1076	-	-	-	-	-	-
EM61 MSEMS	2316	1498	195 27/168	1303 205/1098	-	-	-	-	-	-
MAG MSEMS	3389	1498	195 27/168	1303 205/1098	-	-	-	-	-	-
TEMTADS	-	1464	182 28/154	1282 206/1076	125 20/105	339 214/1125	-	-	-	-
BUD*	-	539	68 9/59	471 59/412	-	-	-	-	-	-
Instrument	Number of Detected Anomalies	Number of Cued Location								
		Overall	Standard		Active Learning		Extended		Second-Pass	
			Training	Test	Training	Test	Training	Test	Training	Test
Metal- Mapper	1617	1561	154 26/128	1407 204/1203	-	-	-	-	-	-

\* BUD collected data over only a sub-area of the site.

## **APPENDIX B: PRIMARY SCORING RESULTS**

This appendix presents the primary scoring results for each of the 62 ranked anomaly lists submitted at Camp San Luis Obispo. Results are labeled by the demonstration team that created the ranked anomaly list, the instrument that collected the data, the classification algorithm that processed the data, and the test set to which the algorithm was applied.

Results consist of the primary ROC-like classification performance curves, a list of all true TOI locations that incorrectly rose above the demonstrator's prospectively chosen "don't dig threshold" (the dark-blue dot on the performance curve), and a list of all true TOI locations that fell between the demonstrator's "don't dig threshold" and the retrospective "95% don't dig threshold" (pink dot). (The "95% don't dig threshold" is the threshold that would have minimized the *Number of Non-TOI Below Threshold* while the *Percent of TOI Below Threshold* was greater than 95%.) In the rare case that the demonstrators' "don't dig threshold" was placed further down the ranked anomaly list than the "95% don't dig threshold," then only those true TOI locations that rose above the "95% don't dig threshold" are listed. In all cases, true TOI locations that rose above the demonstrators' "don't dig threshold" are listed in blue with an asterisk, and true TOI locations that fell between the two thresholds are listed in pink with no asterisk.

Unless otherwise stated, (1) each demonstration team extracted its own parameters from the data to input into its classification algorithm, (2) each classification algorithm was optimized over the Standard Training Set and then applied to the Standard Test Set, and (3) all ranked anomaly lists were created before the demonstration teams received ground truth information on the Standard Test Set.

### **SURVEY INSTRUMENTS**

This section presents results based on survey instruments: the EM61 CART, the EM61 ARRAY, the MAG ARRAY, and the EM61 MSEMS sensor. One set of results is based on cooperative inversions of the EM61 MSEMS and MAG MSEMS sensors.

## EM61 CART

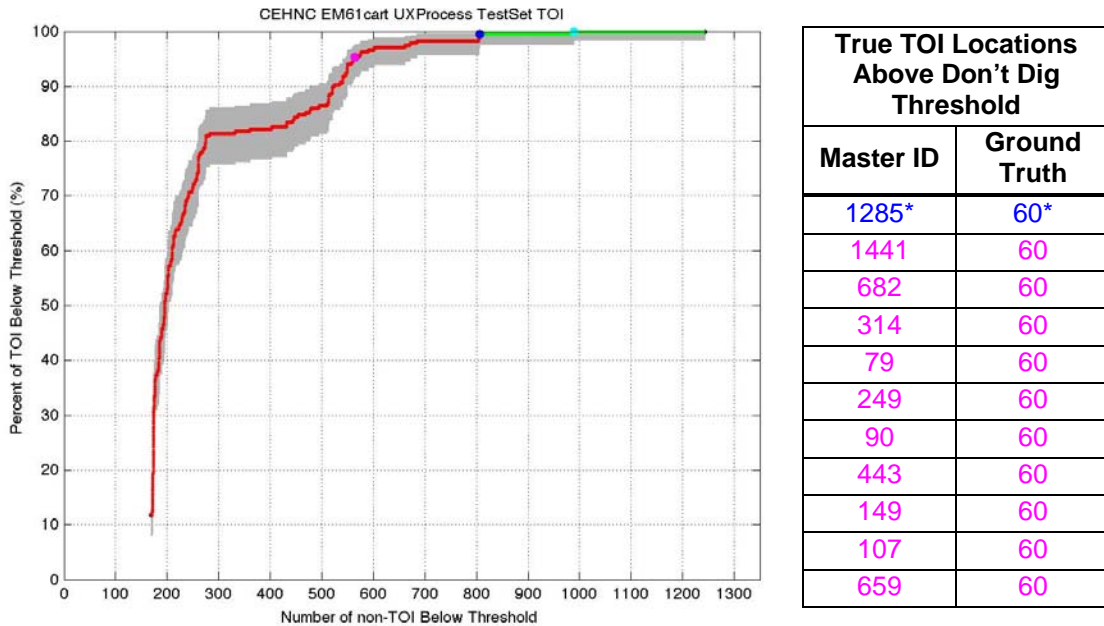


Figure 64: CEHNC’s primary scoring results for the EM61 CART and the UX-Process classification software, first iteration. One true TOI location rose above the demonstrator’s prospective “don’t dig threshold” (dark-blue dot).

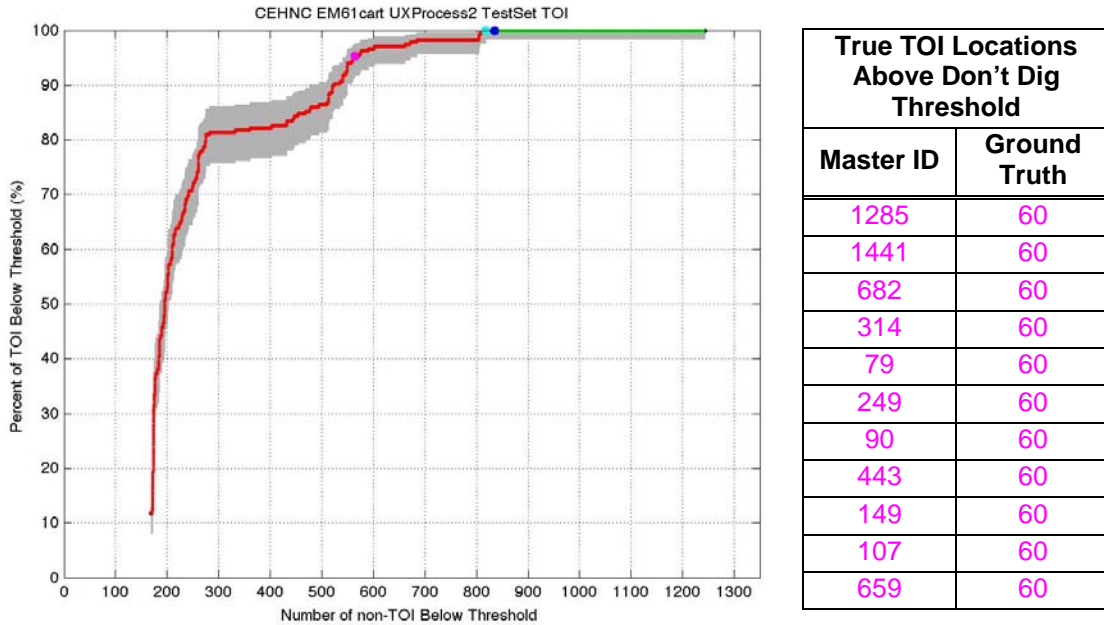
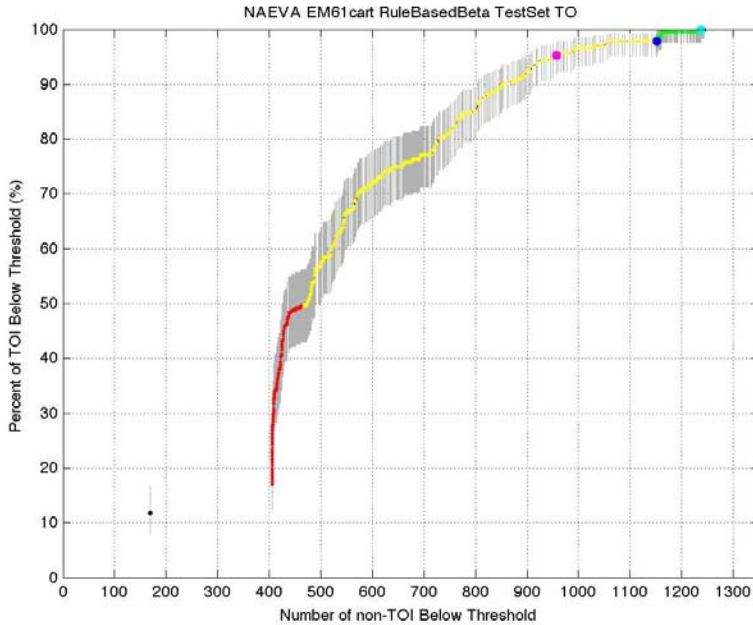
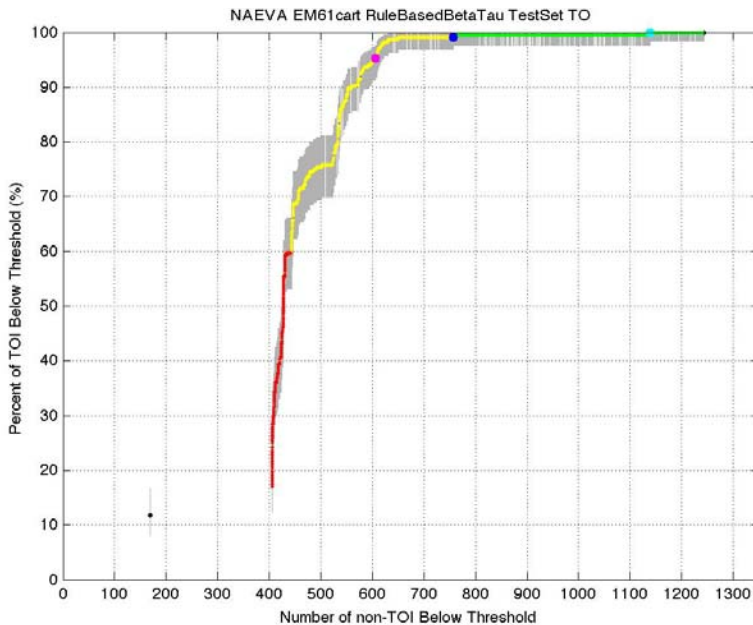


Figure 65: CEHNC’s primary scoring results for the EM61 CART and the UX-Process classification software, second pass. The software was optimized over the Standard Training Set *plus* the subset of the Standard Test Set that had fallen below the demonstrator’s “don’t dig threshold” during the first classification pass. The software was then reapplied to the entire Standard Test Set. No true TOI locations rose above the demonstrator’s revised “don’t dig threshold” in the second classification pass (dark-blue dot).



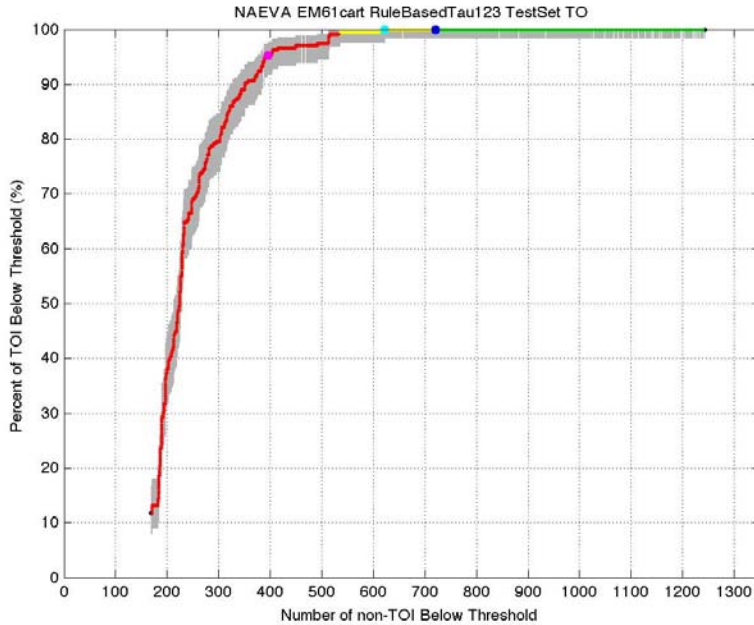
True TOI Locations Above Don't Dig Threshold	
Master ID	Ground Truth
326*	4.2*
404*	4.2*
365*	4.2*
304*	60*
188*	2.36*
367	60
66	60
79	60
290	60
197	60
249	60

Figure 66: NAEVA’s primary scoring results for the EM61 CART and the “Rule Based Beta” classification algorithm. Five true TOI locations rose above the prospective “don’t dig threshold” (dark-blue dot).



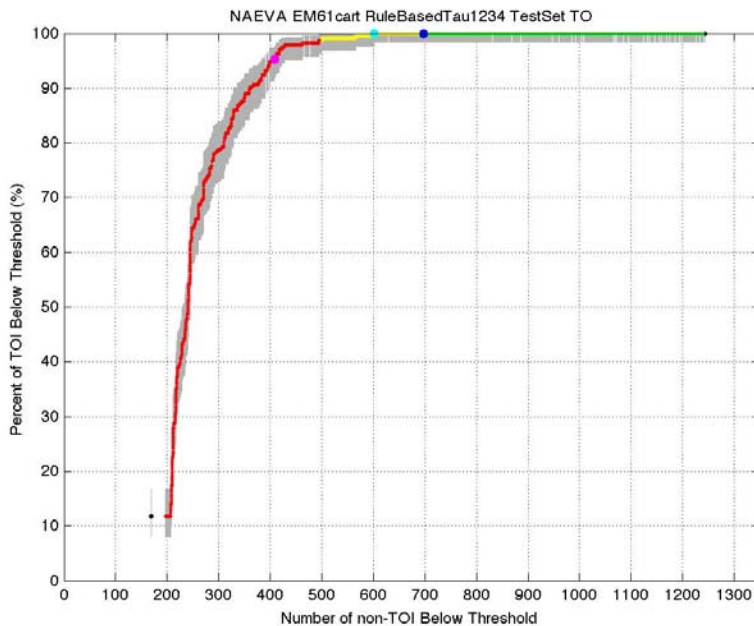
True TOI Locations Above Don't Dig Threshold	
Master ID	Ground Truth
326*	4.2*
404*	4.2*
60	60
1456	60
59	60
1108	60
160	60
275	60
1483	60
443	60
19	60

Figure 67: NAEVA’s primary scoring results for the EM61 CART and the “Rule Based Beta Tau” classification algorithm. Two true TOI locations rose above the prospective “don’t dig threshold” (dark-blue dot).



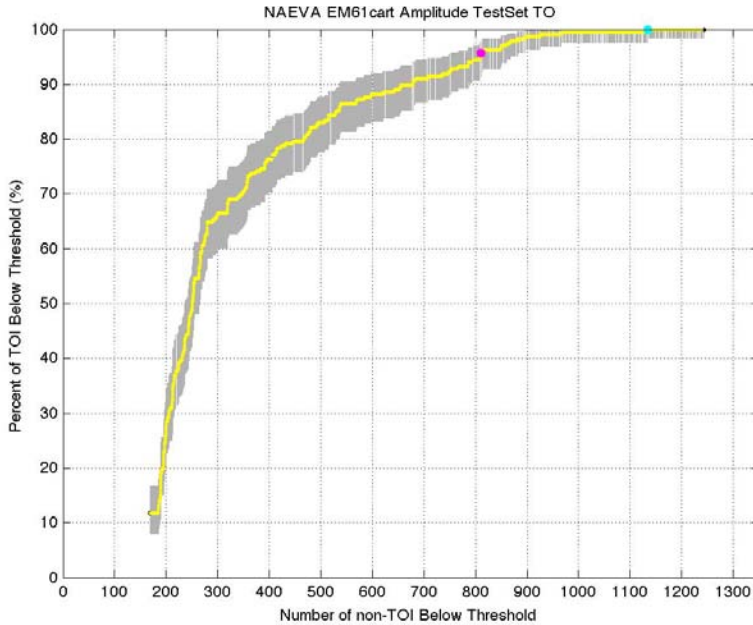
True TOI Locations Above Don't Dig Threshold	
Master ID	Ground Truth
60	60
188	2.36
59	60
1615	60
1444	60
443	60
53	2.36
90	60
19	60
457	60
149	60

Figure 68: NAEVA’s primary scoring results for the EM61 CART and the “Rule Based Beta 123” classification algorithm. No true TOI locations rose above the prospective “don’t dig threshold” (dark-blue dot). (The ranked anomaly list was created after NAEVA received ground truth information for the Test Set.)



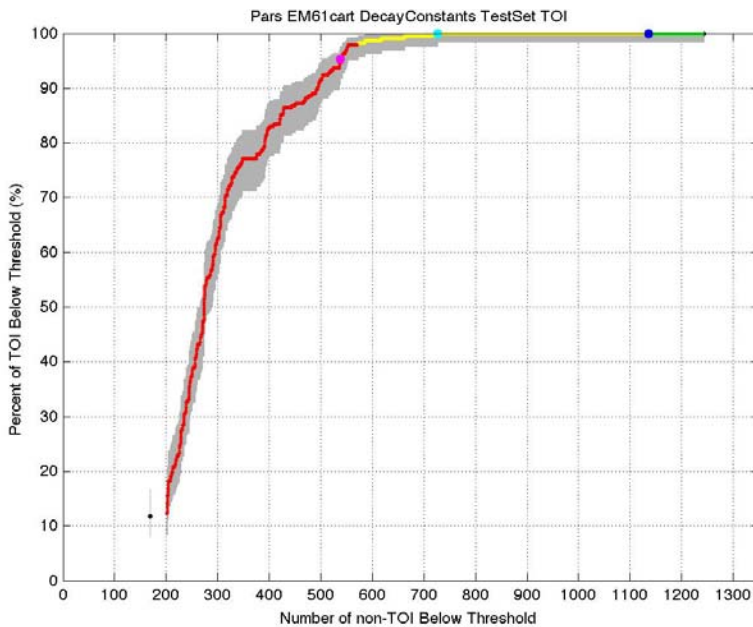
True TOI Locations Above Don't Dig Threshold	
Master ID	Ground Truth
60	60
53	2.36
188	2.36
443	60
90	60
19	60
59	60
457	60
149	60
1615	60
1444	60

Figure 69: NAEVA’s primary scoring results for the EM61 CART and the “Rule Based Tau 1234” classification algorithm. No true TOI locations rose above the prospective “don’t dig threshold” (dark-blue dot). (The ranked anomaly list was created after NAEVA received ground truth information for the Test Set.)



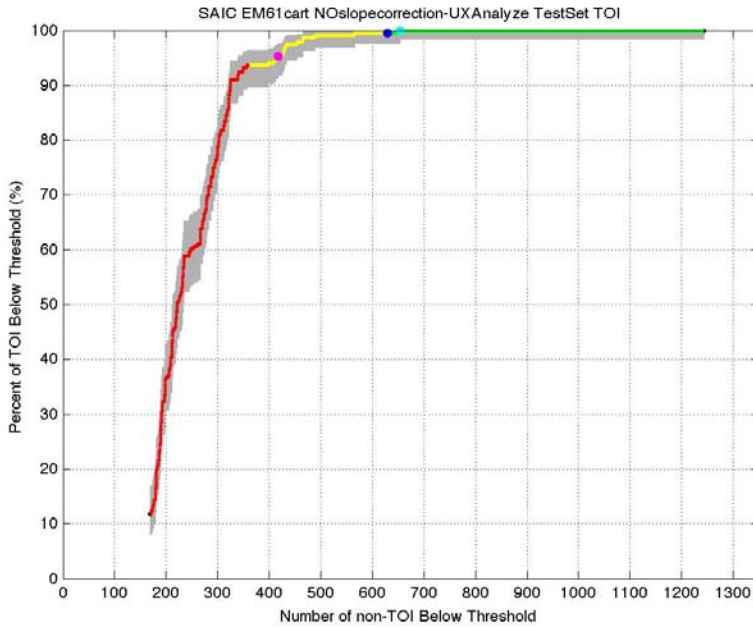
True TOI Locations Above Don't Dig Threshold	
Master ID	Ground Truth
90	60
19	60
59	60
457	60
149	60
1615	60
1444	60
443	60
494	60
441	60
90	60

Figure 70: NAEVA’s primary scoring results for the EM61 CART instrument and the “Amplitude” classification algorithm. No true TOI locations rose above the prospective “don’t dig threshold” (dark-blue dot). (The ranked anomaly list was created after NAEVA received ground truth for the Test Set.)



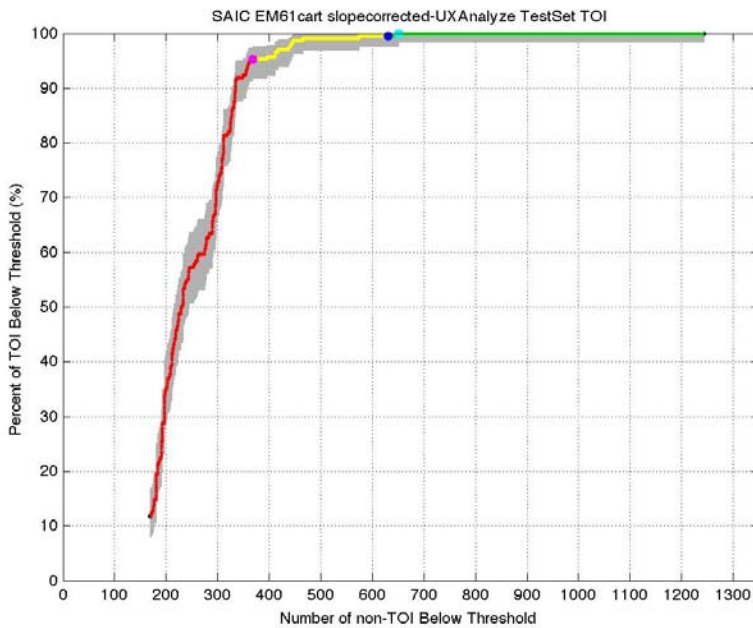
True TOI Locations Above Threshold	
Master ID	Ground Truth
19	60
1372	2.36
60	60
512	60
66	60
1072	4.2
1311	81
517	81
231	81
626	4.2
294	4.2

Figure 71: Parsons’ primary scoring results for the EM61 CART and the “Decay Constants” classification algorithm. No true TOI locations rose above the prospective “don’t dig threshold” (dark-blue dot).



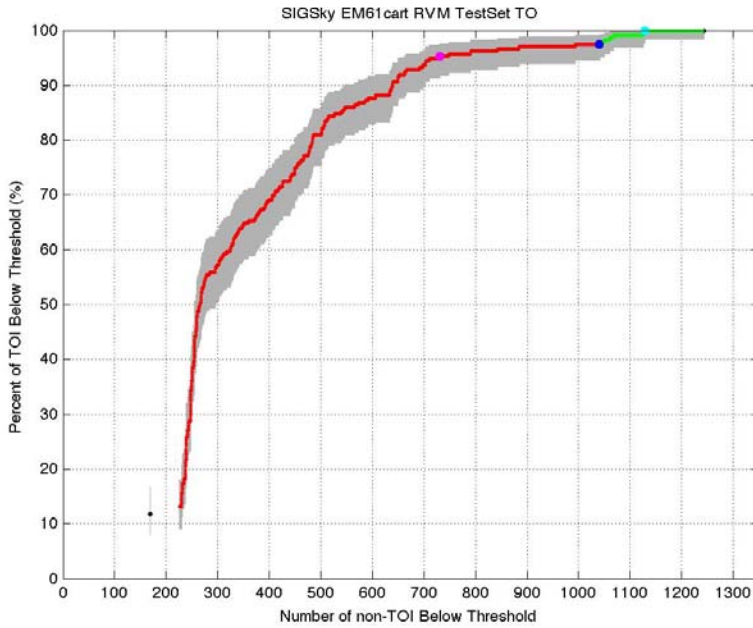
True TOI Locations Above Don't Dig Threshold	
Master ID	Ground Truth
1444*	60*
899	81
1615	60
441	60
160	60
1483	60
775	60
231	81
53	2.36
1372	2.36
301	60

Figure 72: SAIC’s primary scoring results for the EM61 CART (*before* slope correction) and the UX-Analyze classification software. One true TOI location rose above the prospective “don’t dig threshold” (dark-blue dot).



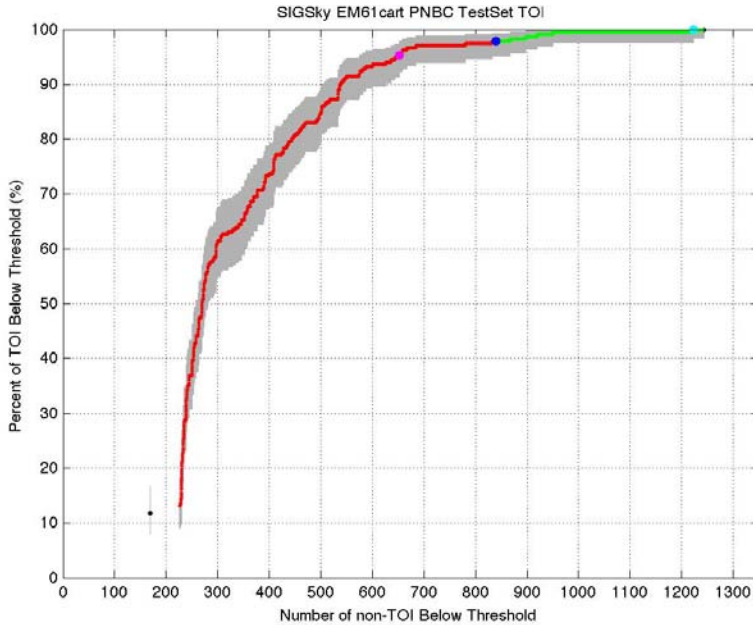
True TOI Locations Above Don't Dig Threshold	
Master ID	Ground Truth
1444*	60*
899	81
1615	60
441	60
1483	60
775	60
160	60
80	60
296	81
907	81
1469	60

Figure 73: SAIC’s primary scoring results for the EM61 CART (*after* slope correction) and the UX-Analyze classification software. One true TOI location rose above the prospective “don’t dig threshold” (dark-blue dot).



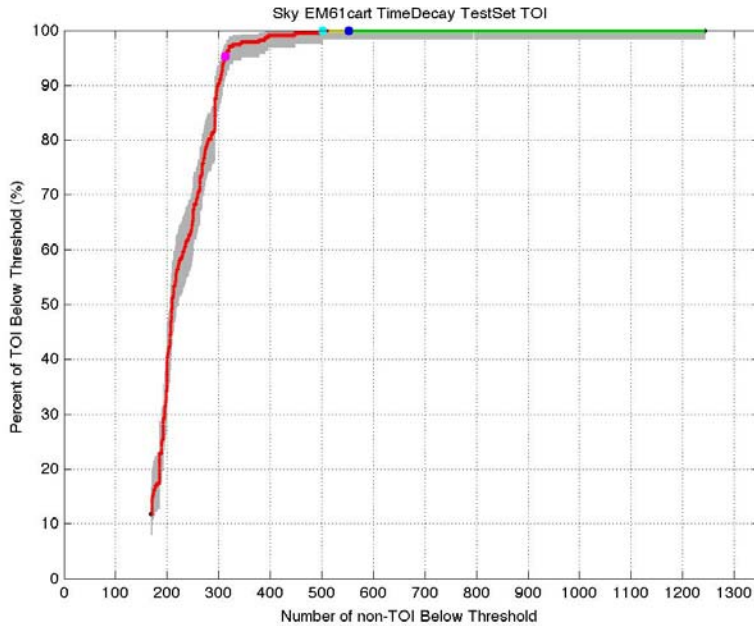
True TOI Locations Above Don't Dig Threshold	
Master ID	Ground Truth
15*	60*
448*	2.36*
1311*	81*
304*	60*
160*	60*
188*	2.36*
290	60
342	60
732	60
675	60
314	60

Figure 74: SIG’s primary scoring results for the EM61 CART and the RVM supervised learning classification algorithm. (Sky estimated the parameters that were input into the algorithm.) Six true TOI locations rose above the prospective “don’t dig threshold” (dark-blue dot).



True TOI Locations Above Don't Dig Threshold	
Master ID	Ground Truth
304*	60*
1311*	81*
314*	60*
160*	60*
290*	60*
249	60
66	60
342	60
1441	60
500	60
372	60

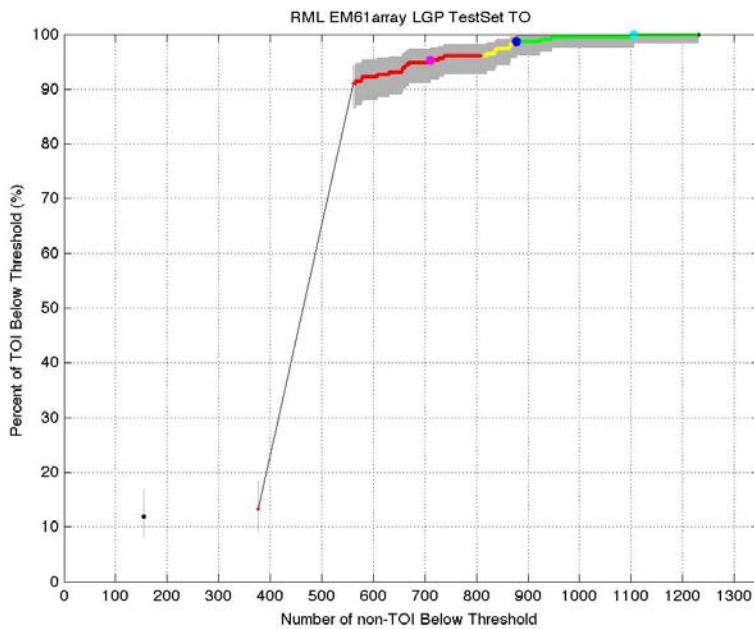
Figure 75: SIG’s primary scoring results for the EM61 CART and the PNBC semi-supervised classification algorithm. (Sky estimated the parameters that were input into the algorithm.) Five true TOI locations rose above the prospective “don’t dig threshold” (dark-blue dot).



True TOI Locations Above Don't Dig Threshold	
Master ID	Ground Truth
1444	60
775	60
1483	60
441	60
907	81
275	60
1455	60
1615	60
207	60
418	60
160	60

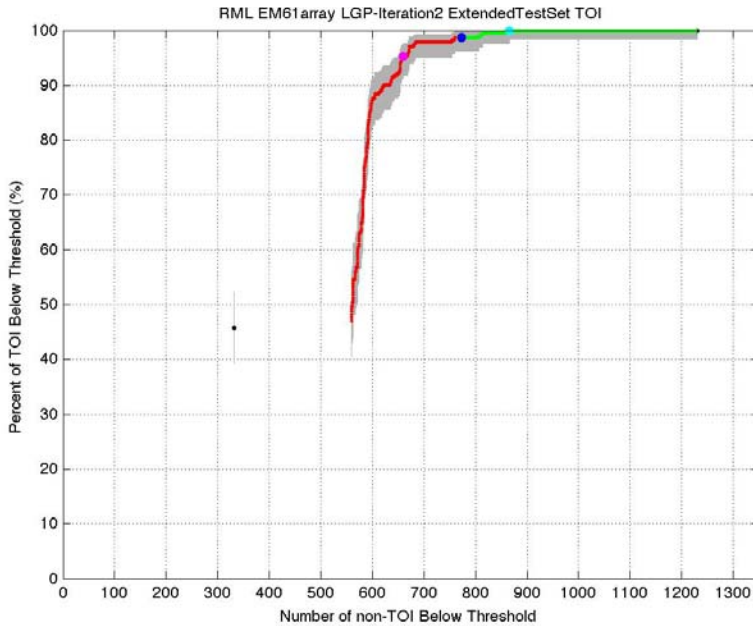
Figure 76: Sky's primary scoring results for the EM61 CART and the "Time Decay" classification algorithm. No true TOI locations rose above the prospective "don't dig threshold" (dark-blue dot).

### EM61 ARRAY



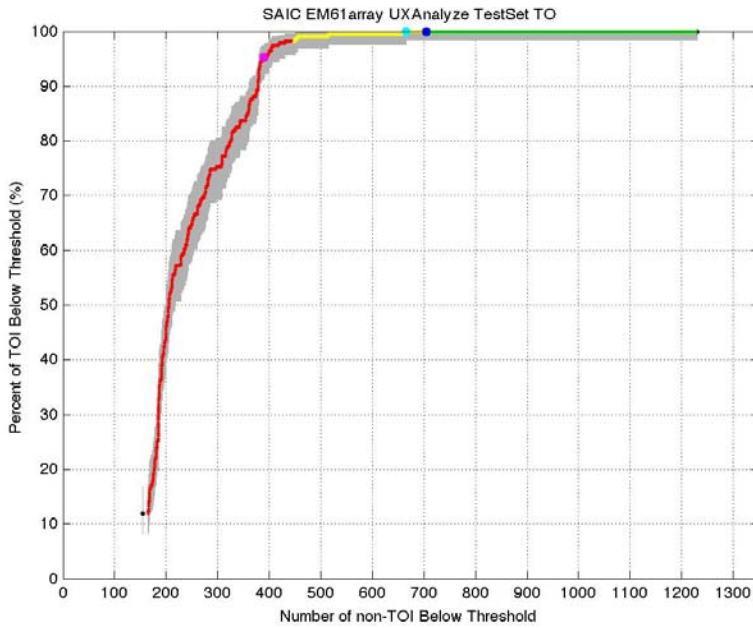
True TOI Locations Above Don't Dig Threshold	
Master ID	Ground Truth
1444*	60*
16*	60*
512*	60*
149	60
59	60
103	60
60	60
444	2.36
722	60
65	60
90	60

Figure 77: RML's primary scoring results for the EM61 ARRAY and the LGP classification algorithm. Three true TOI locations rose above the prospective "don't dig threshold" (dark-blue dot).



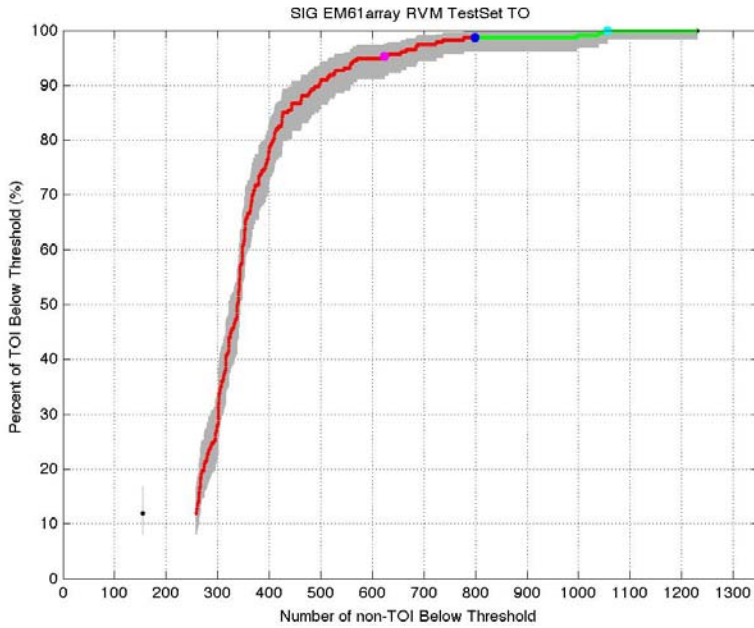
True TOI Locations Above Don't Dig Threshold	
Master ID	Ground Truth
1444*	60*
16*	60*
444*	2.36*
775	60
103	60
59	60
188	2.36
512	60
107	60
25	60
675	60

Figure 78: RML's primary scoring results for the EM61 ARRAY and the LGP classification algorithm. The algorithm was optimized over the Extended Training Set and then applied to the complementary "Extended" Test Set. Three true TOI locations rose above the prospective "don't dig threshold" (dark-blue dot).



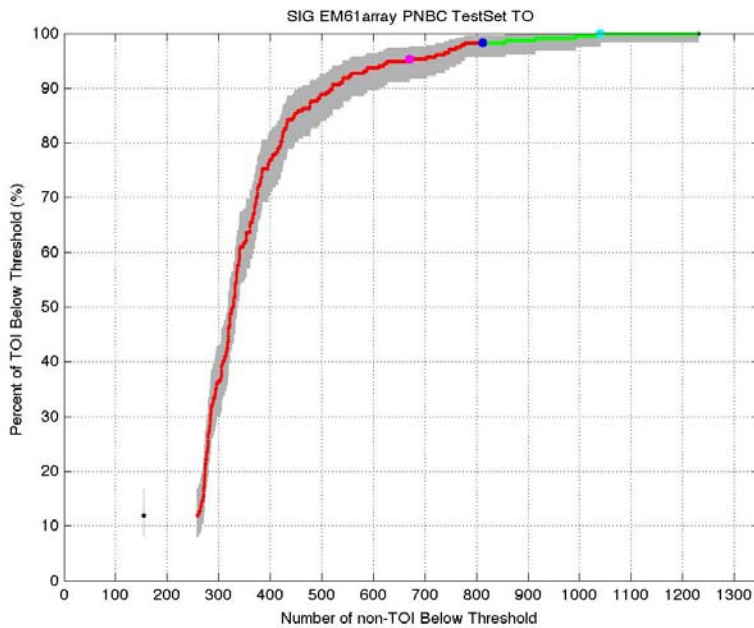
True TOI Locations Above Don't Dig Threshold	
Master ID	Ground Truth
1285	60
899	81
365	4.2
444	2.36
103	60
109	60
28	60
1419	81
585	81
467	81
533	60

Figure 79: SAIC's primary scoring results for the EM61 ARRAY and the UX-Analyze classification software. No true TOI locations rose above the prospective "don't dig threshold" (dark-blue dot).



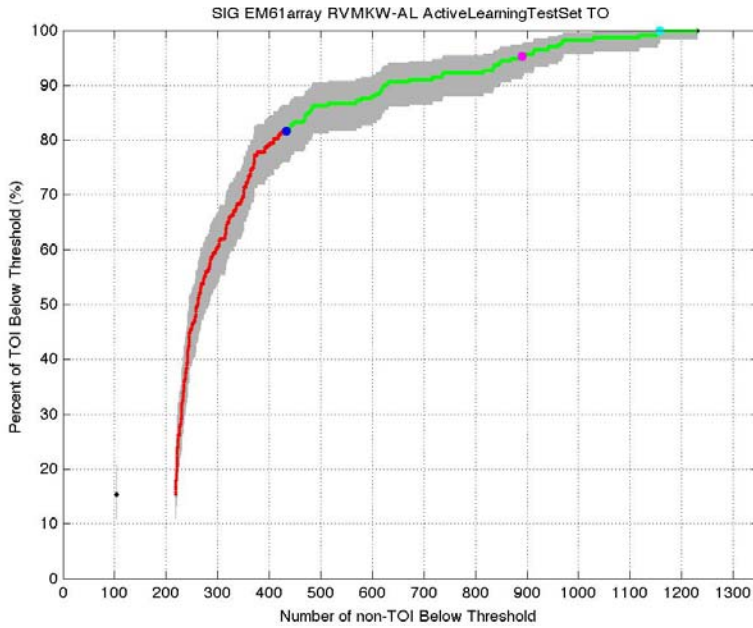
True TOI Locations Above Don't Dig Threshold	
Master ID	Ground Truth
314*	60*
25*	60*
79*	60*
1372	2.36
1285	60
90	60
60	60
1441	60
722	60
1434	81
72	60

Figure 80: SIG's primary scoring results for the EM61 ARRAY and the RVM supervised learning classification algorithm. Three true TOI locations rose above the prospective "don't dig threshold" (dark-blue dot).



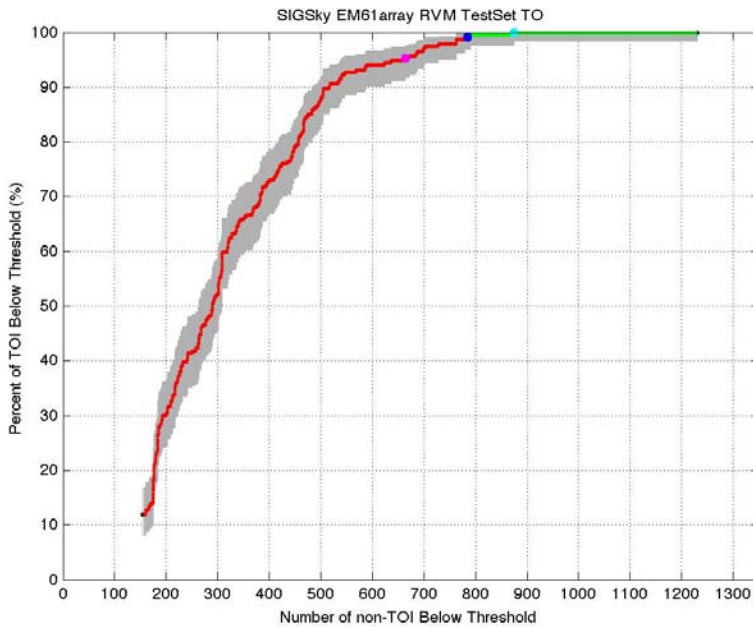
True TOI Locations Above Don't Dig Threshold	
Master ID	Ground Truth
25*	60*
314*	60*
79*	60*
1372*	2.36*
722	60
1285	60
1441	60
90	60
60	60
72	81
275	60

Figure 81: SIG's primary scoring results for the EM61 ARRAY and the PNBC semi-supervised learning classification algorithm. Four true TOI locations rose above the prospective "don't dig threshold" (dark-blue dot).



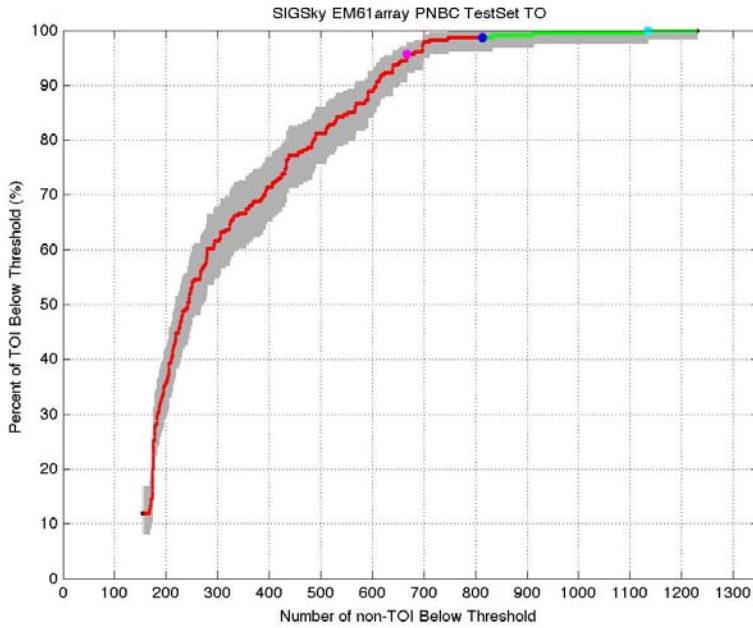
True TOI Locations Above Don't Dig Threshold	
Master ID	Ground Truth
314*	60*
25*	60*
79*	60*
1372*	2.36*
60*	60*
1441*	60*
1285*	60*
22*	60*
241*	2.36*
275*	60*
722*	60*

**Figure 82: SIG’s primary scoring results for the EM61 ARRAY and the RVM supervised learning classification algorithm. The algorithm was optimized over the Active Learning Training Set and applied to the complementary Active Learning Test Set. Forty-three true TOI locations rose above the prospective “don’t dig threshold” (dark-blue dot), the first 11 of which are listed in blue.**



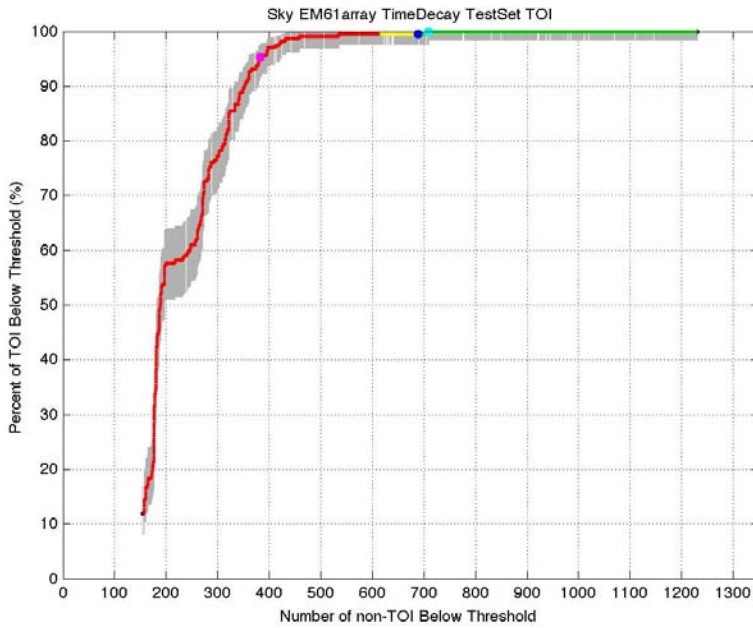
True TOI Locations Above Don't Dig Threshold	
Master ID	Ground Truth
275*	60*
1285*	60*
775	60
365	4.2
361	4.2
626	4.2
276	4.2
175	4.2
152	4.2
865	81
466	81

**Figure 83: SIG’s primary scoring results for the EM61 ARRAY and the RVM supervised learning classification algorithm. (Sky estimated the parameters input to the algorithm.) Two true TOI locations rose above the prospective “don’t dig threshold” (dark-blue dot).**



True TOI Locations Above Don't Dig Threshold	
Master ID	Ground Truth
241*	2.36*
275*	60*
1285*	60*
103	60
90	60
314	60
160	60
38	60
249	2.36
79	60
241	60

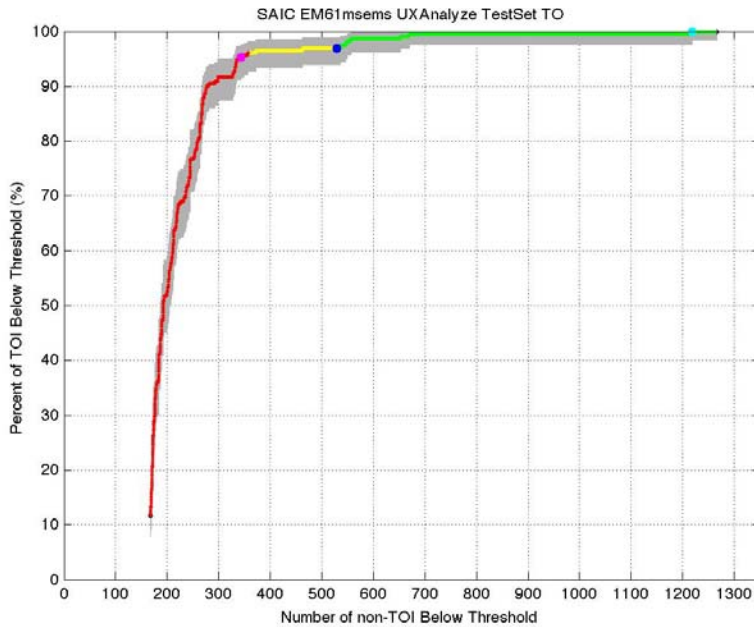
**Figure 84: SIG’s primary scoring results for the EM61 ARRAY and the PNBC semi-supervised learning classification algorithm (Sky estimated the parameters input to the algorithm.) Three true TOI locations rose above the prospective “don’t dig threshold” (dark-blue dot).**



True TOI Locations Above Don't Dig Threshold	
Master ID	Ground Truth
1444*	60*
160	60
775	60
1388	81
585	81
1455	81
1419	81
312	81
121	81
550	81
325	81

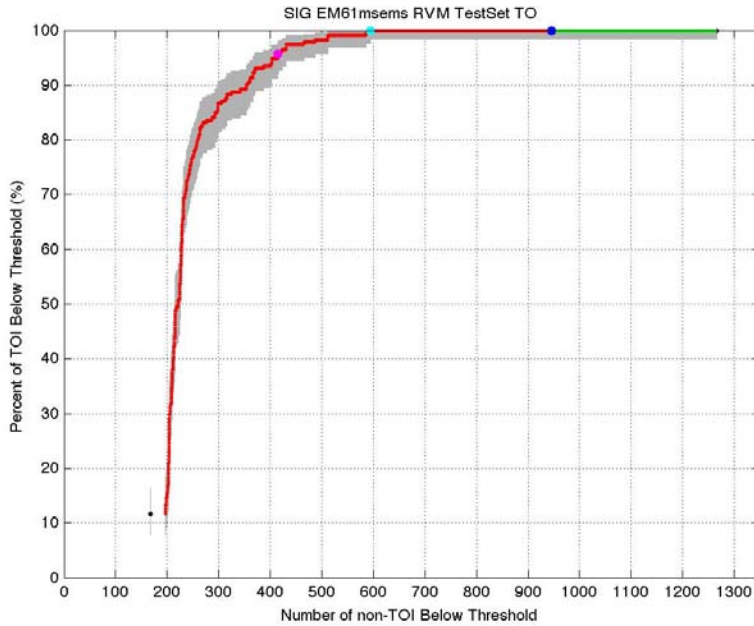
**Figure 85: Sky’s primary scoring results for the EM61 ARRAY and the “Time Decay” classification algorithm. One true TOI location rose above the prospective “don’t dig threshold” (dark-blue dot).**

## EM61 MSEMS



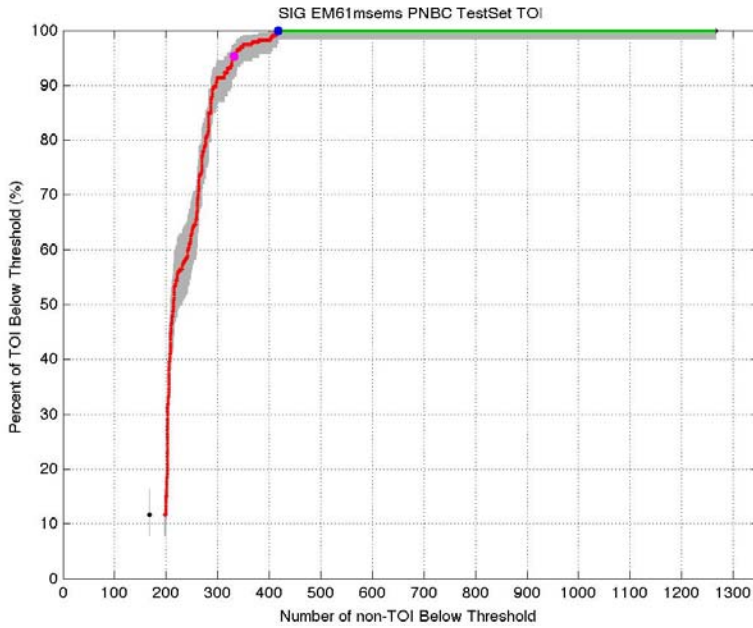
True TOI Locations Above Don't Dig Threshold	
Master ID	Ground Truth
444*	2.36*
1444*	60*
314*	60*
675*	60*
1441*	60*
1285*	60*
775*	60*
899	81
711	60
441	60
160	60

**Figure 86: SAIC's primary scoring results for the EM61 MSEMS and the UX-Analyze classification software. Seven true TOI locations rose above the prospective "don't dig threshold" (dark-blue dot).**



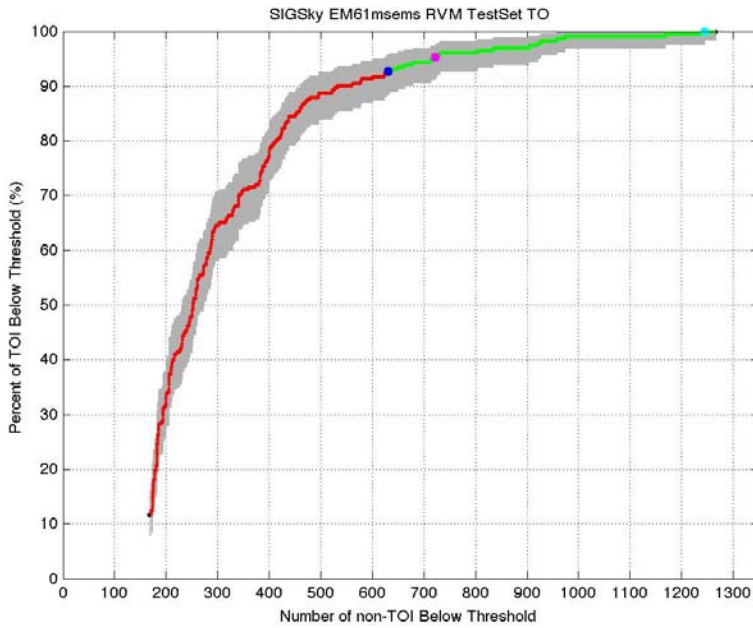
True TOI Locations Above Don't Dig Threshold	
Master ID	Ground Truth
1441	60
675	60
290	60
19	60
514	60
1403	60
90	60
437	60
79	60
65	60

**Figure 87: SIG's primary scoring results for the EM61 MSEMS and the RVM supervised learning classification algorithm. No true TOI locations rose above the prospective "don't dig threshold" (dark-blue dot).**



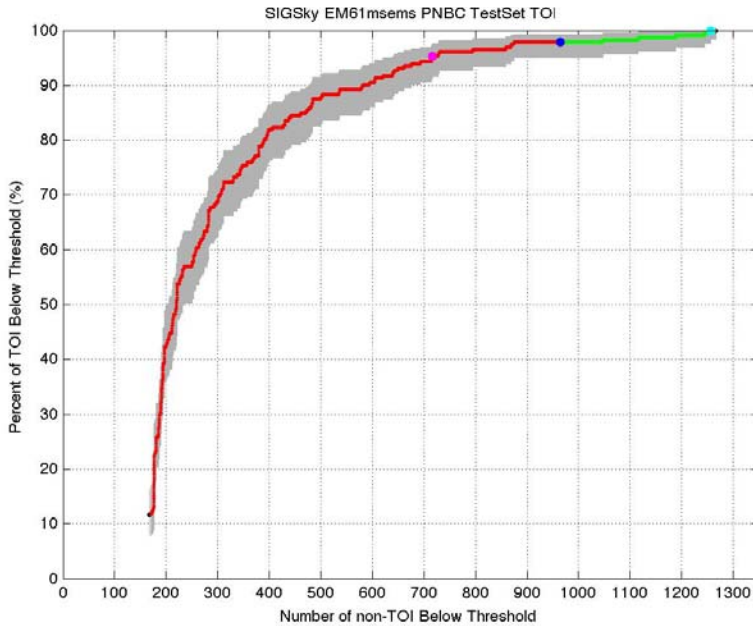
True TOI Locations Above Don't Dig Threshold	
Master ID	Ground Truth
19	60
66	60
1444	60
775	60
160	60
65	60
1483	60
1108	60
1403	60
122	60
59	60

Figure 88: SIG’s primary scoring results for the EM61 MSEMS and the PNBC semi-supervised learning classification algorithm. No true TOI locations rose above the prospective “don’t dig threshold” (dark-blue dot).



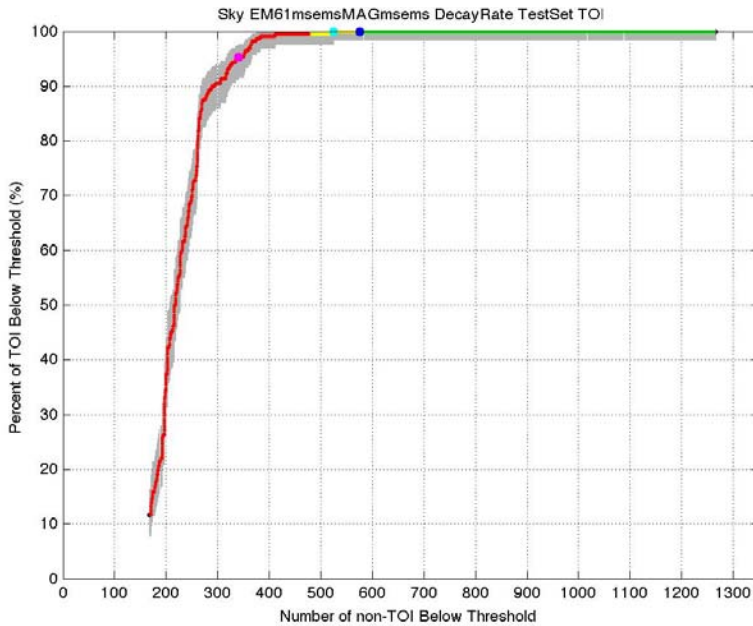
True TOI Locations Above Don't Dig Threshold	
Master ID	Ground Truth
418*	60*
1615*	60*
249*	60*
722*	60*
192*	60*
194*	2.36*
546*	60*
500*	60*
1502*	37*
19*	60*
38*	2.36*

Figure 89: SIG’s primary scoring results for the EM61 MSEMS and the RVM supervised learning classification algorithm. (Sky estimated the parameters input to the algorithm.) Seventeen true TOI locations rose above the prospective “don’t dig threshold” (dark-blue dot), the first 11 of which are listed in blue.



True TOI Locations Above Don't Dig Threshold	
Master ID	Ground Truth
192*	60*
194*	2.36*
500*	60*
418*	60*
1615*	60*
249	60
722	60
546	60
1502	37
38	2.36
19	60

Figure 90: SIG's primary scoring results for the EM61 MSEMS and the PNBC semi-supervised learning classification algorithm. (Sky estimated the parameters input to the algorithm.) Five true TOI locations rose above the prospective "don't dig threshold" (dark-blue dot).



True TOI Locations Above Don't Dig Threshold	
Master ID	Ground Truth
775	60
19	60
585	81
315	60
160	60
1483	60
1444	60
767	60
500	60
550	81
59	60

Figure 91: Sky's primary scoring results for cooperative inversions of the EM61 MSEMS and MAG MSEMS sensors and the "Decay Rate" classification algorithm. No true TOI locations rose above the prospective "don't dig threshold" (dark-blue dot).

## MAG ARRAY

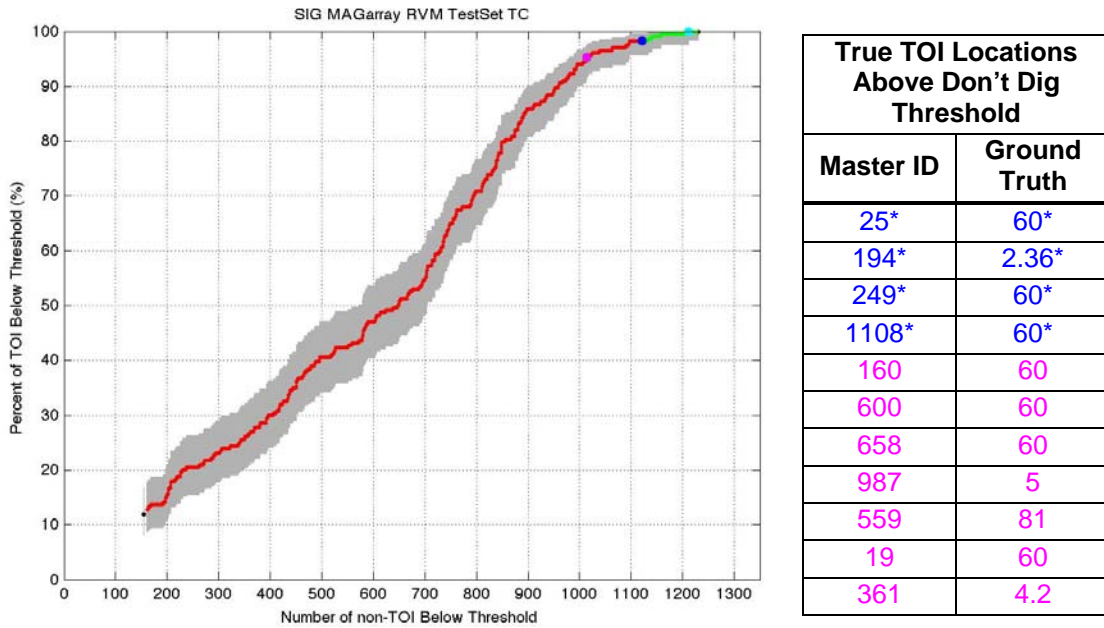


Figure 92: SIG's primary scoring results for the MAG ARRAY and the RVM supervised learning classification algorithm. Four true TOI locations rose above the prospective "don't dig threshold" (dark-blue dot).

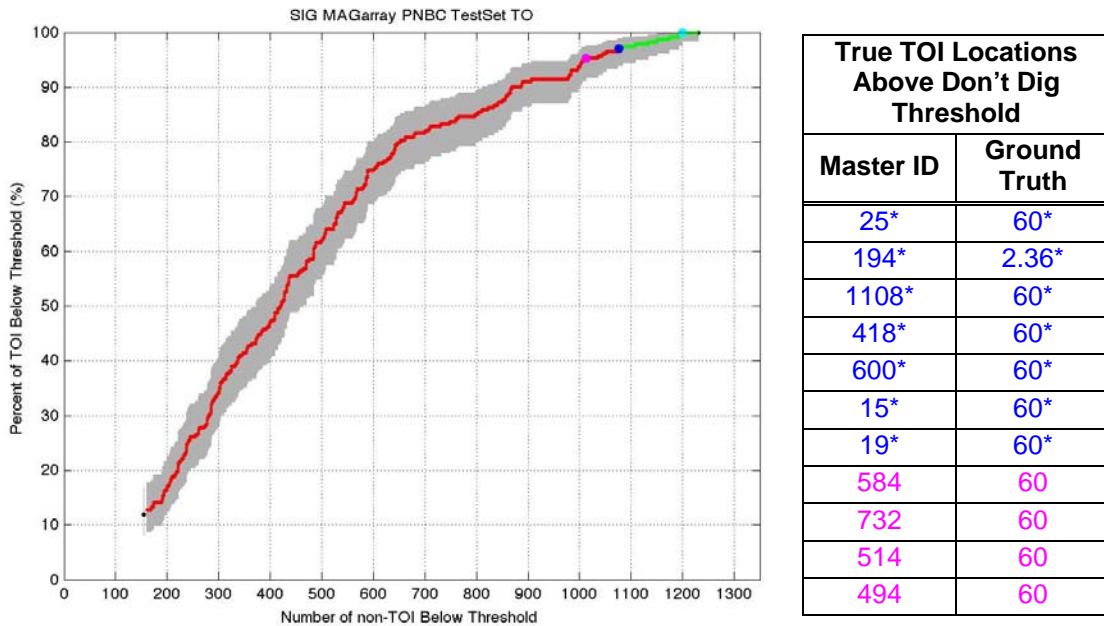
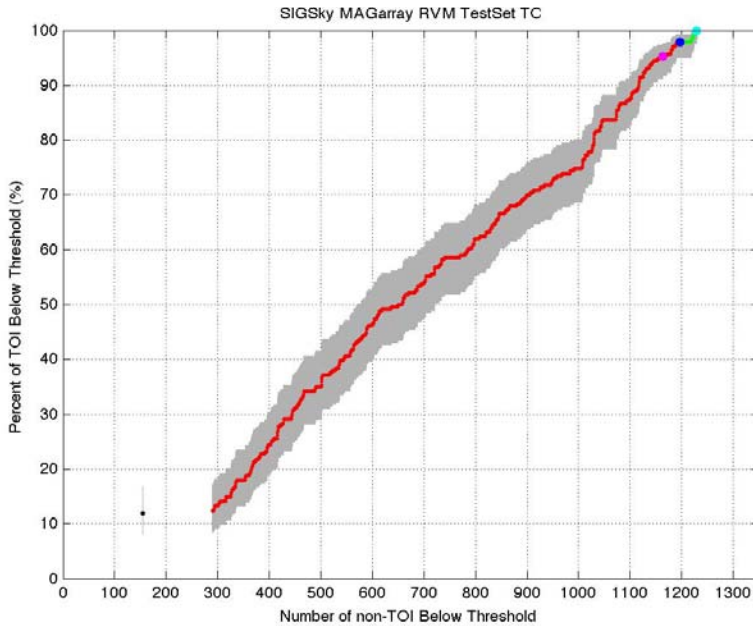
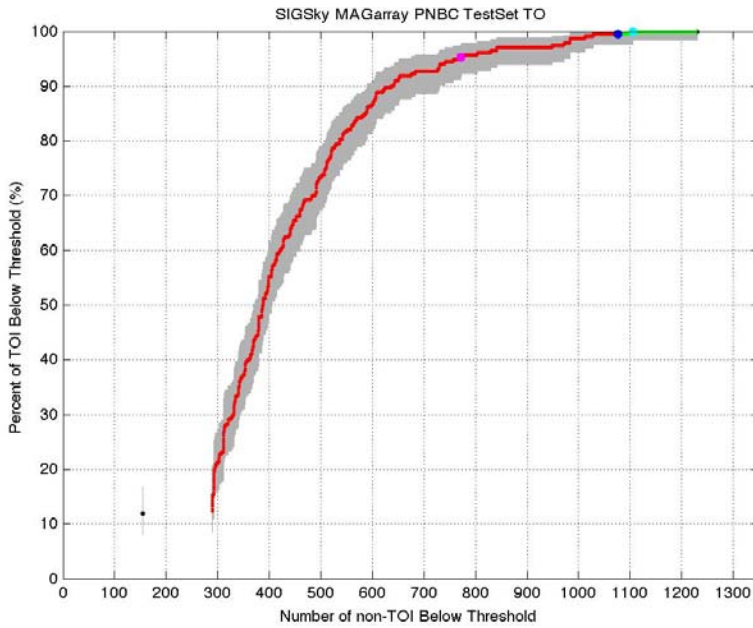


Figure 93: SIG's primary scoring results for the MAG ARRAY and the PNBC semi-supervised learning classification algorithm. Seven true TOI locations rose above the prospective "don't dig threshold" (dark-blue dot).



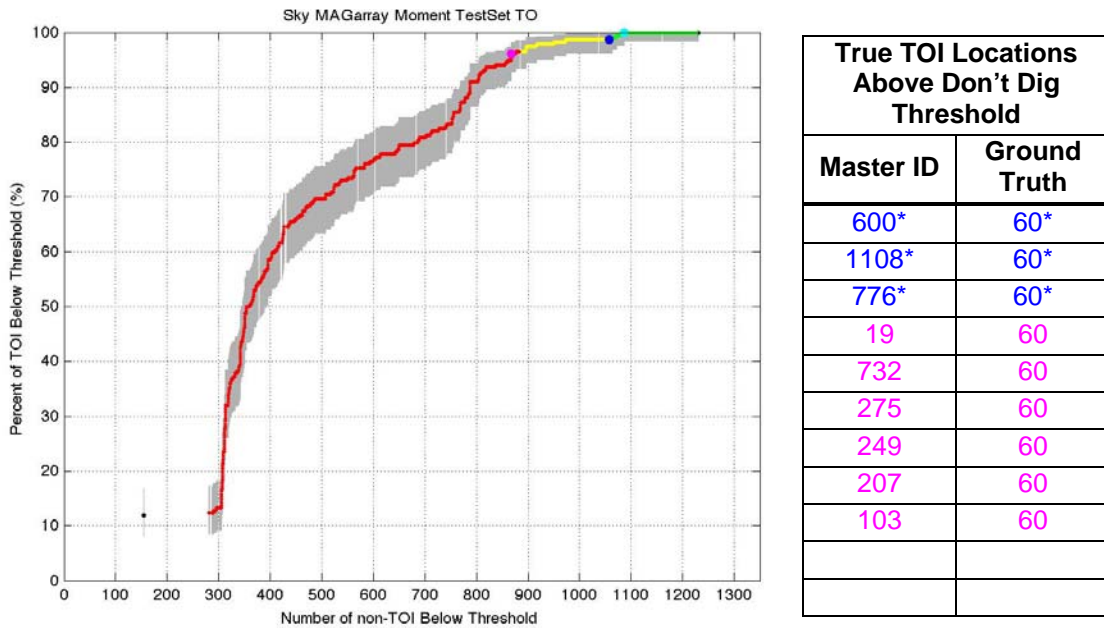
True TOI Locations Above Don't Dig Threshold	
Master ID	Ground Truth
1420*	2.36*
241*	2.36*
1032*	4.2*
361*	4.2*
505*	4.2*
626	4.2
591	4.2
462	4.2
1006	4.2
326	4.2
189	4.2

Figure 94: SIG’s primary scoring results for the MAG ARRAY and the RVM supervised learning classification algorithm. (Sky estimated the parameters input to the algorithm.) Five true TOI locations rose above the prospective “don’t dig threshold” (dark-blue dot).



True TOI Locations Above Don't Dig Threshold	
Master ID	Ground Truth
600*	60*
1108	60
776	60
103	60
732	60
464	2.36
19	60
1189	81
708	60
15	60
192	60

Figure 95: SIG’s primary scoring results for the MAG ARRAY and the PNBC semi-supervised learning classification algorithm. (Sky estimated the parameters input to the algorithm.) One true TOI location rose above the prospective “don’t dig threshold” (dark-blue dot).



**Figure 96: Sky's primary scoring results for the MAG ARRAY and the "Moment" classification algorithm. Three true TOI locations rose above the prospective "don't dig threshold" (dark-blue dot).**

## CUED INSTRUMENTS

This section presents results based on cued instruments: the TEMTADS, the MetalMapper, and the BUD. The BUD results were scored on only the sub-area of the site over which the BUD collected data, resulting in coarser classification performance curves.

# TEMTADS

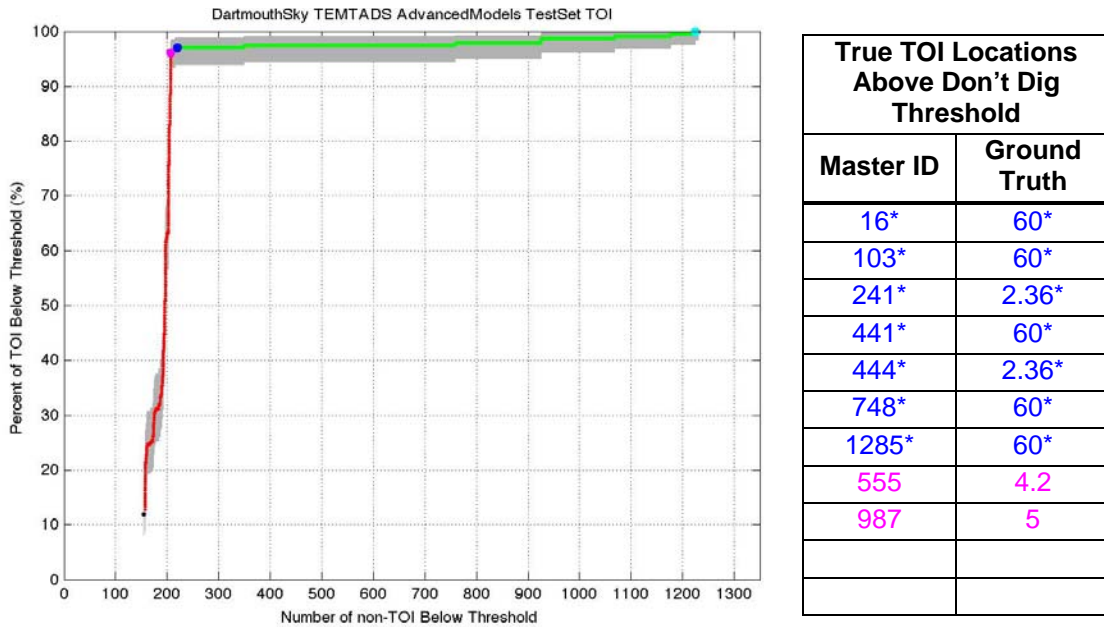


Figure 97: Dartmouth’s primary scoring results for TEMTADS and the “Advanced Models” classification algorithm. (Sky estimated the parameters input to the algorithm.) Seven true TOI locations rose above the prospective “don’t dig threshold” (dark-blue dot).

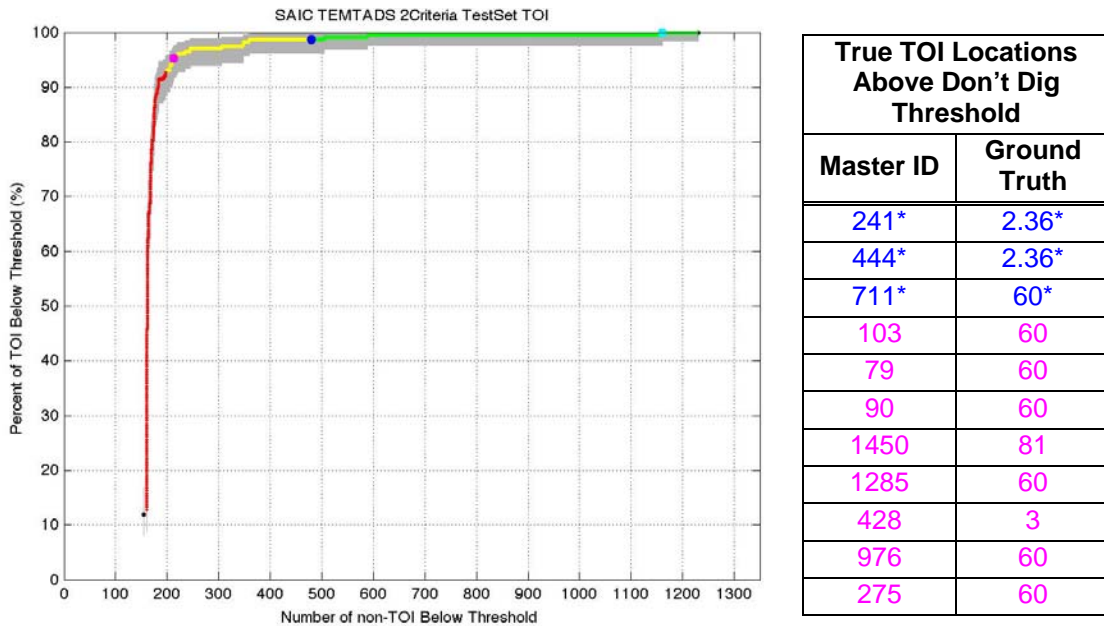
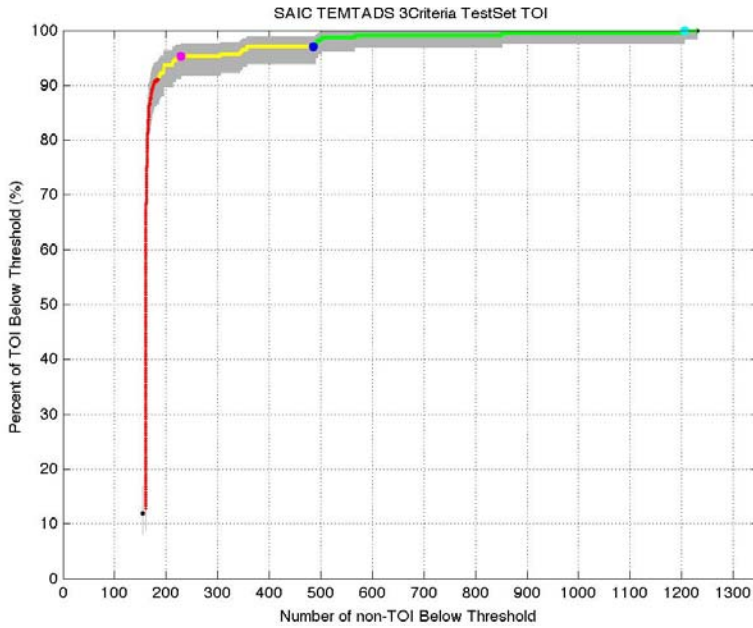
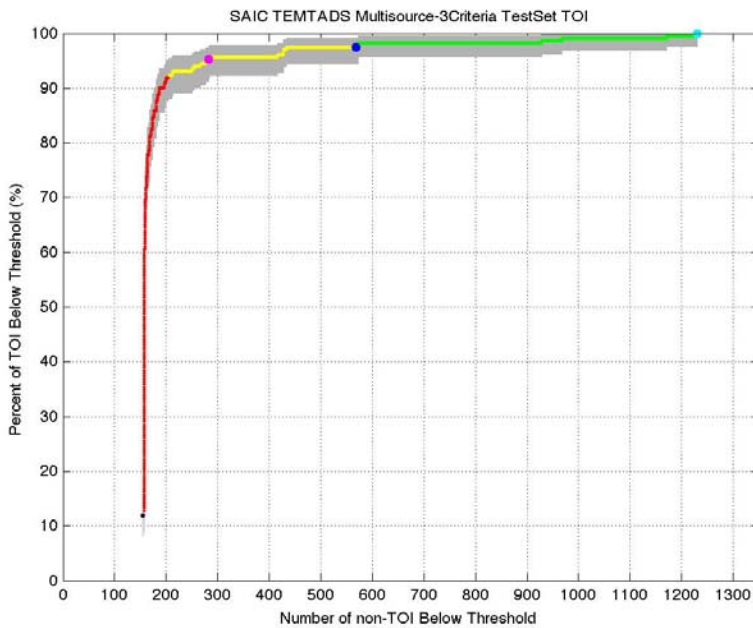


Figure 98: SAIC’s primary scoring results for the TEMTADS and the “2 Criteria” classification algorithm. Three true TOI locations rose above the prospective “don’t dig threshold” (dark-blue dot).



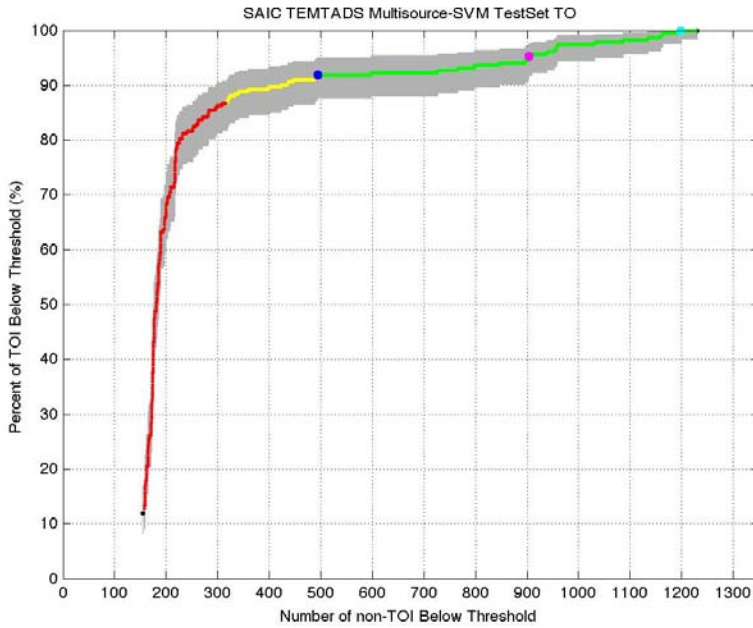
True TOI Locations Above Don't Dig Threshold	
Master ID	Ground Truth
241*	2.36*
711*	60*
444*	2.36*
16*	60*
249*	60*
372*	60*
65*	60*
103	60
90	60
79	60
1450	81

Figure 99: SAIC’s primary scoring results for the TEMTADS and the “3 Criteria” classification algorithm. Seven true TOI locations rose above the prospective “don’t dig threshold” (dark-blue dot).



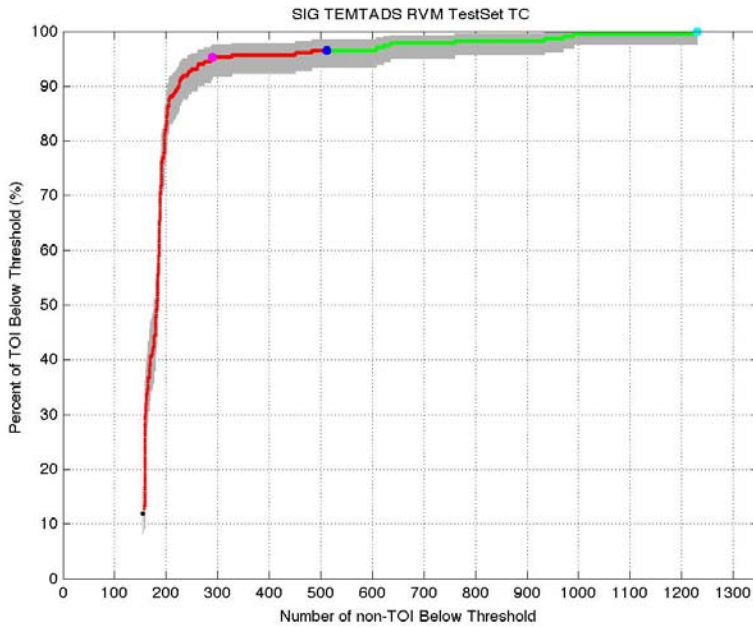
True TOI Locations Above Don't Dig Threshold	
Master ID	Ground Truth
1415*	4.2*
241*	2.36*
775*	60*
444*	2.36*
441*	60*
987*	5*
90	60
103	60
79	60
711	60
722	60

Figure 100: SAIC’s primary scoring results for the TEMTADS and the “Multisource - 3 Criteria” classification algorithm. Six true TOI locations rose above the prospective “don’t dig threshold” (dark-blue dot).



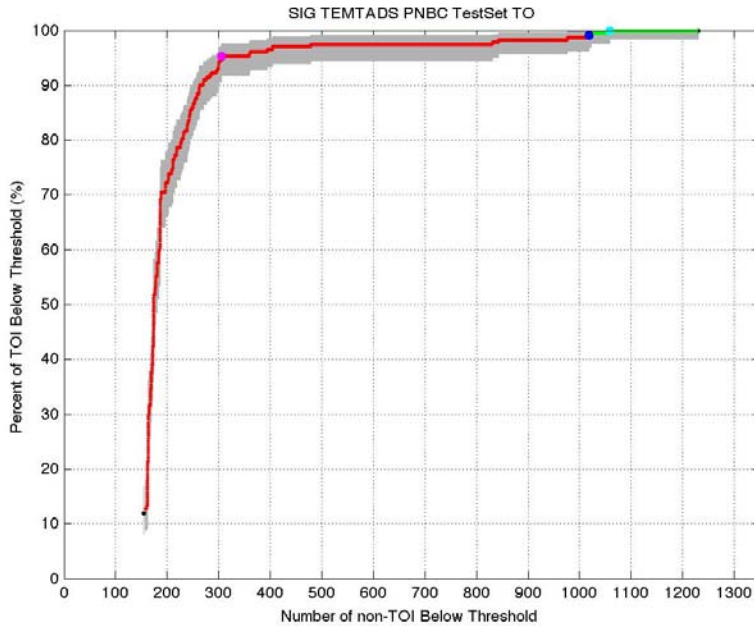
True TOI Locations Above Don't Dig Threshold	
Master ID	Ground Truth
444*	2.36*
1415*	4.2*
241*	2.36*
1450*	81*
90*	60*
722*	60*
118*	4.2*
152*	4.2*
987*	5*
249*	60*
711*	60*

Figure 101: SAIC’s primary scoring results for the TEMTADS and the “Multisource - SVM” classification algorithm. Nineteen true TOI locations rose above the prospective “don’t dig threshold” (dark-blue dot), the first 11 of which are listed above in blue.



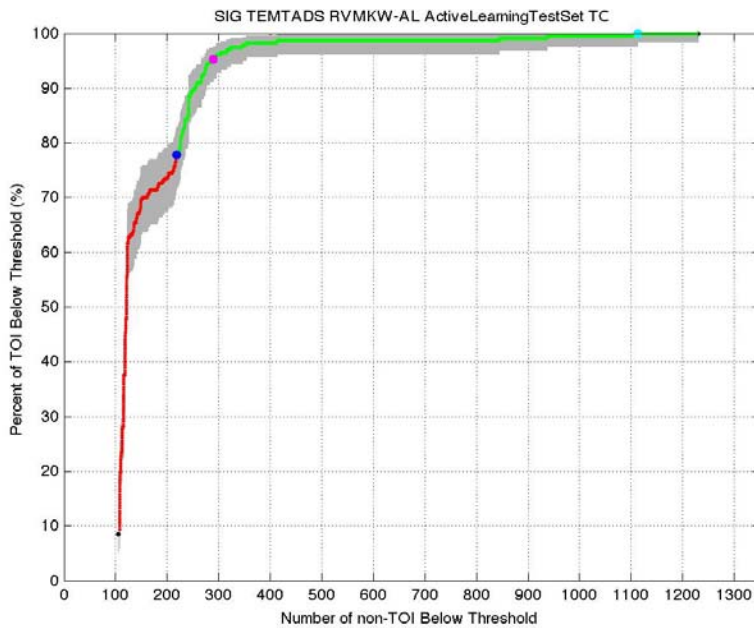
True TOI Locations Above Don't Dig Threshold	
Master ID	Ground Truth
444*	2.36*
241*	2.36*
555*	4.2*
1450*	81*
21*	4.2*
850*	4.2*
1285*	60*
208*	4.2*
1386	81
711	60
722	60

Figure 102: SIG’s primary scoring results for the TEMTADS and the RVM supervised learning classification algorithm. Eight true TOI locations rose above the prospective “don’t dig threshold” (dark-blue dot).



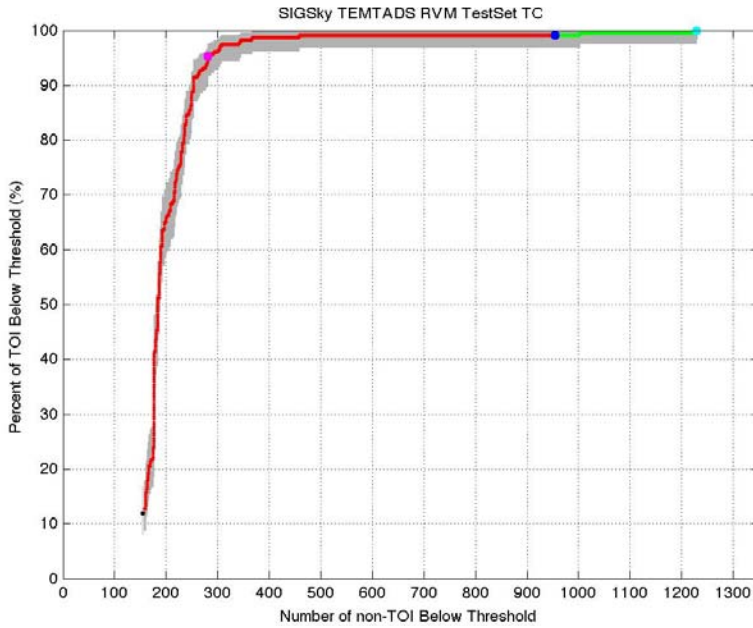
True TOI Locations Above Don't Dig Threshold	
Master ID	Ground Truth
444*	2.36*
1285*	60*
722	60
241	2.36
1450	81
1386	81
21	4.2
748	60
16	60
103	60
55	60

Figure 103: SIG’s primary scoring results for the TEMTADS and the PNBC semi-supervised learning classification algorithm. Two true TOI locations rose above the prospective “don’t dig threshold” (dark-blue dot).



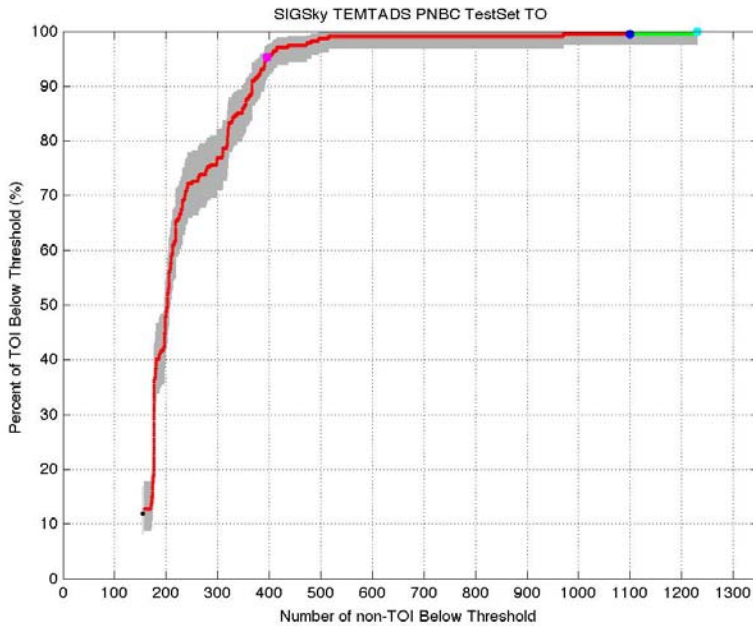
True TOI Locations Above Don't Dig Threshold	
Master ID	Ground Truth
241*	2.36*
1450*	81*
1285*	60*
410*	60*
107*	60*
103*	60*
444*	2.36*
748*	60*
122*	60*
22*	60*
275*	60*

Figure 104: SIG’s primary scoring results for the TEMTADS and the RVM supervised learning classification algorithm. The algorithm was optimized over the Active Learning Training Set and then applied to the complementary Active Learning Test Set. Fifty-two true TOI locations rose above the prospective “don’t dig threshold” (dark-blue dot), the first 11 of which are listed above in blue.



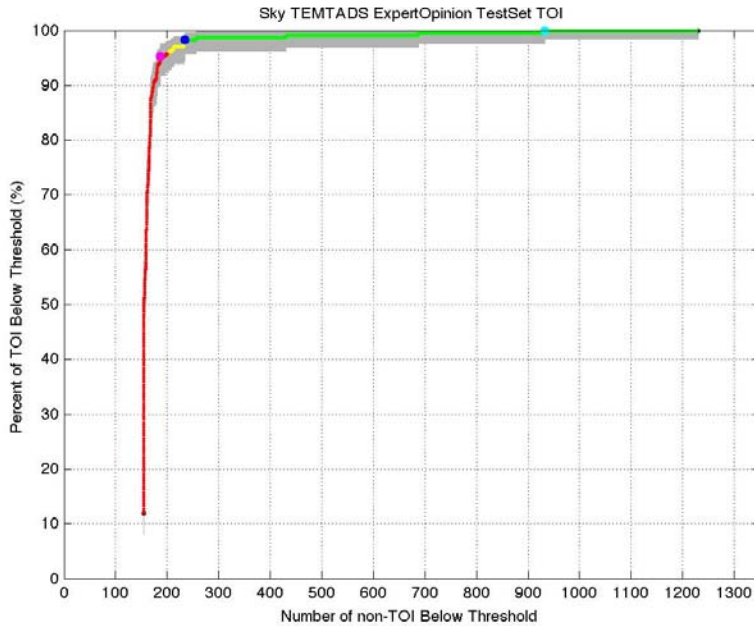
True TOI Locations Above Don't Dig Threshold	
Master ID	Ground Truth
241*	2.36*
1450*	81*
208	4.2
987	5
103	60
55	60
107	60
444	2.36
122	60
1444	60
109	60

Figure 105: SIG’s primary scoring results for the TEMTADS and the RVM supervised learning classification algorithm. (Sky estimated the parameters input to the algorithms.) Two true TOI locations rose above the prospective “don’t dig threshold” (dark-blue dot).



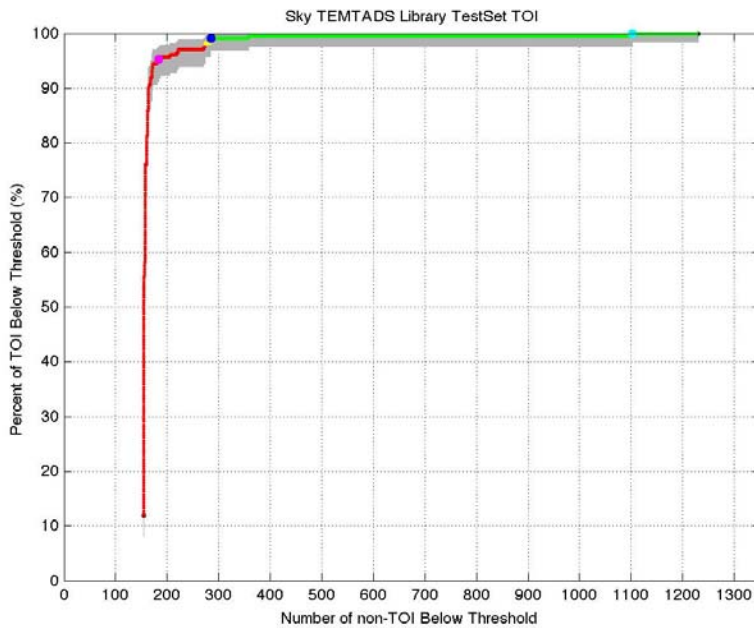
True TOI Locations Above Don't Dig Threshold	
Master ID	Ground Truth
241*	2.36*
1450	81
55	60
444	2.36
987	5
208	4.2
1444	60
160	60
60	60
109	60
775	60

Figure 106: SIG’s primary scoring results for the TEMTADS and the PNBC semi-supervised learning classification algorithm. (Sky estimated the parameters input to the algorithms.) One true TOI location rose above the prospective “don’t dig threshold” (dark-blue dot).



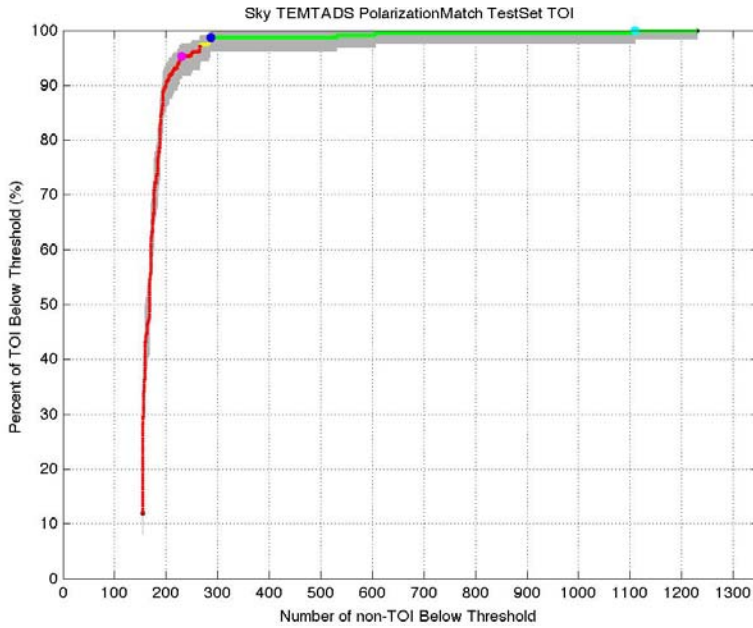
True TOI Locations Above Don't Dig Threshold	
Master ID	Ground Truth
241*	2.36*
16*	60*
103*	60*
1285*	60*
314	60
365	4.2
444	2.36
441	60
249	60
711	60
443	60

Figure 107: Sky’s primary scoring results for the TEMTADS and the “Expert Opinion” classification algorithm. Four true TOI location rose above the prospective “don’t dig threshold” (dark-blue dot).



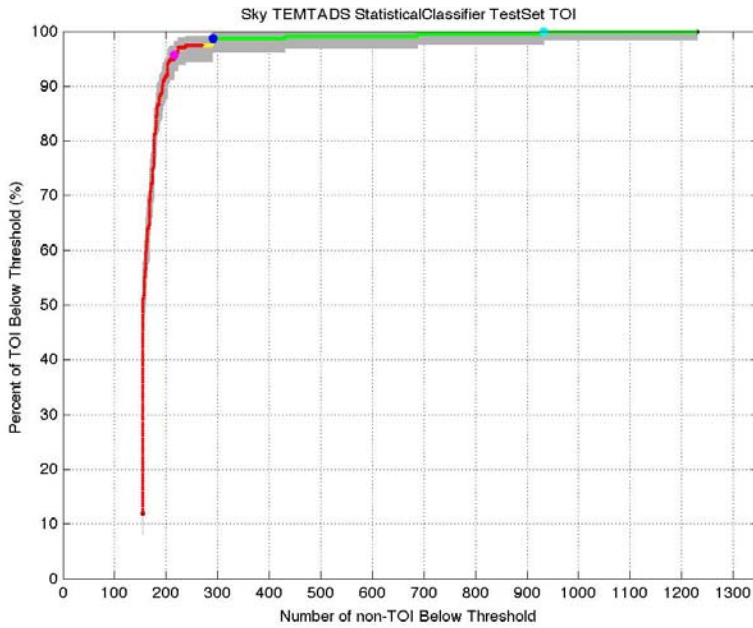
True TOI Locations Above Don't Dig Threshold	
Master ID	Ground Truth
241*	2.36*
711*	60*
314	60
365	4.2
444	2.36
208	4.2
452	81
722	60
372	60
207	60
103	60

Figure 108: Sky’s primary scoring results for the TEMTADS and the “Library” classification algorithm. Two true TOI locations rose above the prospective “don’t dig threshold” (dark-blue dot).



True TOI Locations Above Don't Dig Threshold	
Master ID	Ground Truth
241*	2.36*
103*	60*
16*	60*
314	60
365	4.2
444	2.36
79	60
90	60
443	60
60	60
72	60

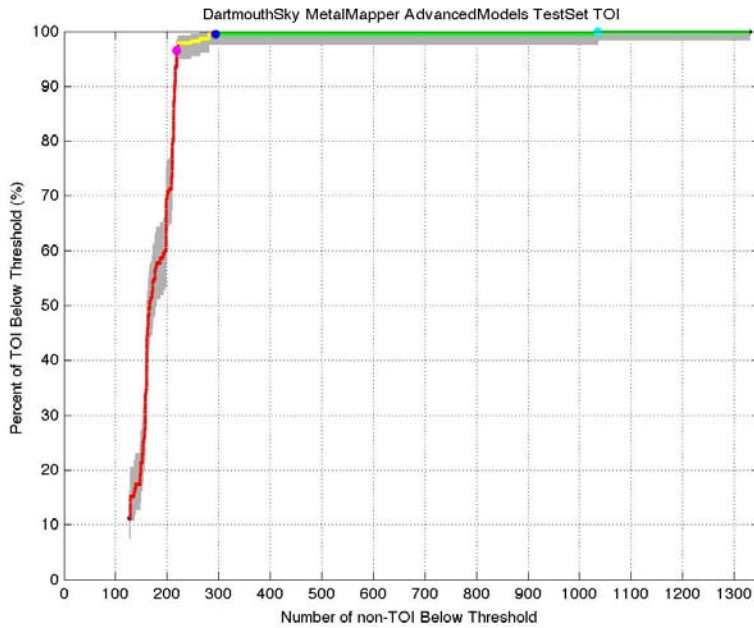
Figure 109: Sky’s primary scoring results for the TEMTADS and the “Polarization Match” classification algorithm. Three true TOI locations rose above the prospective “don’t dig threshold” (dark-blue dot).



True TOI Locations Above Don't Dig Threshold	
Master ID	Ground Truth
241*	2.36*
16*	60*
103*	60*
314	60
365	4.2
444	2.36
443	60
1285	60
441	60
60	60
241	2.36

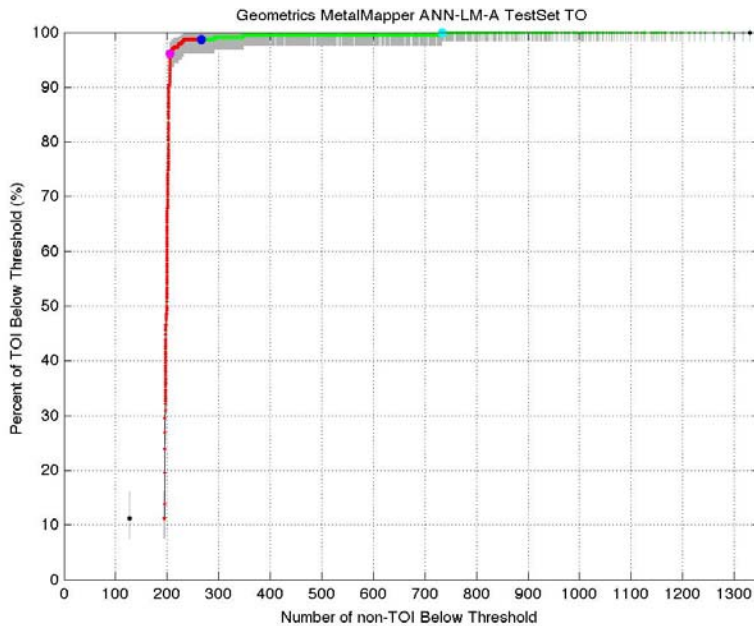
Figure 110: Sky’s primary scoring results for the TEMTADS and the “Statistical Classifier” classification algorithm. Three true TOI locations rose above the prospective “don’t dig threshold” (dark-blue dot).

## MetalMapper



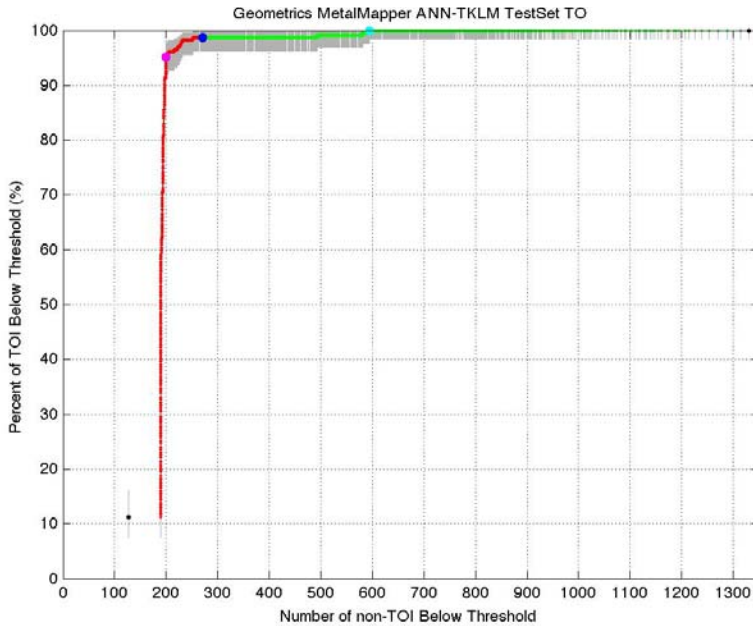
True TOI Locations Above Don't Dig Threshold	
MM ID	Ground Truth
737*	60*
254	60
292	37
852	60
1604	81
31	60
40	60
50	60

Figure 111: Dartmouth’s primary scoring results for the MetalMapper and the “Advanced Models” classification algorithm. (Sky estimated the parameters input to the algorithm.) One true TOI location rose above the prospective “don’t dig threshold” (dark-blue dot).



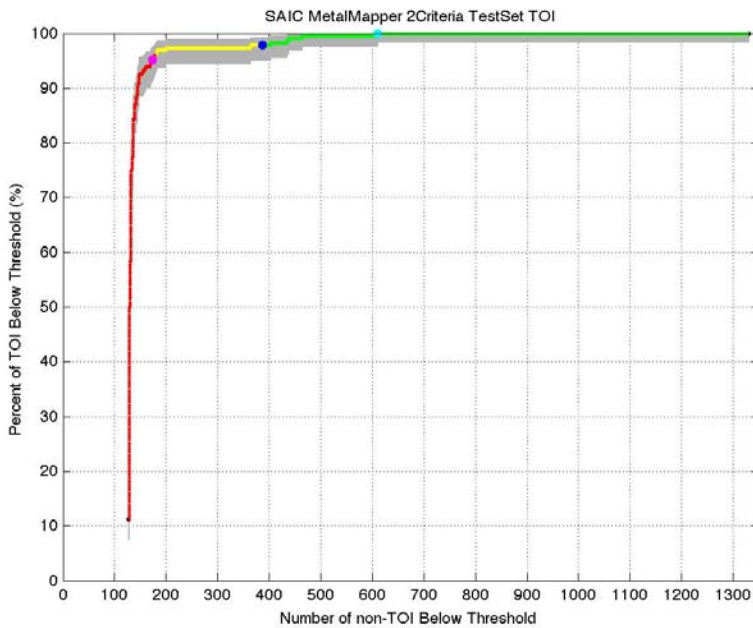
True TOI Locations Above Don't Dig Threshold	
MM ID	Ground Truth
1177*	60*
292*	37*
1718*	2.36*
737	60
493	60
2195	2.36
2149	60
368	60
852	60

Figure 112: Geometrics’ primary scoring results for the MetalMapper and the “ANN-LM-A” classification algorithm. Three true TOI locations rose above the prospective “don’t dig threshold” (dark-blue dot).



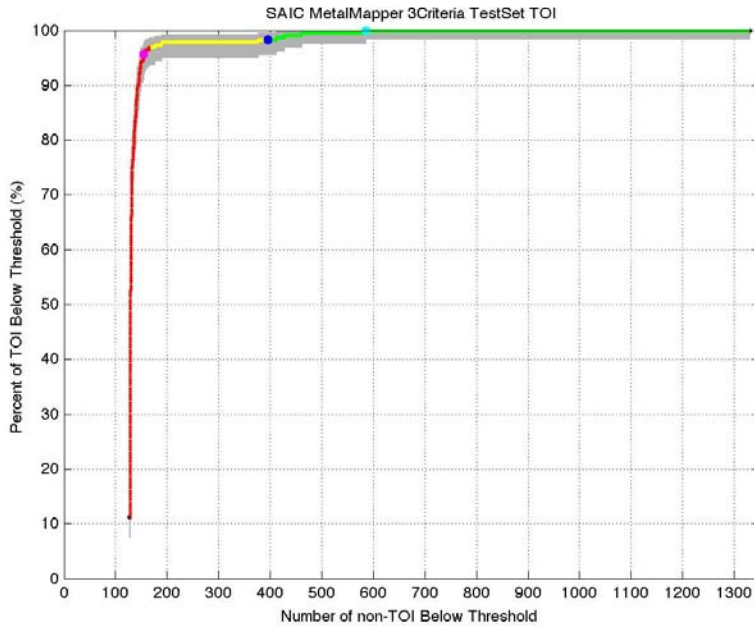
True TOI Locations Above Don't Dig Threshold	
MM ID	Ground Truth
292*	37*
1718*	2.36*
1177*	60*
1771	60
886	5
493	60
737	60
988	81
595	60
1626	3
2149	60

Figure 113: Geometrics' primary scoring results for the MetalMapper and the "ANN-TKLM" classification algorithm. Three true TOI locations rose above the prospective "don't dig threshold" (dark-blue dot).



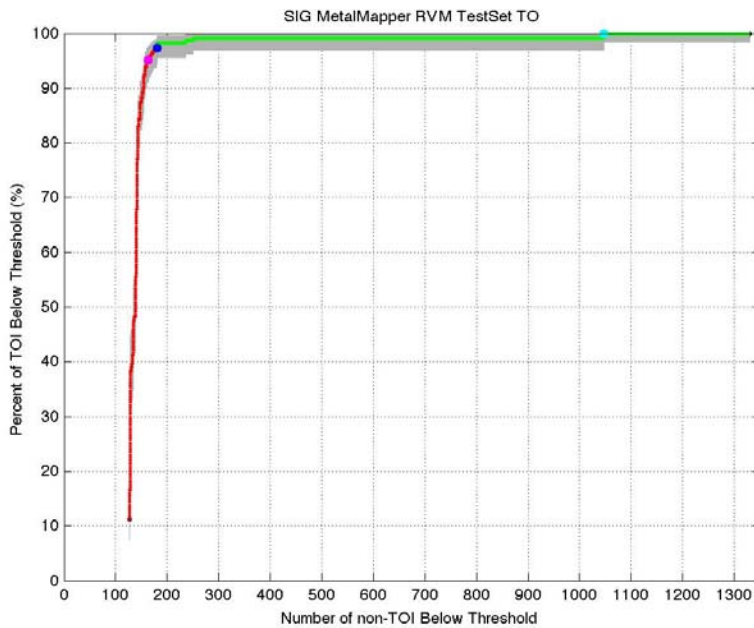
True TOI Locations Above Don't Dig Threshold	
MM ID	Ground Truth
1177*	60*
737*	60*
680*	2.36*
493*	60*
852*	60*
1718	2.36
292	37
1626	3
2306	60
781	60
2410	60

Figure 114: SAIC's primary scoring results for the MetalMapper and the "2 Criteria" classification algorithm. Five true TOI locations rose above the prospective "don't dig threshold" (dark-blue dot).



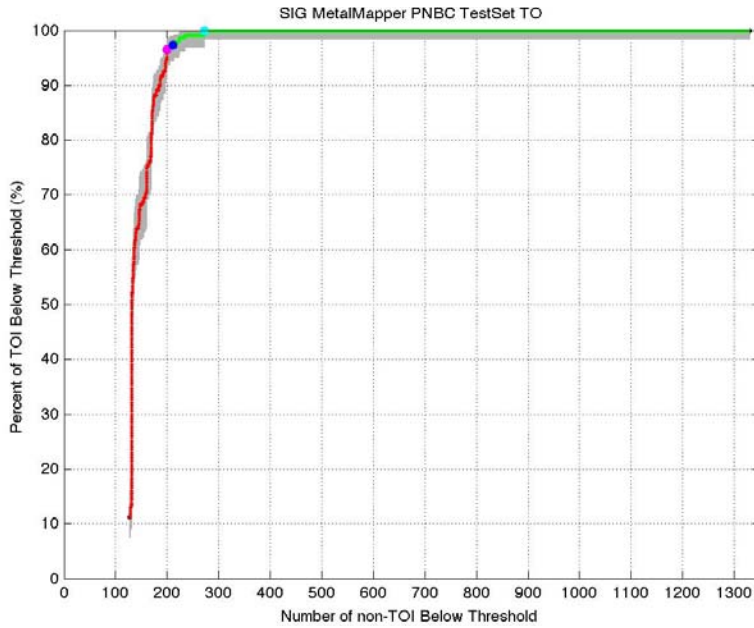
True TOI Locations Above Don't Dig Threshold	
MM ID	Ground Truth
1177*	60*
493*	60*
852*	60*
680*	2.36*
1718	2.36
292	37
737	60
1160	60
2104	2.36
163	2.36
1177	60

Figure 115: SAIC’s primary scoring results for the MetalMapper and the “3 Criteria” classification algorithm. Four true TOI locations rose above the prospective “don’t dig threshold” (dark-blue dot).



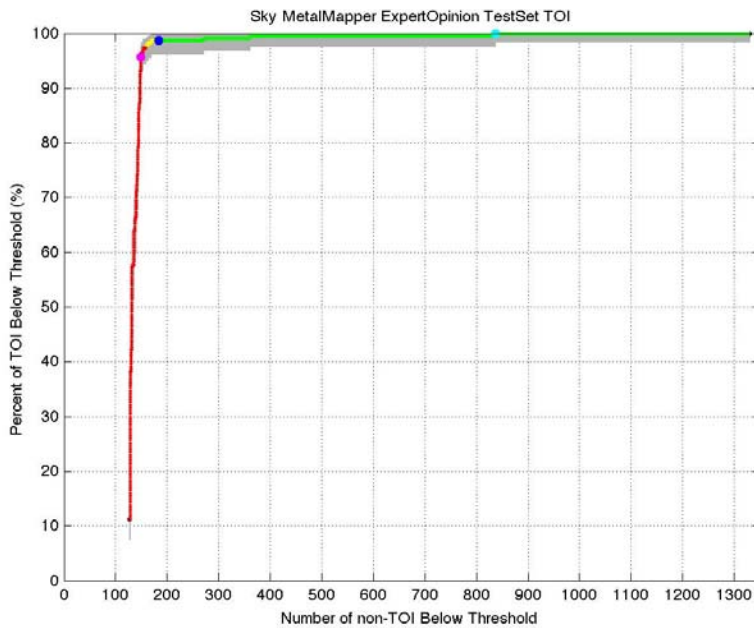
True TOI Locations Above Don't Dig Threshold	
MM ID	Ground Truth
292*	37*
2420*	81*
1177*	60*
1718*	2.36*
746*	60*
737*	60*
771	81
1626	3
886	5
781	60
1754	81

Figure 116: SIG’s primary scoring results for the MetalMapper and the RVM supervised learning classification algorithm. Six true TOI locations rose above the prospective “don’t dig threshold” (dark-blue dot).



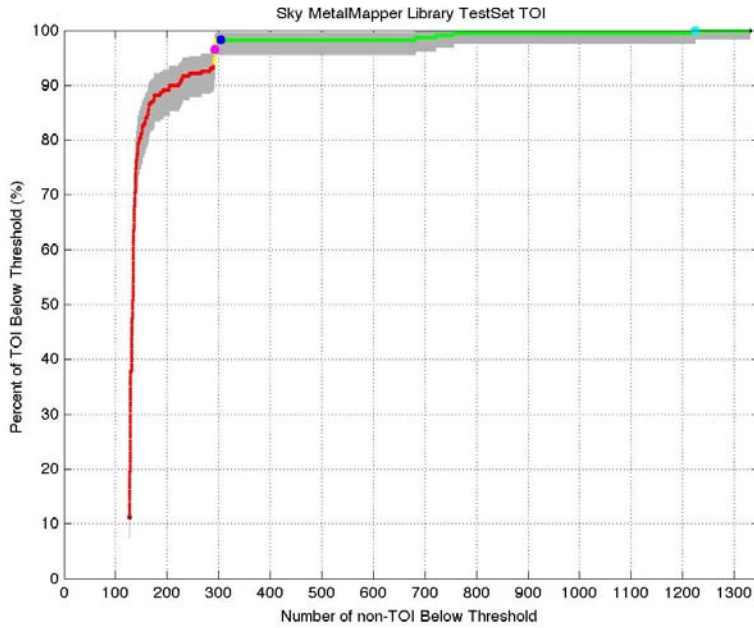
True TOI Locations Above Don't Dig Threshold	
MM ID	Ground Truth
1718*	2.36*
1177*	60*
746*	60*
781*	60*
292*	37*
2420*	81*
529	60
499	60

Figure 117: SIG’s primary scoring results for the MetalMapper and the PNBC semi-supervised learning classification algorithm. Six true TOI locations rose above the prospective “don’t dig threshold” (dark-blue dot).



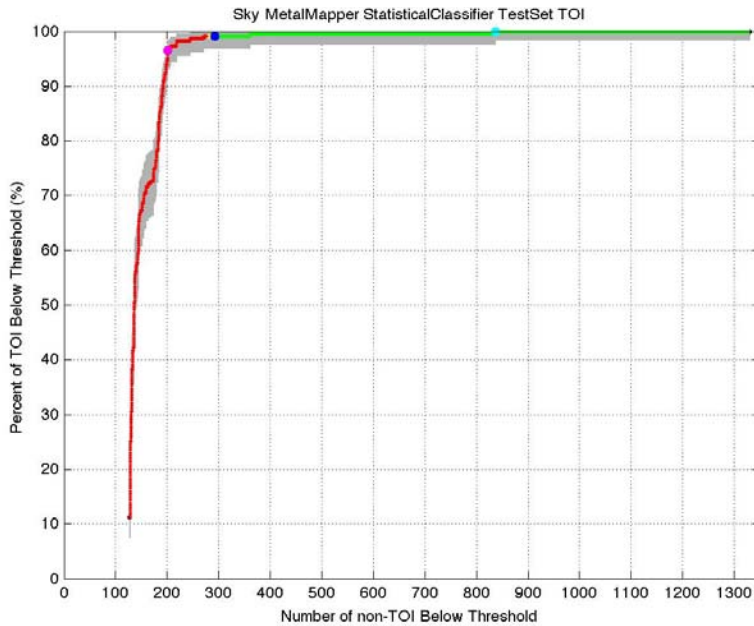
True TOI Locations Above Don't Dig Threshold	
MM ID	Ground Truth
1718*	2.36*
292*	37*
1177*	60*
737	60
1771	60
781	60
746	60
1915	60
493	60
731	60
1718	2.36

Figure 118: Sky’s primary scoring results for the MetalMapper and the “Expert Opinion” classification algorithm. Three true TOI locations rose above the prospective “don’t dig threshold” (dark-blue dot).



True TOI Locations Above Don't Dig Threshold	
MM ID	Ground Truth
1718*	2.36*
1177*	60*
1771*	60*
2420*	81*
371	60
595	60
564	2.36
410	60

Figure 119: Sky’s primary scoring results for the MetalMapper and the “Library” classification algorithm. Four true TOI locations rose above the prospective “don’t dig threshold” (dark-blue dot).



True TOI Locations Above Don't Dig Threshold	
MM ID	Ground Truth
1718*	2.36*
292*	37*
1177	60
781	60
746	60
1915	60
493	60
731	60

Figure 120: Sky’s primary scoring results for the MetalMapper and the “Statistical Classifier” classification algorithm. Two true TOI locations rose above the prospective “don’t dig threshold” (dark-blue dot).

## BUD

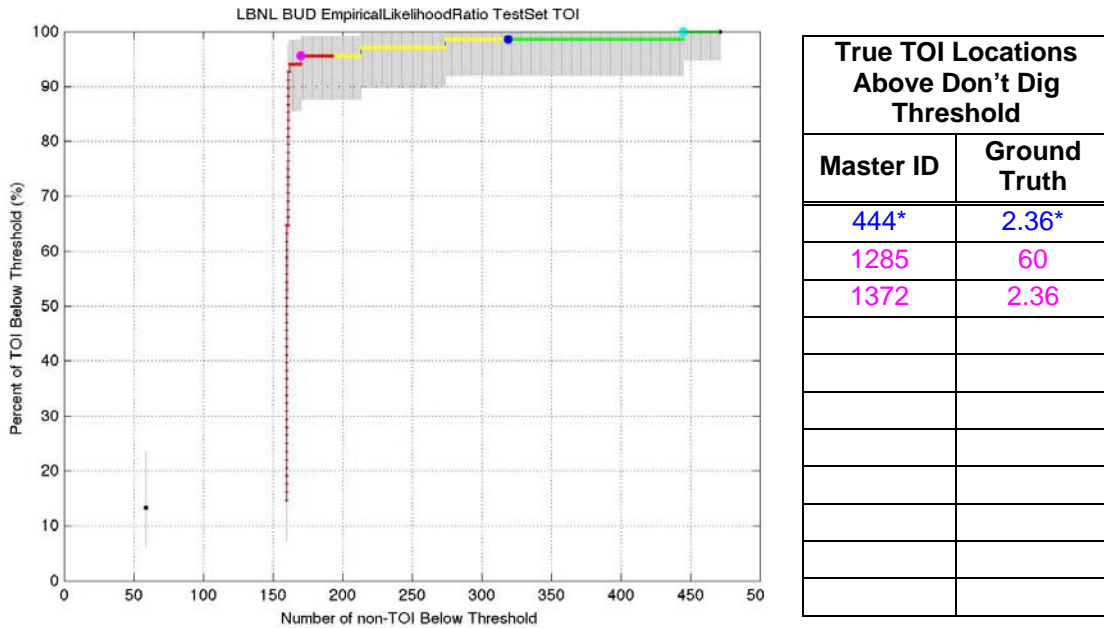


Figure 121: LBNL’s primary scoring results for the BUD and the “Empirical Likelihood Ratio” classification algorithm. Results were scored over only the sub-areas of the site where the BUD collected data. One true TOI location rose above the prospective “don’t dig threshold” (dark-blue dot).

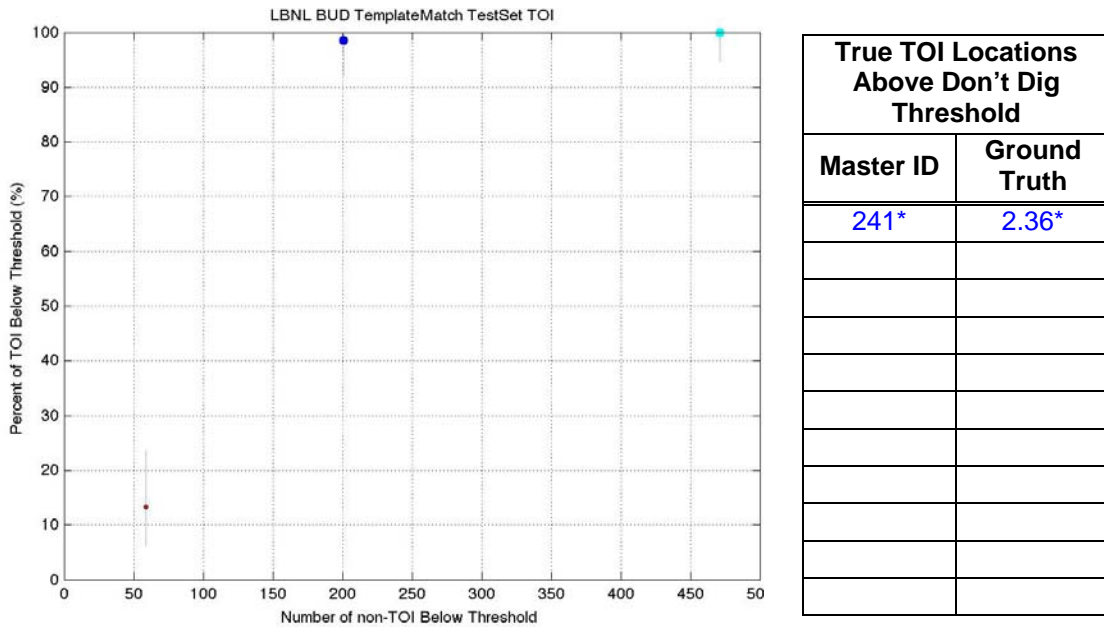
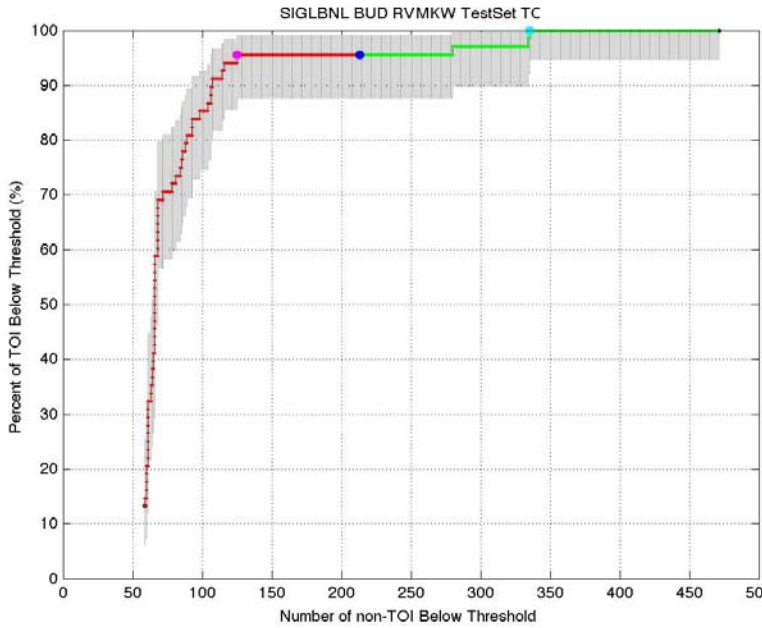
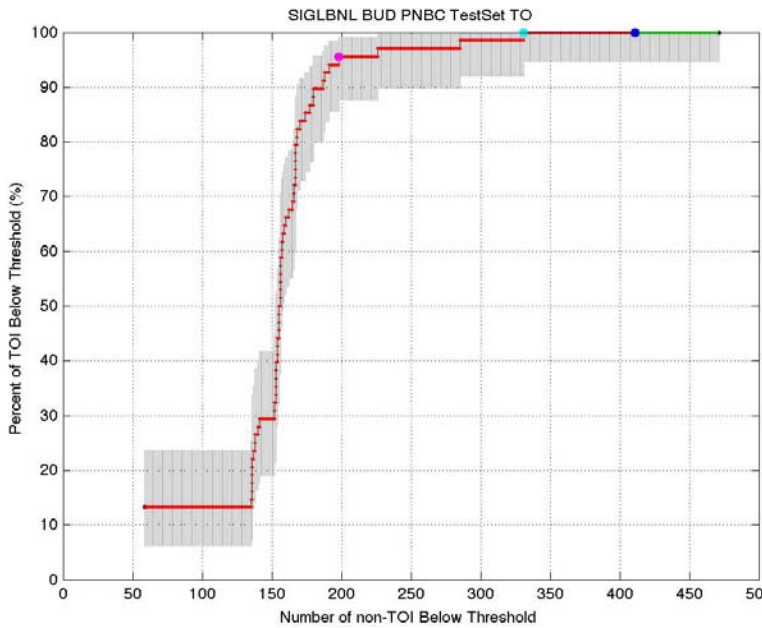


Figure 122: LBNL’s primary scoring results for the BUD and the “Template Match” classification algorithm. Results were scored over only the sub-areas of the site where the BUD collected data. Rather than ordering the BUD cued locations into a ranked anomaly list, LBNL simply classified them as either “Likely TOI” or “Likely Non-TOI.” One true TOI location was incorrectly classified as “Likely Non-TOI” (dark-blue dot). (The classifications were made after LBNL received ground truth for the Test Set.)



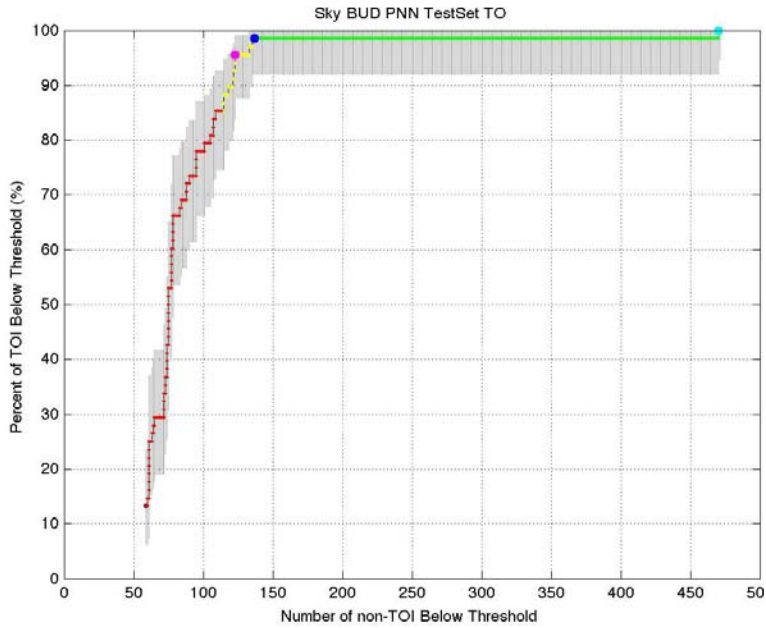
True TOI Locations Above Don't Dig Threshold	
Master ID	Ground Truth
241*	2.36*
1285*	60*
1372*	2.36*

Figure 123: SIG's primary scoring results for the BUD and the RVM supervised learning classification algorithm. (LBNL estimated the parameters input to the algorithm.) Results were scored over only the sub-areas of the site where the BUD collected data. Three true TOI locations rose above the prospective "don't dig threshold" (dark-blue dot), all of which are listed in blue. (The ranked anomaly list was created after SIG received ground truth for the Test Set.)



True TOI Locations Above Don't Dig Threshold	
Master ID	Ground Truth
241	2.36
1372	2.36
1285	60

Figure 124: SIG's primary scoring results for the BUD and the PNBC semi-supervised learning classification algorithm. (LBNL estimated the parameters input to the algorithm.) Results were scored over only the sub-areas of the site where the BUD collected data. No true TOI locations rose above the prospective "don't dig threshold" (dark-blue dot). (The ranked anomaly list was created after SIG received ground truth for the Test Set.)



True TOI Locations Above Don't Dig Threshold	
Master ID	Ground Truth
241*	2.36*
444	2.36
1444	60

**Figure 125: Sky’s primary scoring results for the BUD and the PNN classification algorithm. Results were scored over only the sub-areas of the site where the BUD collected data. One true TOI location rose above the prospective “don’t dig threshold” (dark-blue dot). (The ranked anomaly list was created after Sky received the ground truth for the Test Set.)**



## REFERENCES

- [1] “2008 ESTCP UXO Classification Study, San Luis Obispo, CA,” ESTCP, September 2008.
- [2] “Adaptive and Interactive Processing Techniques for Overlapping Signatures: Technical Summary Report,” AETC Inc., March 2006.
- [3] “Draft Final Report: LGP Discrimination and Residual Risk Analysis: 2008-9 ESTCP UXO Classification Study, Camp Sibert and Camp San Luis Obispo,” ESTCP Project #MM-0811, SAIC and RML Technologies Inc.
- [4] “EM61-Mk2 Cart Data Collection and Analysis: Former Camp San Luis Obispo,” NAEVA Geophysics Inc., April 2009.
- [5] “EMI Array for Cued UXO Discrimination: Draft Data Collection Report: Former Camp San Luis Obispo,” ESTCP Project #MM-00601, SAIC, July 2009.
- [6] “Draft Demonstration Data Report: Former Camp San Luis Obispo: Magnetometer and EM61 MkII Surveys,” ESTCP Project #MM-0744, Nova Research Inc., July 2009.
- [7] “Feature Extraction and Classification of Magnetic and EMI Data: Camp San Luis Obispo,” ESTCP Project #MM-0504, Sky Research Inc., March 2010.
- [8] “Final Site Inspections Report: Former Camp San Luis Obispo,” Parsons Inc., September 2007.
- [9] “Former Camp San Luis Obispo: SAIC Final Report,” SAIC, March 2010.
- [10] “Report of the Defense Science Board Task Force on Unexploded Ordnance,” Office of the Under Secretary of Defense for Acquisition, Technology, and Logistics, December 2003.
- [11] “Slope Correction and Anomaly Memorandum: Former Camp San Luis Obispo,” Nova Research Inc., May 2009.
- [12] Carin, L., et al., “2009 ESTCP UXO Discrimination Study, San Luis Obispo, CA,” ESTCP Project #MM-200501, Signals Innovations Group, April 2010.
- [13] Cazares, S., et al., “The UXO Discrimination Study at the Former Camp Sibert,” IDA Document D-3572, Institute for Defense Analyses, January 2009.
- [14] Gasperikova, E., “Technology Demonstration Plan Draft: ESTCP UXO Discrimination Study,” ESTCP Project #MM-0838, Lawrence Berkeley National Laboratory, January 2009.
- [15] Macshassy, S., and Provost, F., “Confidence Bands for ROC Curves: Methods and Empirical Study, *Proc. 1st Workshop on ROC Analysis in AI*, 2004.
- [16] May, M., and Tuley, M., “Interpreting Results from the Standardized UXO Test Sites,” IDA Document D-3280, Institute for Defense Analyses, January 2007.
- [17] Nelson, H., et al., “ESTCP Pilot Program: Classification Approaches in Munitions Response: San Luis Obispo, California,” ESTCP, May 2010.

- [18] Paski, A., "Memorandum: Description of Additional EM61 Cart Prioritized Dig Lists," NAEVA Geophysics Inc., November 2009.
- [19] Prouty, M., "Data Collection Report: MetalMapper System: Camp San Luis Obispo Discrimination Study," ESTCP Project #MM-0603, Geometrics Inc., July 2009.
- [20] Prouty, M., "Draft Demonstration Plan: Detection and Classification with the MetalMapper at the Former Camp San Luis Obispo," ESTCP Project #MM-0603, Geometrics Inc., March 2009.
- [21] Siegel, R., "MSEMS SLO Draft Data Report," SAIC, August 2009.
- [22] Tuley, M., et al., "UXO Classification Study: Blind Seed Plan at the Former Camp San Luis Obispo," Institute for Defense Analyses, October 2008.
- [23] Walker, A., "Memorandum: Classification of SLO EM61-MK2 Cart Targets," U.S. Army Engineering and Support Center, Huntsville, January 2010.
- [24] Walker, A., "Memorandum: Update to Classification of SLO EM61-MK2 Cart Targets," U.S. Army Engineering and Support Center, Huntsville, January 2010.

## ACRONYMS

$\beta$	EMI polarizability
$\tau$	EMI polarizability decay rate
BUD	Berkeley UXO Discriminator
CEHNC	Corps of Engineers – Huntsville Center
DGPS	Differential Global Positioning System
EMI	Electromagnetic induction
ESTCP	Environmental Security Technology Certification Program
FN	False negative
FP	False positive
GLRT	Generalized likelihood ratio test
GPS	Global Positioning System
IDA	Institute for Defense Analyses
IMU	Inertial measurement unit
IVS	Instrument Verification Strip
MSEMS	Man-portable Simultaneous Magnetometer and Electromagnetic System
MTADS	Multi-sensor Towed Array Detection System
N/A	Not applicable
$P_d$	Probability of detection
PNBC	Parameterized neighborhood-based classification
PNN	Probabilistic neural network
ROC	Receiver operating characteristic
RTK	Real time kinematic
RVM	Relevance Vector Machine
SAIC	Science Applications International Corporation
SERDP	Strategic Environmental Research and Development Program
SIG	Signals Innovations Group
SLO	San Luis Obispo
SNR	Signal-to-noise ratio
TEMTADS	Time-domain Electromagnetic Multi-sensor Towed Array Detection System
TOI	Target of interest

TP  
UXO

True positive  
Unexploded ordnance

**REPORT DOCUMENTATION PAGE***Form Approved*  
OMB No. 0704-0188

The public reporting burden for this collection of information is estimated to average 1 hour per response, including the time for reviewing instructions, searching existing data sources, gathering and maintaining the data needed, and completing and reviewing the collection of information. Send comments regarding this burden estimate or any other aspect of this collection of information, including suggestions for reducing the burden, to Department of Defense, Washington Headquarters Services, Directorate for Information Operations and Reports (0704-0188), 1215 Jefferson Davis Highway, Suite 1204, Arlington, VA 22202-4302. Respondents should be aware that notwithstanding any other provision of law, no person shall be subject to any penalty for failing to comply with a collection of information if it does not display a currently valid OMB control number.

**PLEASE DO NOT RETURN YOUR FORM TO THE ABOVE ADDRESS.**

1. REPORT DATE September 2010		2. REPORT TYPE Final		3. DATES COVERED (From–To) May 2008 – January 2010	
4. TITLE AND SUBTITLE  The UXO Classification Demonstration at San Luis Obispo, CA				5a. CONTRACT NUMBER DASW01 04 C 0003	
				5b. GRANT NUMBER	
				5c. PROGRAM ELEMENT NUMBER	
6. AUTHOR(S)  Shelley Cazares Michael Tuley				5d. PROJECT NUMBER	
				5e. TASK NUMBER AM-2-1528	
				5f. WORK UNIT NUMBER	
7. PERFORMING ORGANIZATION NAME(S) AND ADDRESS(ES)  Institute for Defense Analyses 4850 Mark Center Drive Alexandria, VA 22311-1882				8. PERFORMING ORGANIZATION REPORT NUMBER  IDA Document D-4148 Log: H10-000937	
9. SPONSORING / MONITORING AGENCY NAME(S) AND ADDRESS(ES)  Environmental Security Technology Certification Program 901 N. Stuart Street, Suite 303 Arlington, VA 22203				10. SPONSOR/MONITOR'S ACRONYM(S)	
				11. SPONSOR/MONITOR'S REPORT NUMBER(S)	
12. DISTRIBUTION/AVAILABILITY STATEMENT  Approved for public release; distribution is unlimited. (8 March 2011)					
13. SUPPLEMENTARY NOTES					
14. ABSTRACT Under a task titled "ESTCP/SERDP: Assessment of Traditional and Emerging Approaches to the Detection and Identification of Surface and Buried Unexploded Ordnance," the Institute for Defense Analyses (IDA) was assigned the responsibility to assist ESTCP in planning, executing, and scoring the classification demonstration carried out at San Luis Obispo, CA. IDA's principal functions were to provide seed emplacement locations and burial procedures, create a master anomaly list, develop scoring protocols, and score demonstrators' detection and classification results. This document provides a comprehensive final report describing the demonstration.					
15. SUBJECT TERMS  Unexploded Ordnance, classification, electromagnetic induction, magnetometer, receiver operating characteristics curves					
16. SECURITY CLASSIFICATION OF:			17. LIMITATION OF ABSTRACT	18. NUMBER OF PAGES	19a. NAME OF RESPONSIBLE PERSON
a. REPORT Uncl.	b. ABSTRACT Uncl.	c. THIS PAGE Uncl.			Dr. Herbert Nelson
			SAR	148	19b. TELEPHONE NUMBER (include area code) 703-696-8726

